

Consortium



for

Small-Scale Modelling

Technical Report No. 30

A Turbulence Kinetic Energy – Scalar Variance Turbulence Parameterization Scheme

April 2017

DOI: 10.5676/DWD_pub/nwv/cosmo-tr_30

Deutscher Wetterdienst

MeteoSwiss

Ufficio Generale Spazio Aereo e Meteorologia

ΕΘΝΙΚΗ ΜΕΤΕΩΡΟΛΟΓΙΚΗ ΥΠΗΡΕΣΙΑ

Instytucje Meteorologii i Gospodarki Wodnej

Administratia Nationala de Meteorologie

ROSHYDROMET

Agenzia Regionale per la Protezione Ambientale del Piemonte

Agenzia Regionale Prevenzione Ambiente Energia Emilia Romagna

Centro Italiano Ricerche Aerospaziali

Amt für GeoInformationswesen der Bundeswehr



www.cosmo-model.org

Editor: Massimo Milelli, ARPA Piemonte

*A Turbulence Kinetic Energy – Scalar Variance
Turbulence Parameterization Scheme*

by

Dmitrii V. Mironov¹ and Ekaterina E. Machulskaya

German Weather Service,
Offenbach am Main,
Germany

¹Corresponding author address: Deutscher Wetterdienst, FE14, Frankfurter Str. 135, D-63067 Offenbach am Main, Germany. Phone: +49-69-8062 2705, fax: +49-69-8062 3721. E-mail: dmitrii.mironov@dwd.de

Contents	2
1 Introduction	4
2 Quasi-Conservative Variables	7
3 Transport Equations for Second-Order Moments	7
4 Truncated Reynolds-Stress and Scalar-Flux Equations	10
5 Parameterization of Pressure Scrambling, Third-Order Transport and Dissipation Effects	11
5.1 Pressure Scrambling	11
5.2 Third-Order Transport	14
5.3 Dissipation	15
6 Time and Length Scales	15
7 Effect of Clouds on Mixing	17
8 Boundary-Layer Approximation	24
9 The (So-Called) Stability Functions	26
10 Interaction with the Underlying Surface	33
11 Equation for Scalar Skewness	35
12 Conclusions	38
13 Appendices	40

A Turbulence Kinetic Energy – Scalar Variance Turbulence Parameterization Scheme

Dmitrii V. Mironov[†] and Ekaterina E. Machulskaya

German Weather Service, Offenbach am Main, Germany

Abstract

A turbulence kinetic energy – scalar variance (TKESV) closure model (parameterization scheme) for moist atmosphere is developed. The scheme is formulated in terms of variables that are approximately conserved for phase changes in the absence of precipitation. These are the total water specific humidity and the liquid water potential temperature (or, if cloud ice is present, the ice-liquid water potential temperature). The scheme carries prognostic equations for the turbulence kinetic energy and for the variances and covariance of scalar quantities. The other second-moment equations, namely, the equations for the Reynolds stress and for the scalar fluxes, are reduced to the diagnostic algebraic expressions. In the present report, the set of governing equations of the TKESV scheme and parameterizations (closure assumptions) for the pressure-scrambling terms, the third-order transport (diffusion) terms, and the molecular destruction (dissipation) terms are discussed. Particular attention is paid to the pressure-scrambling terms in the Reynolds-stress and scalar-flux equations. The other issues that receive careful consideration are the effect of clouds on mixing (treated with the aid of statistical cloud schemes) and the interaction of the boundary layer with the underlying surface. Estimates of disposable parameters of the TKESV scheme are given.

[†]Corresponding author address: Deutscher Wetterdienst, FE14, Frankfurter Str. 135, D-63067 Offenbach am Main, Germany. Phone: +49-69-8062 2705, fax: +49-69-8062 3721. E-mail: dmitrii.mironov@dwd.de

1 Introduction

A turbulence parameterization scheme is an integral part of a physical parameterization package of any model of atmospheric circulation, including numerical weather prediction (NWP) and climate models. The importance of turbulence parameterization schemes will likely further increase as the resolution of the atmospheric models is refined. As the mesh size becomes small, quasi-organized flow structures, such as deep convective plumes that are chiefly responsible for non-local convective transport of momentum and scalars, are increasingly resolved. The focus of parameterizations of the sub-grid scale processes is then shifted towards motions at smaller scales and towards other issues, as e.g. the anisotropy of turbulence near the surface and in stably-stratified regions of the flow, and the interaction between boundary-layer turbulence and shallow clouds. Turbulence closure schemes based on truncated second-order moment equations are viable tools for describing these features.

There are many quite sophisticated and physically sound turbulence models (parameterization schemes) which proved to be very useful research tools. There is little chance, however, to use them in operational NWP and related applications for those schemes are computationally prohibitively expensive and are often specific to a particular mixing regime. A turbulence parameterization scheme should no doubt account for the essential physics of atmospheric turbulence. On the other hand, a usable scheme should be computationally efficient and should give a reasonably accurate solution for all mixing regimes (stably-stratified boundary layer, dry convective boundary layer, convective boundary layers capped by cumulus or stratus clouds, etc.) around the clock and at any point on the globe. Therefore, the key issue in developing turbulence parameterization schemes for NWP and related applications is to find the best compromise between physical realism and computational economy.

The so-called one-equation turbulence parameterizations schemes have been very popular in geophysical applications over several decades. Those schemes carry the turbulence kinetic energy (TKE) equation, including the time-rate-of-change (or substantial derivative if the TKE advection is included) and the third-order turbulent transport (diffusion) terms. All other second-moment equations, viz., the equations for the Reynolds stress, for the fluxes of scalar quantities (e.g. temperature and humidity), and for the scalar variances and scalar covariance, are reduced to diagnostic algebraic expressions. In spite of their numerous shortcomings (see a discussion in Mironov, 2009), one-equation TKE schemes (and even simpler algebraic schemes) have been and still are the draft horses of atmospheric turbulence modelling in NWP, climate studies, and related applications.

The present report describes a TKE – Scalar Variance (TKESV) turbulence parameterization scheme that is a natural step beyond one-equation TKE schemes. Apart from the TKE equation, the TKESV scheme carries prognostic transport equations for the scalar variances and covariance (see section 2 for the definition of quasi-conservative scalars utilized by the TKESV scheme). It is the authors' opinion that the level of complexity of the TKESV scheme is likely the minimum level of complexity that is required for NWP, climate modelling and related applications in terms of essential physics. A justification of this opinion is almost trivial. The key issue in modelling of any turbulent flow is an adequate description of the flow energy. In neutrally stratified flows, the kinetic energy of turbulence is a major concern. This explains why the one-equation schemes have been successfully used in modelling neutral flows. The situation is very different in flows where the buoyancy stratification is not neutral. In such flows, the turbulence potential energy (TPE) plays an important part along with the TKE. The TKE is spent to work against the gravity and is converted into the TPE in stably stratified flows. In convective flows, the TKE grows at the expense of the TPE. Since the atmospheric flows are virtually never hydrostatically neutral, and the TKE and the

TPE in stratified flows are equally important, it is difficult to adduce plausible arguments in favour of one form of energy over the other. Both energies possess equal rights and should be treated in a similar way. In the atmosphere, the TPE is characterized by the variances and covariance of the scalar quantities (see Appendix C). Hence, the scalar (co)variances should be treated as accurately as the TKE. An improved treatment of scalar (co)variances helps to improve the performance of atmospheric models in several respects. These are, for example, a consistent treatment of counter-gradient fluxes of scalars (which is not possible with the one-equation TKE schemes) and an improved representation of the fractional cloudiness. Furthermore, the TKESV scheme provides a framework for a consistent unified treatment of boundary-layer turbulence and shallow convection.

Examples of turbulence parameterization schemes that carry transport equations for both the TKE and the scalar variances are given in Kenjereš and Hanjalić (2002) (for the temperature-stratified atmosphere) and Nakanishi and Niino (2004) (for the moist atmosphere). Worthy of mention is a more complex scheme termed CLUBB (Cloud Layers Unified By Binormals), an assumed-PDF (probability distribution function) unified parameterization of turbulence and cloud processes in the Earth's atmosphere (numerous references and further information about CLUBB can be found at <https://people.uwm.edu/vlarson/clubb/>).

Interestingly enough, it was stated already by Mellor and Yamada in their popular 1974 paper (Mellor and Yamada, 1974) that the scheme (level 3 in their nomenclature) that carries transport equations for the TKE and for the potential-temperature variance is particularly attractive. The level 3 scheme outperforms an algebraic closure scheme, and little is gained if a more complex scheme that carries transport equations for all second-order moments involved is used. Thus the level 3 scheme represents an optimal choice. Mention should also be made of the analysis of the second-moment budgets in the cloud-topped boundary layers performed by Heinze et al. (2015) using large-eddy simulation (LES) data. It was found (among other things) that the third-order transport is of secondary importance in the Reynolds-stress and scalar-flux budgets but it plays a key role in maintaining the TKE and the scalar (co)variance budgets. These results support the design of the TKESV scheme.

In the present report, governing equations and closure assumptions (parameterizations) of the TKE–Scalar Variance scheme are formulated, and estimates of disposable parameters are given. In the remainder of this section, an outline of the report is given.

The TKESV scheme is formulated in terms of variables that are approximately conserved for phase changes in the absence of precipitation. These are the total water specific humidity and the liquid water potential temperature. If cloud ice is present, the ice-liquid water potential temperature is used. Quasi-conservative thermodynamic variables are introduced in section 2. Transport equations for the second-order moments of fluctuating velocity and scalar fields are given in section 3. The TKESV scheme carries “full” prognostic equations, i.e. the equations including the substantial derivative (that reduces to the time-rate-of-change in one-dimensional case, where the flow variables depend on the vertical coordinate only) and the third-order turbulent transport terms, for the TKE and for the variances and covariance of the scalar quantities. The equations for the Reynolds stress and for the scalar fluxes are reduced (truncated) to the diagnostic algebraic expressions by neglecting the substantial derivative and the third-order transport terms. The truncated Reynolds-stress and scalar-flux equations are presented in section 4.

The system of governing second-moment equations is not closed. There are four groups of terms that require parameterizations (closure assumptions). These are the pressure-scrambling terms in the Reynolds-stress and the scalar-flux equations, the third-order turbulent transport terms in the equations for the TKE and for the scalar variances and covariance, the dissipation rates of the TKE and of the scalar variances and covariance, and the buoy-

ancy terms (incorporating correlations of the velocity and scalars with the virtual potential temperature) in the Reynolds-stress, scalar-flux and TKE equations. Parameterizations of these terms are presented in sections 5 and 7. Particular attention is paid to the pressure-scrambling terms. Although parameterization of the pressure-scrambling effects is probably the most crucial issue in modelling atmospheric turbulence, this issue receives unduly little attention in the atmospheric modelling community. Formulations of the turbulence time and length scales are presented in section 6. An algebraic interpolation formula for the turbulence length scale that accounts for the limiting effect of stable density stratification is presented. A more advanced non-local length-scale formulation is also discussed. In section 7, we consider the effect of clouds on mixing intensity. The second-moment equations are coupled to a statistical cloud scheme, and parameterizations of the buoyancy terms in the Reynolds-stress, scalar-flux and TKE equations are developed with due regard for the presence of cloud condensate.

In section 8, the so-called boundary-layer approximation is invoked to obtain a one-dimensional version of the TKESV scheme. Note that in the majority of NWP models, including ICON and COSMO, one-dimensional schemes are used to parameterize turbulent mixing (unless these models are used in the LES mode). The so-called stability functions that appear in the algebraic formulations for the Reynolds stress and scalar fluxes (see e.g. Mellor and Yamada, 1974) are discussed in section 9 in much detail. The stability functions, resulting from the truncated Reynolds-stress and scalar-flux equations (where the third-order and the time-rate-of-change terms are neglected) with the linear parameterizations of the pressure-scrambling terms (linear in the second-order moments involved), are ill-behaved over a certain range of governing parameters (e.g. mean velocity shear and mean temperature gradient). Using rather plausible physical arguments, we develop regularized stability functions that are well-behaved in the entire range of governing parameters. The interaction of the boundary-layer flow with the underlying surface is discussed in section 10, where the focus is on the lower boundary conditions for the scalar variances and covariance.

The emphasis in sections 5 through 10 is on the baseline version of the TKESV scheme (TKESV-Bas). This somewhat simplified version of the scheme is based on the linear parameterizations of the pressure-scrambling terms, the simplest isotropic down-gradient parameterizations of the third-order transport terms, and the algebraic interpolation formula for the turbulence length scale. It utilizes an ad hoc correction to the Gaussian statistical cloud scheme to account for shallow cumuli (enhanced mixing due to clouds in spite of low fractional cloud cover). The lower boundary conditions for the scalar variances and covariance do not account for the heterogeneity of the underlying surface. It is the baseline version of the TKESV scheme in the boundary-layer approximation (i.e. the one-dimensional TKESV-Bas) that is intended for use within NWP models ICON and COSMO in the near future.

In the medium-term prospective, an extended version of the scheme (TKESV-Ext) can be used. TKESV-Ext incorporates advanced formulations of the pressure-scrambling terms and of the third-order transport terms, non-local formulation of the turbulence length scale, lower boundary conditions for the scalar (co)variances that are consistent with the tile approach to compute the surface fluxes over heterogeneous surfaces, and a statistical cloud scheme capable of describing cumulus regimes. These formulations are discussed in the respective sections under the heading *Advanced Features*. The use of an advanced statistical cloud scheme, e.g. the scheme proposed by Naumann et al. (2013), requires knowledge of the triple correlations (skewness) of scalar quantities (more specifically, of linearized saturation deficit/excess). The scalar-skewness prognostic equation is developed in section 11.

Conclusions are given in section 12. The present report contains several Appendices. The aim

of the report is not only to present the governing equations and parameterization assumptions of the TKESV scheme, but also to elucidate their physical meaning and, importantly, their limitations. To this end, detailed derivations of at least some parameterizations should be presented (most notably, of the pressure-scrambling terms). Since the derivations are rather lengthy, they are given in Appendices. This allows to keep the main body of the text more concise.

2 Quasi-Conservative Variables

In order to account for the presence of cloud condensate, turbulence and shallow-convection models are formulated in terms of variables that are approximately conserved for phase changes in the absence of precipitation (Betts, 1973; Deardorff, 1976; Betts, 1986). One pair of moist quasi-conservative variables consists of the total water specific humidity q_t and the liquid water potential temperature θ_l defined as

$$q_t = q + q_l, \quad (1)$$

$$\theta_l = \theta - \frac{\theta}{T} \frac{L_v}{c_p} q_l. \quad (2)$$

Here, q is the water vapour specific humidity (the mass of water vapour per unit mass of moist air), q_l is the liquid water specific humidity (the mass of cloud water per unit mass of moist air), c_p is the specific heat of air at constant pressure, L_v is the heat of vapourization, θ is the potential temperature related to the absolute temperature T through $\theta = T(P_0/P)^{R_d/c_p}$, P and P_0 being the atmospheric pressure and its reference value, respectively, and R_d being the gas constant for dry air. No supersaturation is assumed, so that $q_l = q_t - q_s$ if $q_t > q_s$, where q_s is the saturation specific humidity, and $q_l = 0$ otherwise. Clearly, q_t and θ_l reduce to the dry variables q and θ , respectively, in unsaturated conditions. For the sake of simplicity the total water specific humidity and the liquid water potential temperature will also be referred to as simply humidity and temperature, respectively.

Advanced Features

The $q_t - \theta_l$ system outlined above can be extended to the case of three phases including cloud ice (Deardorff, 1976). To this end, the total water specific humidity is generalized to account for the presence of ice, and the ice-liquid water (i.e. total water) potential temperature is introduced:

$$q_t = q + q_l + q_i, \quad (3)$$

$$\theta_t = \theta - \frac{\theta}{T} \frac{L_v}{c_p} q_l - \frac{\theta}{T} \frac{L_i}{c_p} q_i, \quad (4)$$

where q_i is the solid water specific humidity (the mass of cloud ice per unit mass of moist air), and L_i is the heat of sublimation.

3 Transport Equations for Second-Order Moments

The basis for the development of second-order closure schemes is the set of transport equations for the second-order moments of fluctuating fields (e.g. Monin and Yaglom, 1971;

Mironov, 2009). For the moist atmosphere characterized by quasi-conservative variables θ_l and q_t , these are the equations for the Reynolds stress $\langle u'_i u'_j \rangle$, u_i being the velocity components¹, for the scalar fluxes $\langle u'_i \theta'_l \rangle$ and $\langle u'_i q'_t \rangle$, for the scalar variances $\langle \theta'^2_l \rangle$ and $\langle q'^2_t \rangle$, and for the scalar covariance $\langle \theta'_l q'_t \rangle$. The angle brackets denote mean quantities, and a prime denotes a turbulent fluctuation. Using the Boussinesq approximation and assuming that the Reynolds number is sufficiently high to neglect the molecular diffusion terms in the second-moment budget equations (a good approximation for the atmospheric flows), the equations read

$$\begin{aligned} & \left(\frac{\partial}{\partial t} + \langle u_k \rangle \frac{\partial}{\partial x_k} \right) \langle u'_i u'_j \rangle = \\ & - \left(\langle u'_i u'_k \rangle \frac{\partial \langle u_j \rangle}{\partial x_k} + \langle u'_j u'_k \rangle \frac{\partial \langle u_i \rangle}{\partial x_k} \right) - (\beta_i \langle u'_j \theta'_v \rangle + \beta_j \langle u'_i \theta'_v \rangle) \\ & - 2 (\epsilon_{imk} \Omega_m \langle u'_k u'_j \rangle + \epsilon_{jmk} \Omega_m \langle u'_k u'_i \rangle) + \left\langle p' \left(\frac{\partial u'_i}{\partial x_j} + \frac{\partial u'_j}{\partial x_i} \right) \right\rangle \\ & - \frac{\partial}{\partial x_k} (\langle u'_k u'_i u'_j \rangle + \delta_{kj} \langle p' u'_i \rangle + \delta_{ki} \langle p' u'_j \rangle) - \epsilon_{ij}, \end{aligned} \quad (5)$$

$$\begin{aligned} & \left(\frac{\partial}{\partial t} + \langle u_k \rangle \frac{\partial}{\partial x_k} \right) \langle u'_i \theta'_l \rangle = - \langle u'_k \theta'_l \rangle \frac{\partial \langle u_i \rangle}{\partial x_k} - \langle u'_i u'_k \rangle \frac{\partial \langle \theta_l \rangle}{\partial x_k} - \beta_i \langle \theta'_l \theta'_v \rangle \\ & - 2 \epsilon_{imk} \Omega_m \langle u'_k \theta'_l \rangle - \left\langle \theta'_l \frac{\partial p'}{\partial x_i} \right\rangle - \frac{\partial}{\partial x_k} \langle u'_k u'_i \theta'_l \rangle - \epsilon_{\theta i}, \end{aligned} \quad (6)$$

$$\begin{aligned} & \left(\frac{\partial}{\partial t} + \langle u_k \rangle \frac{\partial}{\partial x_k} \right) \langle u'_i q'_t \rangle = - \langle u'_k q'_t \rangle \frac{\partial \langle u_i \rangle}{\partial x_k} - \langle u'_i u'_k \rangle \frac{\partial \langle q_t \rangle}{\partial x_k} - \beta_i \langle q'_t \theta'_v \rangle \\ & - 2 \epsilon_{imk} \Omega_m \langle u'_k q'_t \rangle - \left\langle q'_t \frac{\partial p'}{\partial x_i} \right\rangle - \frac{\partial}{\partial x_k} \langle u'_k u'_i q'_t \rangle - \epsilon_{q i}, \end{aligned} \quad (7)$$

$$\frac{1}{2} \left(\frac{\partial}{\partial t} + \langle u_k \rangle \frac{\partial}{\partial x_k} \right) \langle \theta'^2_l \rangle = - \langle u'_k \theta'_l \rangle \frac{\partial \langle \theta_l \rangle}{\partial x_k} - \frac{1}{2} \frac{\partial}{\partial x_k} \langle u'_k \theta'^2_l \rangle - \epsilon_{\theta \theta}, \quad (8)$$

$$\frac{1}{2} \left(\frac{\partial}{\partial t} + \langle u_k \rangle \frac{\partial}{\partial x_k} \right) \langle q'^2_t \rangle = - \langle u'_k q'_t \rangle \frac{\partial \langle q_t \rangle}{\partial x_k} - \frac{1}{2} \frac{\partial}{\partial x_k} \langle u'_k q'^2_t \rangle - \epsilon_{q q}, \quad (9)$$

$$\left(\frac{\partial}{\partial t} + \langle u_k \rangle \frac{\partial}{\partial x_k} \right) \langle \theta'_l q'_t \rangle = - \langle u'_k q'_t \rangle \frac{\partial \langle \theta_l \rangle}{\partial x_k} - \langle u'_k \theta'_l \rangle \frac{\partial \langle q_t \rangle}{\partial x_k} - \frac{\partial}{\partial x_k} \langle u'_k \theta'_l q'_t \rangle - 2 \epsilon_{\theta q}. \quad (10)$$

Here, t is the time, x_i are the space coordinates, $\beta_i = g_i \alpha_T$ is the buoyancy parameter, g_i is the acceleration due to gravity, $\alpha_T = -\rho^{-1} \partial \rho / \partial T$ is the thermal expansion coefficient, ρ is the density, Ω_i is the angular velocity of the reference frame rotation, and p is the kinematic pressure (deviation of pressure from the hydrostatically balanced pressure divided by the reference density ρ_r). The Einstein summation convention for repeated indices is adopted. The last terms on the right-hand sides (r.h.s.) of Eqs. (5)–(10) are the molecular destruction (dissipation) rates of the Reynolds stress, of the scalar fluxes, and of the scalar variances and covariance. The quantity θ_v is the virtual potential temperature that is defined with due regard for the water loading effect (Lilly, 1968; Bannon, 2007),

$$\theta_v = \theta \left[1 + \left(\frac{R_v}{R_d} - 1 \right) q - q_l \right], \quad (11)$$

¹The term ‘‘Reynolds stress’’ is used here in a somewhat loose way. Strictly speaking, the Reynolds stress tensor is $-\rho \langle u'_i u'_j \rangle$, where ρ is the fluid density. See e.g. Pope (2000).

where R_v is the gas constant for water vapour.

Setting $j = i$ in Eq. (5) yields the budget equation for the TKE, $e \equiv \frac{1}{2} \langle u_i'^2 \rangle$,

$$\begin{aligned} \frac{1}{2} \left(\frac{\partial}{\partial t} + \langle u_k \rangle \frac{\partial}{\partial x_k} \right) \langle u_i'^2 \rangle = & - \langle u_i' u_k' \rangle \frac{\partial \langle u_i \rangle}{\partial x_k} - \beta_i \langle u_i' \theta_v' \rangle \\ & - \frac{\partial}{\partial x_k} \left(\frac{1}{2} \langle u_k' u_i'^2 \rangle + \langle u_k' p' \rangle \right) - \epsilon, \end{aligned} \quad (12)$$

where the last term on the r.h.s. is the TKE dissipation rate, $\epsilon \equiv \frac{1}{2} \epsilon_{ii}$.

The pressure gradient-velocity covariance $\langle u_i' \partial p' / \partial x_j \rangle + \langle u_j' \partial p' / \partial x_i \rangle$ describes the combined effect of pressure transport and pressure scrambling in the Reynolds-stress equation. These are different physical processes that should be modelled in a different way. To this end, the pressure gradient-velocity covariance is decomposed to separate out the traceless part which does not alter the TKE but acts to redistribute the energy between the components, thus driving turbulence towards the isotropic state (hence the term ‘‘pressure scrambling’’). The rest of the pressure gradient-velocity covariance describes the transport of the Reynolds stress in space by the fluctuating velocity and pressure fields. It should be mentioned that the decomposition of the pressure gradient-velocity covariance is not unique. Along with a somewhat more traditional decomposition into pressure-strain and pressure transport that is used in Eq. (5),

$$\left\langle u_i' \frac{\partial p'}{\partial x_j} \right\rangle + \left\langle u_j' \frac{\partial p'}{\partial x_i} \right\rangle = - \left\langle p' \left(\frac{\partial u_i'}{\partial x_j} + \frac{\partial u_j'}{\partial x_i} \right) \right\rangle + \left(\frac{\partial}{\partial x_j} \langle p' u_i' \rangle + \frac{\partial}{\partial x_i} \langle p' u_j' \rangle \right), \quad (13)$$

a decomposition into deviatoric and isotropic parts,

$$\begin{aligned} & \left\langle u_i' \frac{\partial p'}{\partial x_j} \right\rangle + \left\langle u_j' \frac{\partial p'}{\partial x_i} \right\rangle = \\ & \left(\left\langle u_i' \frac{\partial p'}{\partial x_j} \right\rangle + \left\langle u_j' \frac{\partial p'}{\partial x_i} \right\rangle - \frac{2}{3} \delta_{ij} \frac{\partial}{\partial x_k} \langle u_k' p' \rangle \right) + \frac{2}{3} \delta_{ij} \frac{\partial}{\partial x_k} \langle u_k' p' \rangle, \end{aligned} \quad (14)$$

has also been advocated (e.g. Speziale, 1985). The difference,

$$\frac{\partial}{\partial x_j} \langle p' u_i' \rangle + \frac{\partial}{\partial x_i} \langle p' u_j' \rangle - \frac{2}{3} \delta_{ij} \frac{\partial}{\partial x_k} \langle u_k' p' \rangle, \quad (15)$$

is both a transport term and a traceless term. Any fraction of this difference may be added to the pressure-strain and subtracted from the pressure transport, thus producing a new decomposition (Lumley, 1975).

The non-uniqueness of decomposition of the pressure gradient-velocity covariance does not matter much if a truncated equation for the Reynolds stress is used, where the third-order transport and pressure transport terms are neglected. No matter which approach is taken, the pressure-strain and the deviatoric part of the pressure gradient-velocity covariance are both traceless tensors that are modelled in the same way. Therefore, there is no general difference between the decompositions (13) and (14), or any other decomposition separating the traceless and the transport parts, as regards the pressure redistribution (the inter-component energy transfer)². The two decompositions are essentially different as regards the pressure transport (Speziale, 1985). The pressure transport of the Reynolds stress is, however, neglected within the framework of the scheme considered here.

²Notice, however, that the way the traceless part of the pressure term is separated out does matter when data, e.g. large-eddy simulation or direct numerical simulation data, are used to evaluate disposable parameters in models (parameterizations) of the pressure redistribution terms.

Advanced Features

If cloud ice is considered, the virtual potential temperature is defined as

$$\theta_v = \theta \left[1 + \left(\frac{R_v}{R_d} - 1 \right) q - q_l - q_i \right]. \quad (16)$$

4 Truncated Reynolds-Stress and Scalar-Flux Equations

Within the framework of the TKESV scheme, the equations for the Reynolds stress and for the scalar fluxes are reduced (truncated) to the diagnostic algebraic expressions by neglecting the substantial derivatives, the third-order transport of $\langle u'_i u'_j \rangle$, $\langle u'_i \theta'_l \rangle$ and $\langle u'_i q'_l \rangle$, and the pressure transport of $\langle u'_i u'_j \rangle$. The resulting algebraic equations are conveniently recast in terms of the departure-from-isotropy tensor defined as

$$a_{ij} = \langle u'_i u'_j \rangle - \frac{2}{3} \delta_{ij} e. \quad (17)$$

Subtracting Eq. (12) times $\frac{2}{3} \delta_{ij}$ from Eq. (5) and neglecting the time-rate-of-change, advection by the mean flow, the third-order transport and the pressure transport, we obtain

$$\begin{aligned} & - \left[\frac{4}{3} e S_{ij} + \left(a_{ik} S_{jk} + a_{jk} S_{ik} - \frac{2}{3} \delta_{ij} a_{km} S_{km} \right) + (a_{ik} W_{jk} + a_{jk} W_{ik}) \right] \\ & - \left(\beta_i \langle u'_j \theta'_v \rangle + \beta_j \langle u'_i \theta'_v \rangle - \frac{2}{3} \delta_{ij} \beta_k \langle u'_k \theta'_v \rangle \right) - 2 (\epsilon_{imk} \Omega_m a_{kj} + \epsilon_{jmk} \Omega_m a_{ki}) \\ & - \Pi_{ij} - \epsilon_{ij}^d = 0, \end{aligned} \quad (18)$$

where $S_{ij} = \frac{1}{2} \left(\frac{\partial \langle u_i \rangle}{\partial x_j} + \frac{\partial \langle u_j \rangle}{\partial x_i} \right)$ and $W_{ij} = \frac{1}{2} \left(\frac{\partial \langle u_i \rangle}{\partial x_j} - \frac{\partial \langle u_j \rangle}{\partial x_i} \right)$ are the symmetric and the antisymmetric parts, respectively, of the mean-velocity gradient tensor, $\epsilon_{ij}^d = \epsilon_{ij} - \frac{2}{3} \delta_{ij} \epsilon$ is the deviatoric part of the Reynolds-stress dissipation tensor, and Π_{ij} is the traceless part of the pressure gradient-velocity covariance in the Reynolds-stress equation, see Eq. (13).

Neglecting the substantial derivative and the third-order transport terms in Eqs. (6) and (7), we obtain algebraic equations for the scalar fluxes $\langle u'_i \theta'_l \rangle$ and $\langle u'_i q'_l \rangle$. They read

$$\begin{aligned} & - \left(\frac{2}{3} e \delta_{ik} + a_{ik} \right) \frac{\partial \langle \theta_l \rangle}{\partial x_k} - (S_{ik} + W_{ik}) \langle u'_k \theta'_l \rangle - \beta_i \langle \theta'_l \theta'_v \rangle - 2 \epsilon_{imk} \Omega_m \langle u'_k \theta'_l \rangle \\ & - \Pi_{\theta i} - \epsilon_{\theta i} = 0, \end{aligned} \quad (19)$$

$$\begin{aligned} & - \left(\frac{2}{3} e \delta_{ik} + a_{ik} \right) \frac{\partial \langle q_l \rangle}{\partial x_k} - (S_{ik} + W_{ik}) \langle u'_k q'_l \rangle - \beta_i \langle q'_l \theta'_v \rangle - 2 \epsilon_{imk} \Omega_m \langle u'_k q'_l \rangle \\ & - \Pi_{qi} - \epsilon_{qi} = 0, \end{aligned} \quad (20)$$

where $\Pi_{\theta i}$ and Π_{qi} denote the pressure gradient-scalar covariances $\langle \theta'_l \partial p' / \partial x_i \rangle$ and $\langle q'_l \partial p' / \partial x_i \rangle$, respectively.

5 Parameterization of Pressure Scrambling, Third-Order Transport and Dissipation Effects

The second-moment equations (8), (9), (10), (12), (18), (19) and (20) are not closed. There are four groups of terms that should be parameterized. These are the pressure-scrambling terms, the third-order transport (diffusion) terms, the molecular destruction (dissipation) terms, and the buoyancy terms (incorporating correlations of the velocity and scalars with the virtual potential temperature). Parameterizations (closure assumptions) for the pressure-scrambling, third-order transport and dissipation terms are developed in sections 5.1, 5.2 and 5.3, respectively. The buoyancy terms are considered in section 7.

5.1 Pressure Scrambling

A common approach nowadays is to decompose the pressure-scrambling terms in the Reynolds-stress and scalar-flux equations into the contributions due to the non-linear turbulence interactions (that stem from the advection term in the equation of motion), mean velocity shear, buoyancy and the Coriolis effects, and to model (parameterize) these contributions separately (see e.g. Zeman, 1981; Mironov, 2001, 2009). Following this approach, we apply the return-to-isotropy parameterizations (Rotta, 1951; Monin, 1965) to the non-linear turbulence contributions to Π_{ij} , $\Pi_{\theta i}$, Π_{qi} (often referred to as slow parts of the pressure-scrambling terms) and utilize the simplest linear parameterizations of the mean velocity shear, buoyancy and Coriolis contributions (referred to as rapid parts of the pressure-scrambling terms). The following parameterizations of the pressure-scrambling terms are used in the TKESV-Bas scheme:

$$\begin{aligned} \Pi_{ij} &= C_t^u \frac{a_{ij}}{\tau_{ru}} \\ &- C_{s1}^u S_{ij} e - C_{s2}^u \left(S_{ik} a_{kj} + S_{jk} a_{ki} - \frac{2}{3} \delta_{ij} S_{kl} a_{kl} \right) - C_{s3}^u (W_{ik} a_{kj} + W_{jk} a_{ki}) \\ &- C_b^u \left(\beta_i \langle u'_j \theta'_v \rangle + \beta_j \langle u'_i \theta'_v \rangle - \frac{2}{3} \delta_{ij} \beta_k \langle u'_k \theta'_v \rangle \right) \\ &- 2C_c^u (\epsilon_{imk} \Omega_m a_{kj} + \epsilon_{jmk} \Omega_m a_{ki}), \end{aligned} \quad (21)$$

$$\Pi_{\theta i} = C_t^\theta \frac{\langle u'_i \theta'_l \rangle}{\tau_{r\theta}} - \left(C_{s1}^\theta S_{ij} + C_{s2}^\theta W_{ij} \right) \langle u'_j \theta'_l \rangle - C_b^\theta \beta_i \langle \theta'_l \theta'_v \rangle - 2C_c^\theta \epsilon_{imj} \Omega_m \langle u'_j \theta'_l \rangle, \quad (22)$$

$$\Pi_{qi} = C_t^q \frac{\langle u'_i q'_l \rangle}{\tau_{rq}} - \left(C_{s1}^q S_{ij} + C_{s2}^q W_{ij} \right) \langle u'_j q'_l \rangle - C_b^q \beta_i \langle q'_l \theta'_v \rangle - 2C_c^q \epsilon_{imj} \Omega_m \langle u'_j q'_l \rangle, \quad (23)$$

where $C_t^u = 1.8$, $C_{s1}^u = 4/5$, $C_{s2}^u = -6\alpha_5$, $C_{s3}^u = \frac{2}{3}(2 + 7\alpha_5)$, $C_b^u = 3/10$, $C_c^u = \frac{1}{3}(2 + 7\alpha_5)$, $C_t^\theta = C_t^q = 5.0$, $C_{s1}^\theta = C_{s1}^q = 3/5$, $C_{s2}^\theta = C_{s2}^q = 1$, $C_b^\theta = C_b^q = 1/3$ and $C_c^\theta = C_c^q = 1/2$ are dimensionless constants. An estimate of the yet undetermined disposable constant α_5 is obtained below. The return-to-isotropy time scales τ_{ru} , $\tau_{r\theta}$ and τ_{rq} in Eqs. (21)–(23) are taken to be proportional to the TKE dissipation time scale, $\tau_{ru} = \tau_{r\theta} = \tau_{rq} = \tau_\epsilon$, where $\tau_\epsilon = e/\epsilon$ and proportionality constants are set to one as they always occur in combination with the other constants. Parameterizations of the various time and length scales are discussed in section 6. A detailed derivation of Eqs. (21)–(23) is given in Appendix A. The properties of linear parameterizations of the pressure-scrambling terms, most notably their limitations, should be discussed in some detail.

It is readily seen that the linear parameterizations of the mean-velocity shear, buoyancy and Coriolis contributions to Π_{ij} , $\Pi_{\theta i}$ and Π_{qi} have the same form as the mean-velocity shear, buoyancy and Coriolis terms in the Reynolds-stress and scalar-flux equations (5)–(7) [or their truncated counterparts (18)–(20)]. Therefore, the effect of linear rapid parts of the pressure-scrambling terms, sometimes referred to as the implicit mean-velocity shear, buoyancy and Coriolis terms, is simply to partially offset the respective explicit terms already present in the Reynolds-stress and scalar-flux equations.

In the linear parameterizations of the pressure-scrambling terms, Eqs. (21)–(23), the numerical values of most dimensionless coefficients are fixed by mathematical constraints. In practice, however, those coefficients are often treated as disposable parameters whose values are adjusted to improve the overall performance of a turbulence model (parameterization scheme) in a particular flow regime. Although this approach may be considered legitimate in practical applications, caution must be exercised. Consider, for example, the coefficient C_b^θ in the buoyancy contribution to the pressure gradient-temperature covariance. As shown in Appendix A, the symmetry (A.11) and the normalization (A.13) constraints require that C_b^θ be equal to 1/3. This value corresponds to the isotropic limit and is consistent with the fact that the linear parameterizations of the pressure-scrambling terms are only valid for the flows where turbulence is not far from the isotropic state. The use of an empirical estimate of $C_b^\theta = 0.5$ advocated by a number of authors would improve the overall turbulence-scheme performance in the convective boundary layer driven by the surface buoyancy flux, but it would violate the isotropic constraint. One more important situation where the linear parameterizations fail is the so-called two-component limit (TCL). This is the limit that turbulence approaches when the velocity component in one direction vanishes. This occurs, for example, near the rigid boundary or in stably stratified layers, where the velocity component (both mean velocity and turbulent fluctuations) normal to the boundary or aligned with the vector of gravity, respectively, is suppressed. In order to satisfy the TCL constraint, C_b^θ should tend to one as the velocity component in one direction tends to zero (see Craft et al., 1996; Mironov, 2001, for details). Clearly, it is impossible to satisfy both the isotropic and the TCL constraints with one and the same value of C_b^θ . This shows a fundamental limitation of the linear parameterizations of the pressure-scrambling terms.

A consistent way out is to leave the coefficients of the linear terms intact, so that the isotropic limit is satisfied, and to include the non-linear terms, e.g. the terms non-linear in a_{ij} (e.g. Ristorcelli et al., 1995; Craft et al., 1996; Mironov, 2001). This would make the resulting turbulence model more flexible (capable of describing various flow regimes) and more suitable for strongly anisotropic flows. Non-linear parameterizations of the pressure-scrambling terms are inevitably complex, however. They are often inconvenient to use and are computationally expensive. It is therefore common in geophysical applications, including NWP, to put up with the shortcomings of linear parameterizations and apply Eqs. (21)–(23) without non-linear extensions. Another practically useful (albeit mathematically inconsistent) approach is to keep the functional form of Eqs. (21)–(23) but to replace some dimensionless constants with dimensionless functions of the flow governing parameters. Those functions should be constructed in such a way as to satisfy a number of limits. An approximation of $C_b^\theta(Ri)$, Ri being the gradient Richardson number, that satisfies that TCL constraint (a large positive Ri) and yields $C_b^\theta = 0.5$ at $Ri \leq 0$ (best-fit value for convective boundary layer) was proposed by Wyngaard (1975).

The TKESV-Bas scheme utilizes Eqs. (21)–(23) with the estimates of dimensionless constants given above. The estimates of the coefficients C_t^u , C_t^θ and C_t^q in the slow (return-to-isotropy) parts of the pressure-scrambling terms may require some fine tuning in order to improve the overall performance of the TKESV scheme. Most other dimensionless coefficients are fixed by mathematical constraints. We utilize their values given above, keeping in mind that these

values are actually suitable for nearly isotropic turbulence and may not be the best estimates for other flow regimes. The only remaining disposable coefficient α_5 should be determined by satisfying an additional constraint deemed important in terms of essential physics and/or practical significance. We determine α_5 so that the resulting equations of the TKESV scheme yield the classical logarithmic velocity profile in the vicinity of the underlying surface. The way this constraint is applied is described in Appendix A. The following expression for α_5 is obtained:

$$\alpha_5 = \frac{1}{22} \left[1 - (1 + 11C_\alpha^*)^{1/2} \right], \quad C_\alpha^* = 1 + \frac{9C_t^u}{4} \left(\frac{4}{3} - C_{s1}^u \right) - \frac{9}{2} \left(\frac{C_t^u}{C_e} \right)^2, \quad (24)$$

where C_e is the dimensionless constant in the expression [third member of Eq. (A.30)] that relates the values of the TKE and of the friction velocity in the near-surface log-layer. Using $C_{s1}^u = 4/5$, $C_t^u = 1.8$ and $C_e = 3.33$, we obtain an estimate of $\alpha_5 = -0.164$. Optionally, the value of $\alpha_5 = -1/10$ can be used [see Eq. (26) and the subsequent text at the end of this section and Appendix B].

Advanced Features

Craft et al. (1996) proposed advanced parameterizations of the pressure-scrambling terms that satisfy both the isotropic limit and the strongly anisotropic two-component limit. Those parameterizations are rather complex and can hardly be used in NWP and related applications, at least in the short-term prospects. However, the TCL parameterizations of the buoyancy contributions $\Pi_{\theta_i}^b$ and $\Pi_{q_i}^b$ to the pressure gradient-scalar covariances can be utilized within the framework of the TKESV scheme without making the scheme unduly complex and computationally expensive. Extending the formulation presented in Craft et al. (1996) to the case of moist air, we obtain

$$\Pi_{\theta_i}^b = -\beta_j \left(\frac{1}{3} \delta_{ij} - a_{ij} \right) \langle \theta'_i \theta'_v \rangle, \quad \Pi_{q_i}^b = -\beta_j \left(\frac{1}{3} \delta_{ij} - a_{ij} \right) \langle q'_i \theta'_v \rangle. \quad (25)$$

In the isotropic limit, $a_{ij} = 0$ and the expressions (25) coincide with the third terms on the r.h.s. of Eqs. (22) and (23), respectively, where $C_b^\theta = C_b^q = 1/3$. In the two-component limit, the buoyancy contributions to the pressure-scrambling terms given by (25) cancel the buoyancy terms in the scalar-flux equations (19) and (20). The use of Eq. (25) helps to avoid spurious generation of scalar fluxes by the buoyancy forces in stably stratified regions of the flow, where the vertical velocity is suppressed and turbulence is driven towards the two-component state.

One point should be stressed in relation to Eq. (25). As discussed in section 7, the covariances $\langle \theta'_i \theta'_v \rangle$ and $\langle q'_i \theta'_v \rangle$ involving virtual potential temperature are parameterized in terms of linear combinations of $\langle \theta_i'^2 \rangle$, $\langle q_i'^2 \rangle$ and $\langle \theta'_i q'_i \rangle$. Since the TKESV scheme carries prognostic transport equations for the variances and covariance of scalar quantities, diagnostic equations (18)–(20) with due regard for the parameterizations (21)–(23), where the third terms on the r.h.s. of Eqs. (22) and (23) are replaced with the TCL formulations (25), remain linear in a_{ij} (and hence in $\langle u'_i u'_j \rangle$), $\langle u'_i \theta'_i \rangle$ and $\langle u'_i q'_i \rangle$. Then, the system of linear equations is readily solved, resulting in explicit diagnostic formulations for the Reynolds-stress and scalar-flux components (see section 9). This is not the case for one-equation TKE schemes, where diagnostic equations for the scalar variances and covariance are used [these are obtained from Eqs. (8)–(10) by neglecting the substantial derivative and the third-order transport terms]. Then, the use of Eq. (25) results in non-linear equations for a_{ij} , $\langle u'_i \theta'_i \rangle$, $\langle u'_i q'_i \rangle$, $\langle \theta_i'^2 \rangle$, $\langle q_i'^2 \rangle$ and $\langle \theta'_i q'_i \rangle$.

As mentioned above, TKESV-Bas utilizes a constant value of dimensionless parameter α_5 .

A more sophisticated approximation was proposed by Shih and Lumley (1985),

$$\alpha_5 = -\frac{1}{10} \left(1 + \frac{4}{5} F_l^{1/2} \right), \quad (26)$$

where $F_l = 1 - \frac{9}{8}(A_2 - A_3)$ is the so-called flatness parameter, and $A_2 = \hat{a}_{ij}\hat{a}_{ij}$ and $A_3 = \hat{a}_{ij}\hat{a}_{jk}\hat{a}_{ki}$ are the second and the third invariants, respectively, of the dimensionless departure-from-isotropy tensor $\hat{a}_{ij} = e^{-1}a_{ij}$. Although the use of Eq. (26) results in non-linear equations for a_{ij} , $\langle u'_i \theta'_l \rangle$ and $\langle u'_i q'_t \rangle$, the non-linearity can be treated in an approximate way, e.g. by evaluating F_l at the previous time step(s) during the integration of turbulence-moment equations in time. It should be mentioned that a constant value of $\alpha_5 = -1/10$ was adopted in a number of studies (e.g. Shih, 1996; Hanjalić, 1999). The value of $\alpha_5 = -1/10$ corresponds to $F_l = 0$, i.e. to the one-component or two-component limit of strongly anisotropic turbulence.

5.2 Third-Order Transport

The second group of terms that require closure assumptions includes turbulent transport (diffusion) terms. These terms enter the equations for the turbulence moments in the divergence form. They describe the transport of the quantity in question by the fluctuating velocity and the fluctuating pressure. Numerous formulations for the third-order turbulent transport have been proposed, ranging from the simplest down-gradient approximations to very complex formulations based on a sophisticated treatment of transport equations for the high-order turbulence moments. Simple isotropic down-gradient formulations have been very popular in various applications.

In the TKESV-Bas scheme, the simplest isotropic down-gradient parameterizations for the third-order transport terms in the TKE, scalar-variance and scalar-covariance equations are used. They read

$$\frac{1}{2} \langle u'_i u'^2_k \rangle + \langle u'_i p' \rangle = -C_e^d \tau_\epsilon e \frac{\partial e}{\partial x_i}, \quad (27)$$

$$\begin{aligned} \langle u'_i \theta'^2_l \rangle &= -C_{\theta\theta}^d \tau_\epsilon e \frac{\partial \langle \theta'^2_l \rangle}{\partial x_i}, & \langle u'_i q'^2_t \rangle &= -C_{qq}^d \tau_\epsilon e \frac{\partial \langle q'^2_t \rangle}{\partial x_i}, \\ \langle u'_i \theta'_l q'_t \rangle &= -C_{\theta q}^d \tau_\epsilon e \frac{\partial \langle \theta'_l q'_t \rangle}{\partial x_i}, \end{aligned} \quad (28)$$

where C_e^d , $C_{\theta\theta}^d$, C_{qq}^d and $C_{\theta q}^d$ are dimensionless coefficients set equal to 0.1. Somewhat higher values of these coefficients may be used as needed. For example, an estimate of $C_{\theta\theta}^d = 0.3$ was advocated by Otić et al. (2005).

Advanced Features

The isotropic down-gradient diffusion formulations often perform poorly in strongly anisotropic flows, e.g. in the flows dominated by the effects of stratification and/or rotation. Generalized down-gradient diffusion approximations (Daly and Harlow, 1970) are somewhat more appropriate for such flows. The formulations for the diffusion terms in the TKE, scalar-variance and scalar-covariance equations read

$$\frac{1}{2} \langle u'_i u'^2_k \rangle + \langle u'_i p' \rangle = -C_e^{dg} \tau_\epsilon \langle u'_i u'_k \rangle \frac{\partial e}{\partial x_k}, \quad (29)$$

$$\begin{aligned}\langle u'_i \theta'^2 \rangle &= -C_{\theta\theta}^{dg} \tau_\epsilon \langle u'_i u'_k \rangle \frac{\partial \langle \theta'^2 \rangle}{\partial x_k}, & \langle u'_i q'^2 \rangle &= -C_{qq}^{dg} \tau_\epsilon \langle u'_i u'_k \rangle \frac{\partial \langle q'^2 \rangle}{\partial x_k}, \\ \langle u'_i \theta'_l q'_l \rangle &= -C_{\theta q}^{dg} \tau_\epsilon \langle u'_i u'_k \rangle \frac{\partial \langle \theta'_l q'_l \rangle}{\partial x_k},\end{aligned}\quad (30)$$

where C_e^{dg} , $C_{\theta\theta}^{dg}$, C_{qq}^{dg} and $C_{\theta q}^{dg}$ are dimensionless coefficients set equal to 0.15. Higher values have also been proposed, e.g. $C_{\theta\theta}^{dg} = 0.22$ (Jones and Musogne, 1988; Hanjalić, 1999; Otić et al., 2005). Equations (29) and (30) reduce to Eqs. (27) and (28), respectively, if the Reynolds-stress anisotropy is neglected, i.e. a_{ij} is set to zero in the expression $\langle u'_i u'_k \rangle = a_{ik} + \frac{2}{3} \delta_{ik} e$.

5.3 Dissipation

Molecular destruction (dissipation) rates of the TKE and of the scalar variances and covariance can be determined from their own transport equations. The dissipation-rate equations are very complex, however. They contain a number of terms whose physical nature is poorly understood. In fact, all terms in the dissipation-rate equations that describe production, destruction and turbulent transport of the dissipation rates should be parameterized, and the validity of those parameterizations is uncertain. It has often been questioned whether prognostic transport equations for the dissipation rates are really necessary, or diagnostic expressions are sufficient, at least for flows in relatively simple geometries. The latter viewpoint is commonly held in geophysical applications.

In the TKESV scheme, the TKE dissipation rate is parameterized in terms of the TKE dissipation time scale τ_ϵ through the following algebraic expression:

$$\epsilon = \frac{e}{\tau_\epsilon}. \quad (31)$$

The dissipation rates of the scalar variances and the scalar covariance are parameterized as

$$\epsilon_{\theta\theta} = \frac{\langle \theta'^2 \rangle}{2\tau_{\theta\theta}}, \quad \epsilon_{qq} = \frac{\langle q'^2 \rangle}{2\tau_{qq}}, \quad \epsilon_{\theta q} = \frac{\langle \theta'_l q'_l \rangle}{2\tau_{\theta q}}, \quad (32)$$

where $\tau_{\theta\theta}$, τ_{qq} and $\tau_{\theta q}$ are the dissipation times scales of the scalar variances and the scalar covariance. These time scales are taken to be proportional to the TKE dissipation time scale (see the next section).

The deviatoric part ϵ_{ij}^d of the Reynolds-stress dissipation tensor is either neglected (on the assumption of local isotropy at small scales) or incorporated into a parameterization of the slow part Π_{ij}^t of the pressure redistribution term. Likewise, the temperature-flux and the humidity-flux dissipation rates, $\epsilon_{\theta i}$ and ϵ_{qi} , are incorporated into parameterizations of $\Pi_{\theta i}^t$ and Π_{qi}^t , respectively.

6 Time and Length Scales

The return-to-isotropy time scales in Eqs. (21)–(23) are taken to be proportional to the TKE dissipation time scale:

$$\tau_{ru} = \tau_{r\theta} = \tau_{rq} = \tau_\epsilon, \quad (33)$$

where proportionality constants between the various time scales are set to one as they always occur in combination with the other constants. Likewise, the dissipation time scales of the

scalar variances and the scalar covariance, Eq. (32), are taken to be proportional to the TKE dissipation time scale:

$$\tau_{\theta\theta} = \tau_{qq} = \tau_{\theta q} = R_\tau \tau_\epsilon, \quad (34)$$

where R_τ is the ratio of the scalar-variance/scalar-covariance dissipation time scale to the TKE dissipation time scale [e.g. $R_\tau = \tau_{\theta\theta}/\tau_\epsilon = \langle \theta'^2 \rangle \epsilon / (2e\epsilon_{\theta\theta})$ for the temperature variance]. The same value of R_τ is used for $\tau_{\theta\theta}$, τ_{qq} and $\tau_{\theta q}$. The estimates of R_τ given in the literature range from 0.3 to 1.0 (e.g. Dol et al., 1997). Following Kenjereš and Hanjalić (1995, 2000) and Hanjalić (2002), the value of $R_\tau = 0.5$ is utilized.

The TKE dissipation time scale is expressed in terms of the turbulence length scale l :

$$\tau_\epsilon = \frac{1}{C_\epsilon} \frac{l}{e^{1/2}}, \quad (35)$$

where $C_\epsilon = C_e^{-3/2}$, and C_e is a constant in the expression that relates the TKE and the friction velocity in the neutrally-stratified near-surface layer characterized by the logarithmic mean-velocity profile [see Eq. (A.30) in Appendix A]. We utilize an estimate of $C_e = 3.33$ (Umlauf and Burchard, 2003; Umlauf et al., 2003). The following interpolation formula is used in the TKESV-Bas scheme to compute the turbulence length scale:

$$\frac{1}{l} = \frac{1}{\kappa x_n} + \frac{1}{l_\infty} + H(N^2) \frac{N}{C_{lb} e^{1/2}}, \quad (36)$$

where κ is the von Kármán constant, x_n is the distance normal to the surface, l_∞ is the length scale characteristic of the flow far away from the underlying surface, N is the buoyancy frequency, $H(\zeta)$ is the Heaviside step function (equal to 1 if $\zeta \geq 0$, and to 0 if $\zeta < 0$), and C_{lb} is a dimensionless constant. If the last term on the r.h.s. is neglected, Eq. (36) reduces to the well-known Blackadar's formula (Blackadar, 1962) that yields the logarithmic velocity profile close to the underlying surface and prevents l from growing without bound far away from the surface. A conventional value of $\kappa = 0.4$ is utilized, and the l_∞ is set to a constant value of 200 m. The last term on the r.h.s. of Eq. (36) limits the length scale in stably stratified layers (where N^2 is positive) by the buoyancy length scale $l_b = C_{lb} N^{-1} e^{1/2}$ (e.g. Stull, 1973; Zeman and Tennekes, 1977; Brost and Wyngaard, 1978; Zilitinkevich and Mironov, 1992). An estimate of $C_{lb} = 1.0$ is used. The buoyancy frequency N is computed with due regard for the effect of cloud condensate on the static stability (see section 9).

Advanced Features

As an alternative to setting the time-scale ratio in Eq. (34) to a constant value, R_τ can be computed as a function of the scalar-flux correlation coefficient. The following expression was proposed by Craft et al. (1996):

$$R_\tau = \frac{2}{3(1 + A_{u\theta})}, \quad A_{u\theta} = \frac{\langle u'_i \theta' \rangle \langle u'_i \theta' \rangle}{e \langle \theta'^2 \rangle}, \quad (37)$$

where $A_{u\theta}$ is the heat-flux correlation coefficient. In the case of moist air, the time-scale ratio for the temperature variance, $R_\tau^{\theta\theta}$, and for the humidity variance, R_τ^{qq} , can be computed from Eq. (37) where θ is replaced with θ_l and q_t , respectively. The time scale ratio for the temperature-humidity covariance is then computed as $R_\tau^{\theta q} = \frac{1}{2} (R_\tau^{\theta\theta} + R_\tau^{qq})$.

Following Bougeault and André (1986), Bougeault and Lacarrère (1989), Bechtold et al. (1992), Lappen and Randall (2001) and Golaz et al. (2002), an advanced non-local formulation for the turbulence length scale can be used instead of Eq. (36). The turbulence length scale is computed from the following relations:

$$e(x_i) = \int_{x_i}^{x_i + l_{up}} \beta_i [\theta_v^{par}(x_i, x'_i) - \theta_v^{env}(x'_i)] dx'_i, \quad (38)$$

$$e(x_i) = \int_{x_i - l_{do}}^{x_i} \beta_i [\theta_v^{env}(x'_i) - \theta_v^{par}(x_i, x'_i)] dx'_i, \quad (39)$$

$$\frac{1}{l} = \frac{1}{\kappa x_n} + \left(\frac{2}{l_{up} l_{do}} \right)^{1/2}. \quad (40)$$

The physical meaning of Eqs. (38)–(40) can be elucidated as follows. Consider a flat horizontal surface. The x_3 -axis is aligned with the vector of gravity $(0, 0, -g_3)$ and is positive upward. The quantity l_{up} (l_{do}) is an estimate of the distance that an air parcel originating at the level x_3 travels upward (downward) until its energy $e(x_3)$ is spent working against gravity (l_{do} is limited by the distance to the surface). The virtual potential temperature $\theta_v^{par}(x_3, x'_3)$ of an ascending/descending air parcel is computed with due regard for the condensation/evaporation. As an air parcel is displaced from the level x_3 to the level x'_3 , the liquid water potential temperature $\theta_l^{par}(x'_3)$ and the total water specific humidity $q_t^{par}(x'_3)$ of the parcel are conserved, i.e. they remain equal to the values $\theta_l^{par}(x_3)$ and $q_t^{par}(x_3)$, respectively. However, the potential temperature θ^{par} , the specific humidity q^{par} and the liquid water specific humidity q_l^{par} , and hence the virtual potential temperature θ_v^{par} , are not conserved (because of phase changes) and are therefore re-computed at each level x'_3 during the parcel ascend/descent. Note that the quantity $2^{-1/2} (l_{up} l_{do})^{1/2}$, where l_{up} and l_{do} are computed from Eqs.(38) and (39), respectively, yields the buoyancy length scale $l_b = C_{lb} N^{-1} e^{1/2}$ with $C_{lb} = 1.0$ in stably stratified fluid characterized by a constant buoyancy frequency N . The first term on the r.h.s. of the interpolation formula (40) is required to recover the logarithmic velocity profile close to the underlying surface.

7 Effect of Clouds on Mixing

The thermodynamic structure of the atmosphere is heavily complicated by the presence of clouds. Clouds produce precipitation and interact with atmospheric radiation, strongly affecting the atmosphere energy budget. They also change the buoyancy of air parcels. As far as the parameterization of turbulence is concerned, the primary goal is to account for the effect of latent heat release/consumption on the buoyancy production/destruction of the Reynolds stress (including its trace, the TKE) and of the scalar fluxes. To this end, the buoyancy terms (the terms with β_i in Eqs. (12), (18), (19) and (20) should be parameterized with due regard for the presence of cloud condensate. The problem essentially amounts to modelling the virtual potential temperature flux $\langle u'_i \theta'_v \rangle$ and the scalar-virtual potential temperature covariances $\langle \theta'_l \theta'_v \rangle$ and $\langle q'_t \theta'_v \rangle$ in terms of other moments that include fluctuations of u_i , θ_l and q_t .

Using the definition of the virtual potential temperature (11), the covariances incorporating θ'_v are represented as

$$\begin{aligned} \langle f' \theta'_v \rangle &= [1 + (R - 1) \langle q_t \rangle - R \langle q_l \rangle] \langle f' \theta'_l \rangle + (R - 1) \langle \theta \rangle \langle f' q'_l \rangle \\ &+ \left\{ \frac{\langle \theta \rangle}{\langle T \rangle} \frac{L_v}{c_p} [1 + (R - 1) \langle q_t \rangle - R \langle q_l \rangle] - R \langle \theta \rangle \right\} \langle f' q'_l \rangle, \end{aligned} \quad (41)$$

where $R = R_v/R_d$, and a generic variable f stands for u_i , θ_l or q_t . In order to obtain Eq. (41), the third-order covariances and the pressure fluctuations are neglected. The latter assumption yields $\theta_l = \theta - \frac{\langle \theta \rangle}{\langle T \rangle} \frac{L_v}{c_p} q_l$. In the “dry” limit, where a given atmospheric-model

grid box is cloud free (but the water vapour may be present), Eq. (41) reduces to

$$\langle f'\theta'_v \rangle_d = [1 + (R - 1) \langle q_t \rangle] \langle f'\theta'_l \rangle + (R - 1) \langle \theta \rangle \langle f'q'_t \rangle, \quad (42)$$

where θ_l and q_t coincide with θ and q , respectively, as $q_l = 0$. In the “wet” limit, the entire atmospheric-model grid box is saturated, i.e. $q_l = q_t - q_s > 0$ at each point of the grid box. Then, $\langle f'\theta'_v \rangle$ can be expressed, to a good approximation, in terms of $\langle f'\theta'_l \rangle$ and $\langle f'q'_t \rangle$ as follows:

$$\begin{aligned} \langle f'\theta'_v \rangle_w &= [1 + (R - 1) \langle q_t \rangle - R \langle q_l \rangle] \langle f'\theta'_l \rangle + (R - 1) \langle \theta \rangle \langle f'q'_t \rangle \\ &+ \left[-\frac{\mathcal{A}\mathcal{P}}{\mathcal{Q}} \langle f'\theta'_l \rangle + \frac{\mathcal{A}}{\mathcal{Q}} \langle f'q'_t \rangle \right]. \end{aligned} \quad (43)$$

Here, $\mathcal{A} = \frac{\langle \theta \rangle L_v}{\langle T \rangle c_p} [1 + (R - 1) \langle q_t \rangle - R \langle q_l \rangle] - R \langle \theta \rangle$, $\mathcal{P} = \frac{\langle T \rangle}{\langle \theta \rangle} \langle q_{sl,T} \rangle$, $\mathcal{Q} = 1 + \frac{L_v}{c_p} \langle q_{sl,T} \rangle$, and $\langle q_{sl,T} \rangle \equiv \frac{\partial q_s}{\partial T} \Big|_{T=\langle T_l \rangle}$, T_l being the liquid water absolute temperature, is computed from the

Clausius-Clapeyron equation, $\frac{\partial q_s}{\partial T} = \frac{L_v q_s}{R_v T^2}$. A first-order Taylor expansion of the saturation specific humidity $q_s(T)$ about $T = \langle T_l \rangle$ is used to express $\langle f'q'_t \rangle$ in terms of $\langle f'\theta'_l \rangle$ and $\langle f'q'_t \rangle$ [the last terms in brackets on the r.h.s. of Eq. (43)]. An expression is needed that is valid not only in the dry and wet limits, but also in the general case of fractional cloudiness. To this end, the following interpolation formula is used:

$$\begin{aligned} \langle f'\theta'_v \rangle &= [1 + (R - 1) \langle q_t \rangle - R \langle q_l \rangle] \langle f'\theta'_l \rangle + (R - 1) \langle \theta \rangle \langle f'q'_t \rangle \\ &+ \hat{\mathcal{R}} \left[-\frac{\mathcal{A}\mathcal{P}}{\mathcal{Q}} \langle f'\theta'_l \rangle + \frac{\mathcal{A}}{\mathcal{Q}} \langle f'q'_t \rangle \right]. \end{aligned} \quad (44)$$

where $\hat{\mathcal{R}}$ is the interpolation variable satisfying $0 \leq \hat{\mathcal{R}} \leq 1$. Equation (44) reduces to Eq. (42) and to Eq. (43) in the dry ($\hat{\mathcal{R}} = 0$) and wet ($\hat{\mathcal{R}} = 1$) limits, respectively.

The simplest way to determine $\hat{\mathcal{R}}$ is to set it equal to the fractional cloud cover $\hat{\mathcal{C}}$. This parameterization is used within the framework of one-equation TKE turbulence scheme of COSMO and ICON (see Raschendorfer, 1999, 2001; Baldauf et al., 2011). In order to compute the fractional cloud cover, a Gaussian statistical cloud scheme is used that is very similar to the scheme proposed by Sommeria and Deardorff (1977) (see also Mellor, 1977). Recall that statistical cloud schemes make use of probability distribution functions of the sub-grid scale (SGS) humidity and temperature (and possibly velocity) fluctuations. Once the PDF is specified, the fractional cloud cover is simply the integral over a saturated part of the PDF. The COSMO/ICON statistical cloud scheme is formulated in terms of s variable (Mellor, 1977) defined as $s = \mathcal{Q}^{-1} (\langle q_t \rangle - \langle q_{sl} \rangle + q'_t - \mathcal{P}\theta'_l)$, where $\langle q_{sl} \rangle = q_s(\langle T_l \rangle)$. The variable s accounts for the combined effect of humidity and temperature fluctuations (the latter ones change the local saturation vapour pressure). It is a measure of local oversaturation/undersaturation. A positive s is nothing but a local value of the liquid water specific humidity q_l computed with respect to the linearized saturation specific humidity curve³. Assuming that no super-saturation occurs, the fractional cloud cover is given by $\hat{\mathcal{C}} = \int_0^\infty G(s) ds$, where $G(s)$ is the PDF of s . The grid-box mean liquid water specific humidity is given by $\langle q_l \rangle = \int_0^\infty sG(s) ds$. Partial or full PDF moments of higher order can be computed in a similar manner. Following

³In fact, the quantity s has already been used above to express $\langle f'q'_t \rangle$ through $\langle f'q'_t \rangle$ and $\langle f'\theta'_l \rangle$ in Eq. (41), leading to Eq. (43)

Sommeria and Deardorff (1977) and Mellor (1977), a Gaussian PDF is utilized within the framework of the COSMO/ICON TKE turbulence scheme. The following relations hold:

$$\hat{C} = \frac{1}{2} \left[1 + \operatorname{erf} \left(\frac{\langle s \rangle}{\sqrt{2}\sigma_s} \right) \right], \quad \langle q_l \rangle = \hat{C} \langle s \rangle + \frac{\sigma_s}{\sqrt{2\pi}} \exp \left(-\frac{\langle s \rangle^2}{2\sigma_s^2} \right), \quad (45)$$

where erf is the error function, $\langle s \rangle = \mathcal{Q}^{-1}(\langle q_l \rangle - \langle q_{sl} \rangle)$ is the mean value of s , and $\sigma_s \equiv \langle s'^2 \rangle^{1/2} = \mathcal{Q}^{-1}(\langle q_t'^2 \rangle + \mathcal{P}^2 \langle \theta_t'^2 \rangle - 2\mathcal{P} \langle q_t' \theta_t' \rangle)^{1/2}$ is its standard deviation. Note that σ_s depends on the variances of q_t and θ_t and on their covariance, providing an important link between the cloud cover and the dynamics of SGS motions. Within the framework of the one-equation TKE turbulence scheme, $\langle q_t'^2 \rangle$, $\langle \theta_t'^2 \rangle$ and $\langle q_t' \theta_t' \rangle$, and hence σ_s , are computed diagnostically through the down-gradient algebraic formulations. This is different from the TKESV scheme that carries prognostic equations for the scalar variances and covariance with due regard for the third-order transport. It is also worth noting that approximations of Eqs. (45) through piecewise polynomial (linear and quadratic) functions are used in COSMO/ICON to compute \hat{C} and $\langle q_l \rangle$ [see Eqs. (22) and (25) in Sommeria and Deardorff (1977) and Eqs. (47) below].

The use of $\hat{\mathcal{R}} = \hat{C}$ in Eq. (44) along with the Gaussian formulations for \hat{C} and $\langle q_l \rangle$ may result in large errors in the determination of the buoyancy terms in the Reynolds-stress and scalar-flux equations. A prominent example is the convective boundary layer with shallow cumuli, where the PDFs of cloud-related variables are highly skewed. In the shallow cumulus regime, the atmospheric-model grid box is undersaturated in the mean and the fractional cloud cover is typically small (certainly, this holds if the horizontal model resolution is not too high and shallow cumulus clouds remain unresolved). However, these highly localized cumulus clouds account for much of the buoyancy terms in the Reynolds-stress, scalar-flux and TKE equations, and $\langle f' \theta_v' \rangle$ is closer to $\langle f' \theta_v' \rangle_w$ than to $\langle f' \theta_v' \rangle_d$. Then, $\hat{\mathcal{R}}$ in Eq. (44) is (considerably) larger than \hat{C} (see e.g. Lewellen and Lewellen, 2004).

In order to account for the skewed nature of convective motions associated with shallow cumuli, the following parameterization that interpolates between the Gaussian and the exponential formulations (Bougeault, 1981; Bechtold et al., 1995) is used within the framework of the TKESV-Bas scheme:

$$f = \begin{cases} f_{Gauss} & \text{at } \tilde{s} \geq 0 \\ 0.5 [(2 + \tilde{s}) f_{Gauss} - \tilde{s} f_{exp}] & \text{at } -2 \leq \tilde{s} \leq 0 \\ f_{exp} & \text{at } \tilde{s} \leq -2, \end{cases} \quad (46)$$

where $\tilde{s} = \langle s \rangle / \sigma_s$, and f stands either for the fractional cloud cover \hat{C} or for the grid-box mean liquid water specific humidity $\langle q_l \rangle$. The Gaussian formulations are given by

$$\begin{aligned} \hat{C}_{Gauss} &= \begin{cases} 1 & \text{at } \tilde{s} \geq 1.6 \\ 0.5 (1 + \tilde{s}/1.6) & \text{at } -1.6 \leq \tilde{s} \leq 1.6 \\ 0 & \text{at } \tilde{s} \leq -1.6, \end{cases} \\ \frac{\langle q_l \rangle_{Gauss}}{\sigma_s} &= \begin{cases} \tilde{s} & \text{at } \tilde{s} \geq 1.6 \\ (\tilde{s} + 1.6)^2 / 6.4 & \text{at } -1.6 \leq \tilde{s} \leq 1.6 \\ 0 & \text{at } \tilde{s} \leq -1.6. \end{cases} \end{aligned} \quad (47)$$

Equations (47) are the piecewise polynomial approximations of Eqs. (45). The exponential formulations are given by

$$\hat{C}_{exp} = \exp(\tilde{s} - 1), \quad \langle q_l \rangle_{exp} = \sigma_s \exp(\tilde{s} - 1). \quad (48)$$

At large negative \tilde{s} , the Gaussian relations (45) give a very small fractional cloud cover, and the approximations (47) give no clouds at all. A relatively thick exponential tail (as

compared to a Gaussian tail) is introduced to account, in an approximate way, for non-zero fractional cloud cover in the shallow cumulus regime. The buoyancy terms in the Reynolds-stress and scalar-flux equations are computed from Eq. (44), where the interpolation variable $\hat{\mathcal{R}}$ is given by

$$\frac{\hat{\mathcal{R}}}{\hat{\mathcal{C}}} = \begin{cases} 1 & \text{at } \tilde{s} \geq 0 \\ 1 - 1.5\tilde{s} & \text{at } -2 \leq \tilde{s} \leq 0 \\ 2 - \tilde{s} & \text{at } \tilde{s} \leq -2. \end{cases} \quad (49)$$

Note that Eq. (49) may underestimate $\hat{\mathcal{R}}$ (perhaps quite considerably) at large negative \tilde{s} . Thus the above formulations with the exponential tail can only be considered as the first-order corrections to the Gaussian formulations. Note further that $\hat{\mathcal{C}}$, $\langle q_l \rangle$, and $\hat{\mathcal{R}}$ given by Eqs. (46)–(49) depend on the mean and the variance of s but do not explicitly depend on higher-order moments such as skewness. That is, the skewed nature of shallow cumulus clouds is accounted for implicitly in a rather ad hoc manner.

It should be recognized that the use of the interpolation formula (44) to determine the buoyancy terms in the Reynolds-stress and the scalar-flux equations can be avoided. If a cloud scheme employs a joint PDF for the scalars q_l and θ_l and for the vertical velocity u_3 , all quantities $\langle f'q_l' \rangle$ including the liquid water specific humidity are determined in a straightforward way by means of integration over the saturated part of the PDF. In other words, the problem reduces to the determination of a number of partial moments using an assumed PDF. This approach is taken within the framework of CLUBB (Cloud Layers Unified By Binormals), an assumed-PDF unified parameterization of turbulence and cloud processes in the Earth's atmosphere (see references at <https://people.uwm.edu/vlarson/papers/>). Apart from its numerous advantages, the approach has shortcomings. For example, the cloud schemes based on a joint PDF require a large number of statistical moments of fluctuating scalar and velocity fields as an input. Furthermore, the joint-PDF schemes may place rather stringent requirements upon the input quality, i.e. a large number of irreducible moments of second, third and possibly higher order should be determined accurately. Comprehensive discussions of various issues related to the parameterization of clouds and cloud-turbulence interaction in atmospheric models are given in Tompkins (2003, 2005) and Machulskaya (2015). A cloud parameterization based on a joint scalar-velocity PDF may be incorporated into the TKESV scheme in the future. The TKESV-Bas scheme employs an interpolation formula (44) with $\hat{\mathcal{C}}$, $\langle q_l \rangle$, and $\hat{\mathcal{R}}$ determined through the approximations (46)–(49).

Advanced Features

Following Larson et al. (2001), Naumann et al. (2013) developed a statistical cloud scheme based on a double-Gaussian PDF of s ,

$$\begin{aligned} G(s) &= aG_1(s) + (1-a)G_2(s) \\ &= \frac{a}{\sqrt{2\pi}\sigma_{s1}} \exp\left[-\frac{1}{2}\left(\frac{s-s_1}{\sigma_{s1}}\right)^2\right] + \frac{1-a}{\sqrt{2\pi}\sigma_{s2}} \exp\left[-\frac{1}{2}\left(\frac{s-s_2}{\sigma_{s2}}\right)^2\right]. \end{aligned} \quad (50)$$

Here, a and $1-a$ are the relative weights of the two Gaussian curves G_1 and G_2 , respectively, and s_1 and s_2 and σ_{s1} and σ_{s2} are, respectively, their means and standard deviations. The PDF given by Eq. (50) is a five-parameter PDF. That is, five irreducible moments of s , e.g. five first moments, should be provided as input arguments to specify a , s_1 , s_2 , σ_{s1} and σ_{s2} . In order to reduce the number of input arguments, Naumann et al. (2013) used observational and numerical LES data to express σ_{s1} and σ_{s2} through the standard deviation σ_s and the skewness $S_s \equiv \langle s'^3 \rangle / \langle s'^2 \rangle^{3/2}$ of s . The following relations are proposed by Naumann et al.

(2013) (cf. Larson et al., 2001):

$$\begin{aligned} \frac{\sigma_{s1}}{\sigma_s} &= \begin{cases} 1 + \gamma_3 \frac{S_s}{(\alpha + S_s^2)^{1/2}} & \text{at } S_s \leq 0 \\ 1 + \gamma_1 \frac{S_s}{\alpha^{1/2}} & \text{at } S_s \geq 0, \end{cases} \\ \frac{\sigma_{s2}}{\sigma_s} &= \begin{cases} 1 - \gamma_4 \frac{S_s}{(\alpha + S_s^2)^{1/2}} & \text{at } S_s \leq 0 \\ 1 - \gamma_2 \frac{S_s}{(\alpha + S_s^2)^{1/2}} & \text{at } S_s \geq 0, \end{cases} \end{aligned} \quad (51)$$

where $\alpha = 2.0$, $\gamma_1 = 0.73$, $\gamma_2 = 0.46$, $\gamma_3 = 0.78$ and $\gamma_4 = 0.73$ are dimensionless constants (the notation used in Naumann et al., 2013, is retained).

With due regard for (51), only three irreducible moments of s should be provided, viz., $\langle s \rangle$, σ_s and S_s . The mean value of s is provided by the host atmospheric model. The variances and the covariance of the scalar quantities required to compute σ_s are determined within the framework of the TKESV scheme from the scalar (co)variance transport equations. The skewness of s is required to close the problem. The way to determine S_s is discussed in section 11. A cloud scheme based on Eqs. (50) and (51) represents a good compromise between physical realism and computational economy and is a viable choice for the extended version of the TKESV scheme. On the one hand, a double-Gaussian distribution (50) is very flexible and is capable of describing both symmetric and skewed PDFs, the latter one is required to describe the cumulus regime. On the other hand, the use of Eqs. (51) reduces the number of PDF input arguments to three (mean, variance, and skewness), making the cloud scheme reasonably inexpensive from the computational viewpoint.

Given the estimates of $\langle s \rangle$, σ_s and S_s , the weighting factor a is determined as a solution to the following equation:

$$\begin{aligned} & S_s - \left\{ a(1-a) \left[1 - a \left(\frac{\sigma_{s1}}{\sigma_s} \right)^2 - (1-a) \left(\frac{\sigma_{s2}}{\sigma_s} \right)^2 \right] \right\}^{1/2} \\ & \times \left\{ 3 \left(\frac{\sigma_{s1}}{\sigma_s} \right)^2 - 3 \left(\frac{\sigma_{s2}}{\sigma_s} \right)^2 + \frac{1-2a}{a(1-a)} \left[1 - a \left(\frac{\sigma_{s1}}{\sigma_s} \right)^2 - (1-a) \left(\frac{\sigma_{s2}}{\sigma_s} \right)^2 \right] \right\} = 0, \end{aligned} \quad (52)$$

where σ_{s1}/σ_s and σ_{s2}/σ_s are given by Eqs. (51). The mean values s_1 and s_2 are computed from

$$\begin{aligned} \frac{s_1 - \langle s \rangle}{\sigma_s} &= \left(\frac{1-a}{a} \right)^{1/2} \left[1 - a \left(\frac{\sigma_{s1}}{\sigma_s} \right)^2 - (1-a) \left(\frac{\sigma_{s2}}{\sigma_s} \right)^2 \right]^{1/2}, \\ \frac{s_2 - \langle s \rangle}{\sigma_s} &= \left(\frac{a}{1-a} \right)^{1/2} \left[1 - a \left(\frac{\sigma_{s1}}{\sigma_s} \right)^2 - (1-a) \left(\frac{\sigma_{s2}}{\sigma_s} \right)^2 \right]^{1/2}. \end{aligned} \quad (53)$$

Then, the fractional cloud cover and the grid-box mean liquid water specific humidity are computed from the following relations:

$$\begin{aligned} \hat{C} &= \frac{a}{2} \left[1 + \operatorname{erf} \left(\frac{s_1}{\sqrt{2}\sigma_{s1}} \right) \right] + \frac{1-a}{2} \left[1 + \operatorname{erf} \left(\frac{s_2}{\sqrt{2}\sigma_{s2}} \right) \right], \\ \langle q_l \rangle &= s_1 \frac{a}{2} \left[1 + \operatorname{erf} \left(\frac{s_1}{\sqrt{2}\sigma_{s1}} \right) \right] + s_2 \frac{1-a}{2} \left[1 + \operatorname{erf} \left(\frac{s_2}{\sqrt{2}\sigma_{s2}} \right) \right] \\ &+ \sigma_{s1} \frac{a}{\sqrt{2\pi}} \exp \left(-\frac{s_1^2}{2\sigma_{s1}^2} \right) + \sigma_{s2} \frac{1-a}{\sqrt{2\pi}} \exp \left(-\frac{s_2^2}{2\sigma_{s2}^2} \right). \end{aligned} \quad (54)$$

The buoyancy terms in the Reynolds-stress and scalar-flux equations are computed from Eq. (44), where the interpolation variable $\hat{\mathcal{R}}$ is given by

$$\frac{\hat{\mathcal{R}}}{\hat{\mathcal{C}}} = \begin{cases} 1 & \text{at } \tilde{s} \geq 0 \\ 1 + 1.5\tilde{s}^2 \exp(0.25S_s) & \text{at } \tilde{s} \leq 0. \end{cases} \quad (55)$$

It is significant that $\hat{\mathcal{R}}$ depends on the skewness of s in an explicit manner. This is different from Eq. (49), where $\hat{\mathcal{R}}$ explicitly depends on $\langle s \rangle$ and σ_s (via $\tilde{s} = \langle s \rangle / \sigma_s$) but there is no explicit dependence on S_s .

In order to obtain the weighting factor a , Eq. (52) with due regard for Eqs. (51) should be solved numerically at each atmospheric-model time step. Since the left-hand side (l.h.s.) of Eq. (52) is the seventh-order polynomial in a , in general no analytical solution $a(S_s)$ exists. In order to save computational resources, an approximate solution is used that interpolates between analytical asymptotic solutions valid at $S_s \rightarrow \pm\infty$ and $S_s \rightarrow \pm 0$. The asymptotic solutions are

$$\begin{aligned} a_{-\infty} &= 1 - \frac{C_{-\infty}}{S_s^2} & \text{at } S_s \rightarrow -\infty \\ a_{-0} &= 1 + C_{-0}S_s & \text{at } S_s \rightarrow -0 \\ a_{+0} &= C_{+0}S_s & \text{at } S_s \rightarrow +0 \\ a_{+\infty} &= \frac{C_{+\infty}}{S_s^2} & \text{at } S_s \rightarrow +\infty, \end{aligned} \quad (56)$$

where $C_{-\infty} = \gamma_3^3(2 - \gamma_3)^3 \approx 0.862$, $C_{-0} = 8\alpha^{-3/2}\gamma_3^3 \approx 1.342$, $C_{+0} = 8\alpha^{-3/2}\gamma_2^3 \approx 0.275$, and $C_{+\infty} \approx 0.570$ are dimensionless constants. The value of $C_{+\infty}$ is a root of the cubic equation $\frac{4\gamma_1^6}{\alpha^3}C_{+\infty}^3 + \left[1 - \frac{3\gamma_1^2}{\alpha}\gamma_2^2(2 - \gamma_2)^2\right]C_{+\infty} - \gamma_2^3(2 - \gamma_2)^3 = 0$. Using (56), the weighting factor is computed from the following interpolation formulae:

$$\begin{aligned} \frac{1}{(1-a)^n} &= \frac{1}{(1-a_{-0})^n} + \frac{1}{(1-a_{-\infty})^n} & \text{at } S_s < 0 \\ a &= \frac{1}{2} & \text{at } S_s = 0 \\ \frac{1}{a^m} &= \frac{1}{a_{+0}^m} + \frac{1}{a_{+\infty}^m} & \text{at } S_s > 0, \end{aligned} \quad (57)$$

where the exponents n and m are tuning parameters estimated at 0.52 and 0.75, respectively.

As seen from Fig. 1, Eqs. (56) and (57) approximate the exact solution of Eqs. (51) and (52) very accurately at $S_s > 0$. A positive (and possibly large) skewness of s is characteristic of shallow cumulus regime that presents major difficulties in terms of modelling the effect of clouds on turbulent mixing. The agreement between the approximation and the exact solution is less favourable in the range of S_s from ca. -1 to ca. -4 . This is not crucial, however. A negative S_s is characteristic of the stratus or stratocumulus clouds, but large negative values of S_s are rarely encountered. In the stratus (stratocumulus) regime, the atmospheric-model grid box is oversaturated in the mean ($\langle s \rangle > 0$), the fractional cloud cover is typically large, and the effect of clouds on mixing can be accounted for with the aid of relatively simple parameterization schemes. For example, assuming $\hat{\mathcal{R}} = \hat{\mathcal{C}}$, as in Eq. (55), does not lead to large uncertainties in the determination of the buoyancy terms in the Reynolds-stress and scalar-flux equations. Note that the error in a caused by the use of Eqs. (56) and (57) instead of the exact solution to Eqs. (51) and (52) does not exceed a few percent. This error is tolerable in the stratus regime.

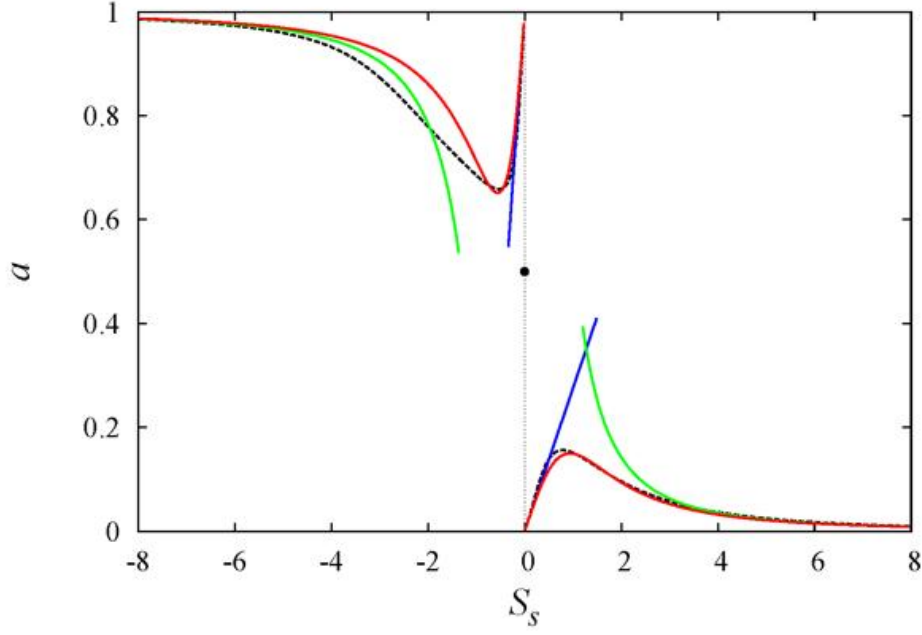


Figure 1: The weighting factor a as function of skewness S_s . Black dashed curves and black dot show numerical solution of Eqs. (51) and (52). Solid curves show the interpolation formulation given by Eqs. (56) and (57) – red, and the asymptotes a_{-0} and a_{+0} – blue, and $a_{-\infty}$ and $a_{+\infty}$ – green.

In order to account for the presence of cloud ice, a generalized total water specific humidity q_t and the ice-liquid (total) water potential temperature θ_t defined through Eqs. (3) and (4), respectively, should be utilized. The use of the $q_t - \theta_t$ system raises various tricky issues. A comprehensive discussion of those issues is beyond the scope of the present report. Here, a way to account for the cloud ice in a very approximate manner is briefly outlined.

Local saturation adjustment is performed in terms of the total cloud condensate $q_c = q_l + q_i$ computed as $q_c = q_t - q_s$ if $q_t > q_s$, and $q_c = 0$ if $q_t \leq q_s$. The saturation specific humidity is specified with respect to the water-ice mixed phase. The following parameterization of the mixed-phase q_s is used:

$$q_{sc} = (1 - F_i) q_{sl} + F_i q_{si}, \quad (58)$$

where $F_i = q_i / (q_l + q_i)$ is the cloud-ice fraction of the total cloud condensate, and q_{sl} and q_{si} are the saturation specific humidity for the vapour-liquid equilibrium and for the vapour-ice equilibrium, respectively. If cloud ice and cloud water are allowed to co-exist over a certain temperature range, a simple (e.g. polynomial) function of temperature can be used to determine F_i . A more attractive alternative is to employ a rate equation for F_i (see e.g. Deardorff, 1976):

$$\frac{dF_i}{dt} = -H(T_{li} - T) \frac{(F_i - 1)}{\tau_{li}} - H(T - T_{il}) \frac{F_i}{\tau_{il}}, \quad (59)$$

where H is the Heaviside step function, τ_{li} and τ_{il} are the e-folding time scales of the liquid water to ice and ice to liquid water conversion, respectively, T_{li} is a threshold temperature, below which the conversion of liquid water to ice is assumed to occur, and T_{il} a threshold temperature, above which the cloud ice melting takes place (T_{il} may be set equal to the

fresh-water freezing point). In the quantities \mathcal{A} , \mathcal{P} and \mathcal{Q} that enter Eqs. (43) and (44), $\langle q_l \rangle$ should be replaced with $\langle q_c \rangle = \langle q_l \rangle + \langle q_i \rangle$, q_{sl} should be replaced with q_{sc} , and L_v should be replaced with the effective heat of vapourization-sublimation L_c . The latter quantity may be approximated through an interpolation formula similar to Eq. (58), that is $L_c = (1 - F_i) L_v + F_i L_i$.

A method to account for the effect of cloud ice described above is rather crude and can only be considered as a zero-order approximation. It should still be advantageous within a parameterization scheme of shallow clouds.

8 Boundary-Layer Approximation

A simplification typically made in geophysical applications, including NWP, is the so-called boundary-layer approximation. This approximation is fairly accurate for large-scale and meso-scale atmospheric models whose grid-box aspect ratio (the ratio of the horizontal grid size to the vertical grid size) is large. Within the framework of the boundary-layer approximation, all derivatives in the x_1 and x_2 horizontal directions in the second-moment equations are neglected and the grid-box mean vertical velocity $\langle u_3 \rangle$ is zero in the second-moment equations (but not in the equations for the mean fields). The equations become one-dimensional, i.e. the flow variables depend on the x_3 vertical coordinate only.

Equations (60)–(67) presented below are obtained using the baseline parameterizations of the third-order transport, dissipation and pressure-scrambling terms in the second-moment equations. The incorporation of more advanced formulations, given in the preceding sections under the heading **Advanced Features**, is fairly straightforward.

With due regard for the (baseline) parameterizations of the third-order transport and the dissipation terms given in sections 5.2, 5.3 and 6, the equations for the TKE and for the scalar variances and covariance in the boundary-layer approximation are

$$\begin{aligned} \frac{\partial e}{\partial t} = & - \left(\langle u'_1 u'_3 \rangle \frac{\partial \langle u_1 \rangle}{\partial x_3} + \langle u'_2 u'_3 \rangle \frac{\partial \langle u_2 \rangle}{\partial x_3} \right) - \beta_3 \langle u'_3 \theta'_v \rangle \\ & + \frac{\partial}{\partial x_3} \left(C_e^d \tau_\epsilon e \frac{\partial e}{\partial x_3} \right) - \frac{e}{\tau_\epsilon}, \end{aligned} \quad (60)$$

$$\frac{1}{2} \frac{\partial \langle \theta_l'^2 \rangle}{\partial t} = - \langle u'_3 \theta_l' \rangle \frac{\partial \langle \theta_l \rangle}{\partial x_3} + \frac{1}{2} \frac{\partial}{\partial x_3} \left(C_{\theta\theta}^d \tau_\epsilon e \frac{\partial \langle \theta_l'^2 \rangle}{\partial x_3} \right) - \frac{\langle \theta_l'^2 \rangle}{2R_\tau \tau_\epsilon}, \quad (61)$$

$$\frac{1}{2} \frac{\partial \langle q_t'^2 \rangle}{\partial t} = - \langle u'_3 q_t' \rangle \frac{\partial \langle q_t \rangle}{\partial x_3} + \frac{1}{2} \frac{\partial}{\partial x_3} \left(C_{qq}^d \tau_\epsilon e \frac{\partial \langle q_t'^2 \rangle}{\partial x_3} \right) - \frac{\langle q_t'^2 \rangle}{2R_\tau \tau_\epsilon}, \quad (62)$$

$$\frac{\partial \langle \theta_l' q_t' \rangle}{\partial t} = - \langle u'_3 q_t' \rangle \frac{\partial \langle \theta_l \rangle}{\partial x_3} - \langle u'_3 \theta_l' \rangle \frac{\partial \langle q_t \rangle}{\partial x_3} + \frac{\partial}{\partial x_3} \left(C_{\theta q}^d \tau_\epsilon e \frac{\partial \langle \theta_l' q_t' \rangle}{\partial x_3} \right) - \frac{\langle \theta_l' q_t' \rangle}{R_\tau \tau_\epsilon}, \quad (63)$$

where the vertical x_3 axis is aligned with the vector of gravity so that the only non-zero component of the buoyancy parameter is β_3 . The virtual potential temperature flux $\langle u'_i \theta'_v \rangle$ is expressed through the fluxes of liquid water potential temperature, $\langle u'_i \theta_l' \rangle$, and the total water specific humidity, $\langle u'_i q_t' \rangle$, using Eq. (44), and the interpolation variable $\hat{\mathcal{R}}$ is computed from Eqs. (46)–(49). The TKE dissipation time scale τ_ϵ is computed from

$$\tau_\epsilon = \frac{1}{C_\epsilon} \frac{l}{e^{1/2}}, \quad \frac{1}{l} = \frac{1}{\kappa x_3} + \frac{1}{l_\infty} + \text{H}(N^2) \frac{N}{C_{ub} e^{1/2}}. \quad (64)$$

In the atmospheric flows, the Coriolis terms in the Reynolds-stress and scalar-flux equations are typically small and can safely be neglected. With due regard for the (baseline) parameterizations of pressure-scrambling terms given in section 5.1 (the deviatoric part of the Reynolds-stress dissipation rate and the dissipation rates of temperature and humidity fluxes are incorporated into the slow parts of the respective pressure-scrambling terms), the algebraic equations for the departure-from-isotropy tensor (and hence for the Reynolds stress) and for the scalar fluxes in the boundary-layer approximation are

$$\begin{aligned}
& C_t^u a_{ij} + (1 - C_{s2}^u) \tau_\epsilon \left(a_{ik} S_{jk} + a_{jk} S_{ik} - \frac{2}{3} \delta_{ij} a_{km} S_{km} \right) \\
& + (1 - C_{s3}^u) \tau_\epsilon (a_{ik} W_{jk} + a_{jk} W_{ik}) \\
& + (1 - C_b^u) \tau_\epsilon \left(\delta_{i3} \beta_3 \langle u'_j \theta'_v \rangle + \delta_{j3} \beta_3 \langle u'_i \theta'_v \rangle - \frac{2}{3} \delta_{ij} \beta_3 \langle u'_3 \theta'_v \rangle \right) \\
& = - \left(\frac{4}{3} - C_{s1}^u \right) \tau_\epsilon e S_{ij}, \tag{65}
\end{aligned}$$

$$\begin{aligned}
& C_t^\theta \langle u'_i \theta'_l \rangle + a_{i3} \tau_\epsilon \frac{\partial \langle \theta_l \rangle}{\partial x_3} + \tau_\epsilon \left[(1 - C_{s1}^\theta) S_{ik} + (1 - C_{s2}^\theta) W_{ik} \right] \langle u'_k \theta'_l \rangle \\
& = - \frac{2}{3} \tau_\epsilon e \delta_{i3} \frac{\partial \langle \theta_l \rangle}{\partial x_3} - (1 - C_b^\theta) \tau_\epsilon \delta_{i3} \beta_3 \langle \theta'_l \theta'_v \rangle, \tag{66}
\end{aligned}$$

$$\begin{aligned}
& C_t^q \langle u'_i q'_l \rangle + a_{i3} \tau_\epsilon \frac{\partial \langle q_l \rangle}{\partial x_3} + \tau_\epsilon [(1 - C_{s1}^q) S_{ik} + (1 - C_{s2}^q) W_{ik}] \langle u'_k q'_l \rangle \\
& = - \frac{2}{3} \tau_\epsilon e \delta_{i3} \frac{\partial \langle q_l \rangle}{\partial x_3} - (1 - C_b^q) \tau_\epsilon \delta_{i3} \beta_3 \langle q'_l \theta'_v \rangle, \tag{67}
\end{aligned}$$

where the covariances $\langle u'_i \theta'_v \rangle$, $\langle \theta'_l \theta'_v \rangle$ and $\langle q'_l \theta'_v \rangle$ incorporating the virtual potential temperature are expressed through $\langle u'_i \theta'_l \rangle$ and $\langle u'_i q'_l \rangle$, $\langle \theta'_l{}^2 \rangle$ and $\langle \theta'_l q'_l \rangle$, and $\langle q'_l{}^2 \rangle$ and $\langle \theta'_l q'_l \rangle$, respectively, using Eq. (44). Within the framework of the boundary-layer approximation, $S_{13} = S_{31} = W_{13} = -W_{31} = \frac{1}{2} \partial \langle u_1 \rangle / \partial x_3$, $S_{23} = S_{32} = W_{23} = -W_{32} = \frac{1}{2} \partial \langle u_2 \rangle / \partial x_3$, and other components of S_{ij} and W_{ij} are zero. Estimates of disposable constants and parameters of TKESV-Bas are summarized in Appendix B.

Equations (65)–(67) constitute a system of 12 linear equations for a_{ij} (six independent components), $\langle u'_i \theta'_l \rangle$ (three independent components), and $\langle u'_i q'_l \rangle$ (three independent components). This system is readily solved, yielding explicit expressions for the Reynolds stress and scalar fluxes. Unfortunately, the solution to Eqs. (65)–(67) is non-realizable. That is, it yields physically meaningless values of a_{ij} (and hence of $\langle u'_i u'_j \rangle$), $\langle u'_i \theta'_l \rangle$ and $\langle u'_i q'_l \rangle$, such as infinite scalar fluxes or negative velocity variances, over a certain range of governing parameters (e.g. mean velocity shear and mean temperature gradient). A plausible way to circumvent these difficulties is considered in the next section.

9 The (So-Called) Stability Functions

The system of linear equations (65)–(67) yields explicit expressions for the Reynolds-stress and scalar-flux components. The expressions for $\langle u'_3 u'_1 \rangle$ and $\langle u'_3 u'_2 \rangle$ (components of the vertical flux of horizontal momentum) have the following down-gradient form:

$$\langle u'_3 u'_1 \rangle = -\mathcal{F}_M \tau_\epsilon e \frac{\partial \langle u_1 \rangle}{\partial x_3}, \quad \langle u'_3 u'_2 \rangle = -\mathcal{F}_M \tau_\epsilon e \frac{\partial \langle u_2 \rangle}{\partial x_3}. \tag{68}$$

The expressions for the vertical scalar fluxes contain both the down-gradient terms and the non-gradient terms that describe the generation of scalar fluxes by buoyancy:

$$\langle u'_3 \theta'_l \rangle = -\mathcal{F}_{\text{H1}} \tau_\epsilon e \frac{\partial \langle \theta_l \rangle}{\partial x_3} - \mathcal{F}_{\text{H2}} \tau_\epsilon \beta_3 \langle \theta'_l \theta'_v \rangle, \quad (69)$$

$$\langle u'_3 q'_t \rangle = -\mathcal{F}_{\text{H1}} \tau_\epsilon e \frac{\partial \langle q_t \rangle}{\partial x_3} - \mathcal{F}_{\text{H2}} \tau_\epsilon \beta_3 \langle q'_t \theta'_v \rangle, \quad (70)$$

where the covariances $\langle \theta'_l \theta'_v \rangle$ and $\langle q'_t \theta'_v \rangle$ are expressed through $\langle \theta_l'^2 \rangle$ and $\langle \theta'_l q'_t \rangle$ and $\langle q_t'^2 \rangle$ and $\langle \theta'_l q'_t \rangle$, respectively, using Eq. (44). The quantities \mathcal{F}_{M} , \mathcal{F}_{H1} and \mathcal{F}_{H2} are referred to as the “stability functions” (Mellor and Yamada, 1974). It should be emphasized at once that the stability functions are merely the notation introduced to represent the formulations of fluxes in a compact form. Basically, \mathcal{F}_{M} , \mathcal{F}_{H1} and \mathcal{F}_{H2} reflect the parameterization assumptions invoked to arrive at the algebraic Reynolds-stress and scalar-flux equations, first of all, the parameterizations of the pressure-scrambling terms.

The functions \mathcal{F}_{M} and \mathcal{F}_{H1} that appear in the down-gradient terms in Eqs. (68)–(70) are functions of three dimensionless parameters. These are the squared dimensionless shear $(\tau_\epsilon S)^2$, the squared dimensionless buoyancy frequency $(\tau_\epsilon N)^2$, and the potential to kinetic energy ratio P/e . Here, S^2 , N^2 and P are given by

$$S^2 = \left(\frac{\partial \langle u_1 \rangle}{\partial x_3} \right)^2 + \left(\frac{\partial \langle u_2 \rangle}{\partial x_3} \right)^2, \quad (71)$$

$$N^2 = -\beta_3 \left(\mathcal{I}_\theta \frac{\partial \langle \theta_l \rangle}{\partial x_3} + \mathcal{I}_q \frac{\partial \langle q_t \rangle}{\partial x_3} \right), \quad (72)$$

$$P = \tau_\epsilon^2 \beta_3^2 [\mathcal{I}_\theta (\mathcal{I}_\theta \langle \theta_l'^2 \rangle + \mathcal{I}_q \langle \theta'_l q'_t \rangle) + \mathcal{I}_q (\mathcal{I}_q \langle q_t'^2 \rangle + \mathcal{I}_\theta \langle \theta'_l q'_t \rangle)], \quad (73)$$

$$\mathcal{I}_\theta = 1 + (R - 1) \langle q_t \rangle - R \langle q_l \rangle - \hat{\mathcal{R}} \frac{\mathcal{A} \mathcal{P}}{\mathcal{Q}}, \quad \mathcal{I}_q = (R - 1) \langle \theta \rangle + \hat{\mathcal{R}} \frac{\mathcal{A}}{\mathcal{Q}}, \quad (74)$$

where \mathcal{A} , \mathcal{P} , \mathcal{Q} and $\hat{\mathcal{R}}$ are defined in section 7. The quantity P characterizes potential energy of the turbulent flow and may be referred to as the turbulence potential energy⁴. Note that the buoyancy frequency and the TPE appear to depend on the interpolation variable $\hat{\mathcal{R}}$ and hence on the fractional cloud cover. As discussed in section 7, the covariances incorporating fluctuation of the virtual potential temperature cannot be computed exactly in the general case of fractional cloudiness. It is the use of the interpolation formula (44) to determine $\langle u'_l \theta'_v \rangle$, $\langle \theta'_l \theta'_v \rangle$ and $\langle q'_t \theta'_v \rangle$ that leads to the interpolation formulae (72) and (73) for N^2 and P , respectively. Instead of $(\tau_\epsilon S)^2$ and $(\tau_\epsilon N)^2$, \mathcal{F}_{M} and \mathcal{F}_{H1} can be presented in terms of $(\tau_\epsilon S)^2$ [or $(\tau_\epsilon N)^2$] and the gradient Richardson number $Ri = N^2/S^2$. The stability function \mathcal{F}_{H2} that appears in the non-gradient terms in Eqs. (69) and (70) depends on $(\tau_\epsilon S)^2$ and $(\tau_\epsilon N)^2$, or, alternatively, on $(\tau_\epsilon S)^2$ [or $(\tau_\epsilon N)^2$] and Ri , but does not depend on P/e .

The stability functions resulting from Eqs. (68)–(70) are ill-behaved over a certain range of governing parameters. Figure 2 shows \mathcal{F}_{M} and \mathcal{F}_{H1} as dependent on Ri and $(\tau_\epsilon S)^2$ at a fixed value of P/e . As seen from the figure, the stability functions have physically meaningless values, i.e. they tend to infinity or become negative over a part of their parameter

⁴Other definitions of TPE have also been used in the analyses of atmospheric turbulence, see Appendix C for a brief discussion.

space. The scalar-flux stability function \mathcal{F}_{H2} (not shown) is well-behaved and poses no complications. The expressions of \mathcal{F}_M , \mathcal{F}_{H1} and \mathcal{F}_{H2} are rather lengthy and are not presented in this section. However, those expressions are drastically simplified in the case of shear-free (and rotation-free) flow, and the ill-behaviour of the stability functions can be easily demonstrated analytically. The analysis is presented in Appendix D.

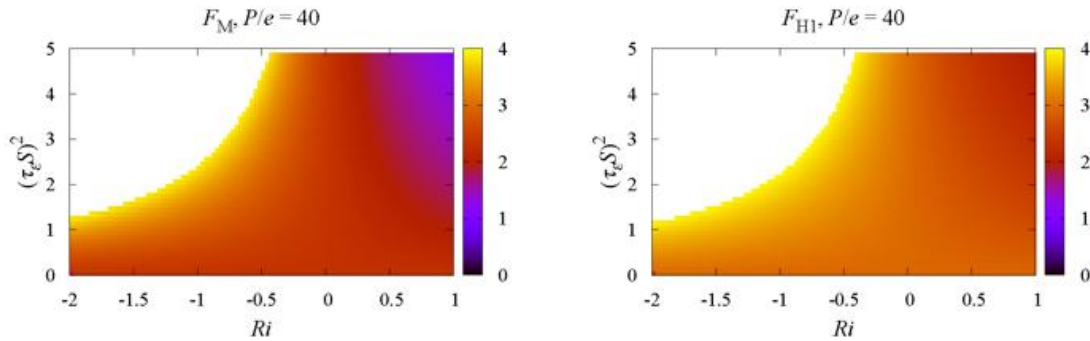


Figure 2: The momentum-flux \mathcal{F}_M (left panel) and the scalar-flux \mathcal{F}_{H1} (right panel) stability functions of the TKESV scheme as dependent on Ri and $(\tau_\epsilon S)^2$ at a fixed value of $P/e = 40$. The functions are computed with the estimates of dimensionless constants given in Table 1 (Appendix B), where the estimates of $C_{s2}^u = 3/5$ and $C_{s3}^u = 13/15$ are used. The values of \mathcal{F}_M and \mathcal{F}_{H1} are indicated by the colour scale. The white area is a part of the parameter space where the stability functions are ill-behaved.

In order to obtain the Reynolds-stress and scalar-flux formulations that remain in force over the entire parameter space, the stability functions should be modified (regularized) in one way or the other. A straightforward approach is to simply impose the upper and lower bounds on the stability functions themselves. Alternatively, realizability constraints may be imposed on the arguments, e.g. on $(\tau_\epsilon S)^2$ and $(\tau_\epsilon N)^2$, so that the stability functions cannot become infinite or negative (see e.g. Mellor and Yamada, 1982; Hassid and Galperin, 1994). These methods applied within the framework a one-equation TKE scheme may lead to either the model blow-up or to physically implausible solutions (Helfand and Labraga, 1988). One more method is to replace the ill-behaved stability functions with more simple functions that reveal no pathological behaviour. For example, the stability functions of the algebraic turbulence parameterization scheme, where all second-moment equations (including the TKE equation) are reduced to the diagnostic algebraic formulations, are well-behaved over their entire parameter space. The use of the algebraic-scheme stability functions within the one-equation TKE scheme yields regular solutions. However, the adjustment of the TKE towards the production-dissipation equilibrium state occurs on a too short time scale. In other words, turbulence responds too quickly to changes in the shear and buoyancy forcing. A more detailed discussion of the above (and some other) regularization methods is given in Helfand and Labraga (1988) (see also Hanjalić and Launder, 2011; Lazeroms et al., 2013, 2015, 2016).

An appealing way to tackle the problem was proposed by Helfand and Labraga (1988) (see also du Vachat, 1989; Helfand and Labraga, 1989). These authors analyzed the stability functions of the one-equation TKE scheme. Using rather plausible physical arguments, they developed regularized functions that reveal no pathological behaviour over their entire parameter space. In what follows, we extend the approach of Helfand and Labraga to the

TKESV scheme⁵. Following Helfand and Labraga (1988), we adhere to the Mellor and Yamada terminology (Mellor and Yamada, 1974, 1982; Yamada, 1977). The level 3 refers to the TKESV-like schemes that carry transport equations for the TKE and for the scalar variances and covariance, and the level 2 refers to the schemes, where all second-moment equations are reduced to the diagnostic algebraic formulations. One-equation TKE schemes are referred to as the level 2.5 schemes.

Within the framework of the level 2.5 scheme, the scalar-variance and scalar-covariance transport equations are truncated to the diagnostic expressions reflecting the steady-state balance between the mean-gradient production and the dissipation. The vertical scalar fluxes are given by the following down-gradient formulations:

$$\langle u'_3 \theta'_l \rangle = -\mathcal{F}_H^{2.5} \tau_\epsilon e \frac{\partial \langle \theta_l \rangle}{\partial x_3}, \quad \langle u'_3 q'_l \rangle = -\mathcal{F}_H^{2.5} \tau_\epsilon e \frac{\partial \langle q_l \rangle}{\partial x_3}, \quad (75)$$

where $\mathcal{F}_H^{2.5}$ is the level 2.5 scalar-flux stability function. The momentum-flux components $\langle u'_3 u'_1 \rangle$ and $\langle u'_3 u'_2 \rangle$ are given by Eqs. (68), where \mathcal{F}_M is replaced with the level 2.5 stability function $\mathcal{F}_M^{2.5}$. The level 2.5 stability functions depend on $(\tau_\epsilon S)^2$ and $(\tau_\epsilon N)^2$, or, alternatively, on $(\tau_\epsilon S)^2$ [or $(\tau_\epsilon N)^2$] and Ri . The level 2.5 functions suffer from the same deficiencies as the level 3 functions, i.e. they are ill-behaved over a part of their parameter space.

Helfand and Labraga (1988) recast the functions $\mathcal{F}_M^{2.5}(Ri, \tau_\epsilon^2 S^2)$ and $\mathcal{F}_H^{2.5}(Ri, \tau_\epsilon^2 S^2)$ in terms of Ri and the ratio e/e_e of the actual TKE $e = e_{2.5}$ of the level 2.5 scheme (hence the subscript) to the equilibrium value of the TKE $e_e = e_2$ of the level 2 scheme. Within the framework of the level 2 scheme, all second-moment transport equations, including the TKE equation, are truncated to the diagnostic expressions by neglecting the time-rate-of-change, advection and third-order transport terms. That is, all second-order moments, including the TKE, are in the state of local production-destruction equilibrium. In order to change the variables $(Ri, \tau_\epsilon^2 S^2)$ to the variables $(Ri, e/e_e)$, the equality $\tau_\epsilon^2 S^2 = (\tau_\epsilon/\tau_{ee})^2 \tau_{ee}^2 S^2 = (e_e/e) \tau_{ee}^2 S^2$ is used, where τ_{ee} is the equilibrium TKE dissipation time scale, i.e. τ_ϵ computed with e_e . The value of e_e , and hence of $\tau_{ee}^2 S^2$, for a given Ri is found by solving the equilibrium TKE equation of the level 2 scheme, which is a quadratic equation in e_e (in $\tau_{ee}^2 S^2$). Since the stability functions \mathcal{F}_M^2 and \mathcal{F}_H^2 are well-behaved over their entire parameter space (any value of Ri), a physically meaningful solution $e_e = e_2$ can always be found. Helfand and Labraga (1988) noticed that $\mathcal{F}_M^{2.5}$ and $\mathcal{F}_H^{2.5}$ become pathological in the case of growing turbulence, $e/e_e < 1$, where the TKE production (locally) dominates over the TKE dissipation. Figure 3 illustrates the pathological behaviour of the level 2.5 stability functions on the $Ri \times e/e_e$ plane. Note that $\mathcal{F}_M^{2.5}$ and $\mathcal{F}_H^{2.5}$ are computed with the estimates of dimensionless constants of TKESV-Bas (where $C_{s2}^u = 3/5$ and $C_{s3}^u = 13/15$), which are somewhat different from the estimates used by Helfand and Labraga (1988). As seen from the figure, $\mathcal{F}_M^{2.5}$ and $\mathcal{F}_H^{2.5}$ are well-behaved in the case of equilibrium or decaying turbulence, $e/e_e \geq 1$, but become pathological at $e/e_e < 1$.

The failure of the level 2.5 scheme is attributed to the closure assumptions used to develop the scheme, namely, (i) the neglect of the substantial derivative and the third order transport of the Reynolds stress, scalar fluxes and scalar variances and covariance, and (ii) the use of linear formulations of the pressure-scrambling terms in the Reynolds-stress and scalar-flux equations (see further discussion at the end of the present section). These closure assumptions are valid for the flows where turbulence is not far from the stationary, homogeneous, and isotropic state. Helfand and Labraga (1988) argue that it is precisely in the regime of growing TKE, where $e/e_e < 1$, that the turbulence becomes strongly anisotropic (also

⁵Helfand and Labraga (1988) considered dry atmosphere, where θ is the only thermodynamic variable that affects buoyancy. Our analysis deals with the moist atmosphere, using thermodynamic variables θ_l and q_l .

non-stationary and possibly non-homogeneous) and the above assumptions are too crude, leading to the ill-behaviour of the stability functions and to non-realizability of the turbulence closure scheme. In order to remedy the situation, Helfand and Labraga proposed to account, in an approximate way, for the effects of time-rate-of-change, advection and diffusion in those truncated second-moment equations in which these effects have been neglected. In other words, the idea is to restore to the second-moment equations some information that has been lost because of truncation. The following approximation was proposed:

$$\frac{d\mathcal{M}/dt + \mathcal{D}_{\mathcal{M}}}{\mathcal{G}_{\mathcal{M}}} = \frac{de/dt + \mathcal{D}_e}{\mathcal{G}_e}. \quad (76)$$

Here, \mathcal{M} stands for the Reynolds stress, scalar fluxes, and (within the framework of the level 2.5 scheme) scalar variances and covariance, d/dt is the substantial derivative that coincides with $\partial/\partial t$ within the framework of the boundary-layer approximation, \mathcal{D} is the diffusion rate of the respective second-order moment, and \mathcal{G} is its production (generation) rate. The production rate $\mathcal{G}_{\mathcal{M}}$ includes the terms due to mean velocity shear and buoyancy (in the Reynolds-stress and scalar-flux equations), and due to mean scalar gradients (in the scalar-flux, scalar-variance and scalar-covariance equations). It should be mentioned that within the framework of the Helfand and Labraga approach the production rate is defined with due regard for the rapid parts of the pressure-scrambling terms. Equation (76) states that the ratio of the tendency of the second-order moment \mathcal{M} due to d/dt and \mathcal{D} to the production rate of \mathcal{M} is the same as the respective ratio for the TKE.

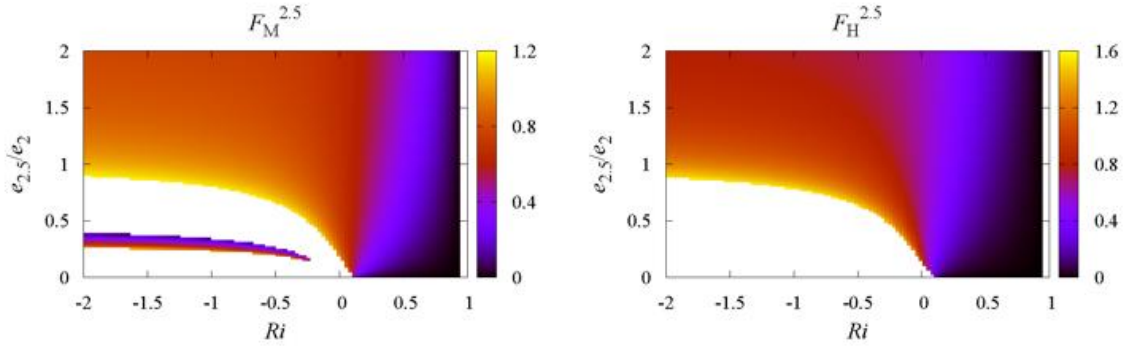


Figure 3: The stability functions of the level 2.5 scheme as dependent on Ri and $e/e_e = e_{2.5}/e_2$. The values of $\mathcal{F}_M^{2.5}$ and $\mathcal{F}_H^{2.5}$ are indicated by the colour scale. The white area is a part of the parameter space where the stability functions are ill-behaved.

Some comments on the validity of Eq. (76) are in order. Equation (76) is obviously exact in the regime of production-destruction equilibrium. In this regime, the production rate of any moment \mathcal{M} , including the TKE, is balanced by the destruction rate of \mathcal{M} due to return-to-isotropy (\mathcal{M} stands for the Reynolds stress or scalar flux) or viscous dissipation (\mathcal{M} stands for the scalar variance, scalar covariance, or TKE). In the regime of production-destruction equilibrium, both the r.h.s. and the l.h.s. of Eq. (76) are zero. Equation (76) is also valid asymptotically if the production rate of the moment \mathcal{M} strongly dominates over its destruction rate. A transport equation for \mathcal{M} can be written in the following form:

$$\frac{d\mathcal{M}/dt + \mathcal{D}_{\mathcal{M}}}{\mathcal{G}_{\mathcal{M}}} = 1 - \frac{\epsilon_{\mathcal{M}}}{\mathcal{G}_{\mathcal{M}}}, \quad (77)$$

where $\epsilon_{\mathcal{M}}$ denotes the destruction rate of the moment \mathcal{M} . The r.h.s. of Eq. (77) approaches one as the ratio $\epsilon_{\mathcal{M}}/\mathcal{G}_{\mathcal{M}}$ tends to zero. If the ratio ϵ/\mathcal{G}_e for the TKE also tends to zero, both the r.h.s. and the l.h.s. of Eq. (76) approach one. In the real-world flows, this never holds exactly. However, $\epsilon_{\mathcal{M}}/\mathcal{G}_{\mathcal{M}} \ll 1$ may hold approximately following a rapid increase of forcing (by mean scalar gradient, mean velocity shear, or buoyancy), i.e. precisely in the regime of growing turbulence.

Using Eq. (76), the truncated, algebraic equations of the level 2.5 scheme can be modified to approximately account for (mimic) the effects of the time-rate-of-change and turbulent diffusion. To this end, approximations $d\mathcal{M}/dt + \mathcal{D}_{\mathcal{M}} = \alpha_e \mathcal{G}_{\mathcal{M}}$, where $\alpha_e = (de/dt + \mathcal{D}_e)/\mathcal{G}_e$ is known from the solution of the TKE equation, are added to the Reynolds-stress, scalar-flux and scalar-variance equations (recall that $d/dt = \partial/\partial t$ within the framework of the boundary-layer approximation). In substance, these modifications amount to multiplying the production terms in the algebraic equations by a factor $1 - \alpha_e$. The resulting system of the Reynolds-stress, scalar-flux and scalar-variance equations remains algebraic and linear. It is readily solved (see Helfand and Labraga, 1988, for details), giving the following expressions for the stability functions of the level 2.5 scheme:

$$\mathcal{F}_M^{2.5} = \mathcal{F}_{Mr}^{2.5} = \mathcal{F}_M^2 \left(\frac{e_{2.5}}{e_2} \right)^{1/2}, \quad \mathcal{F}_H^{2.5} = \mathcal{F}_{Hr}^{2.5} = \mathcal{F}_H^2 \left(\frac{e_{2.5}}{e_2} \right)^{1/2}, \quad (78)$$

where the subscript ‘‘r’’ indicates the modified (regularized) stability functions. The regularized functions given by Eq. (78) are used in the case of growing turbulence, when the actual value of TKE $e_{2.5}$ of the level 2.5 scheme is less than the equilibrium TKE e_2 of the level 2 scheme. In the case of equilibrium or decaying turbulence, the original, non-modified stability functions of the level 2.5 scheme are used that are well-behaved at $e_{2.5}/e_2 \geq 1$ and pose no problem. Recall that the stability functions \mathcal{F}_M^2 and \mathcal{F}_H^2 of the level 2 algebraic scheme are well-behaved over their entire parameter space, and e_2 is found by solving the equilibrium TKE equation (a quadratic equation in e_2 that always has a physically meaningful solution). Figure 4 illustrates the regularized stability functions of the level 2.5 scheme that reveal no pathological behaviour.

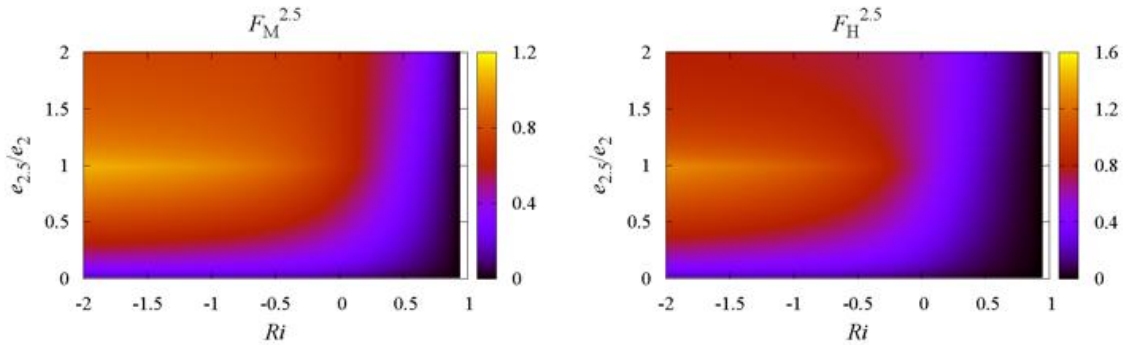


Figure 4: The regularized stability functions of the level 2.5 scheme as dependent on Ri and $e/e_e = e_{2.5}/e_2$. The values of $\mathcal{F}_M^{2.5}$ and $\mathcal{F}_H^{2.5}$ are indicated by the colour scale. In the case of growing turbulence, $e_{2.5}/e_2 < 1$, the stability functions are computed from Eq. (78).

The regularization method of Helfand and Labraga (1988) is now applied to the TKESV (level 3) scheme. Using Eq. (76), the Reynolds-stress and scalar-flux equations are modified, and the resulting system of algebraic equations for a_{ij} , $\langle u'_i \theta'_l \rangle$ and $\langle u'_i q'_l \rangle$ is solved (the

derivations are rather cumbersome and are omitted here). The following expressions of the stability functions $\mathcal{F}_M = \mathcal{F}_M^3$ and $\mathcal{F}_{H1} = \mathcal{F}_{H1}^3$ in Eqs. (68)–(70) are obtained (index “3” refers to the level 3, i.e. to the TKESV, scheme):

$$\mathcal{F}_M^3 = \mathcal{F}_{Mr}^3 = \mathcal{F}_M^{2,p} \left(\frac{e_3}{e_{2,p}} \right)^{1/2}, \quad \mathcal{F}_{H1}^3 = \mathcal{F}_{H1r}^3 = \mathcal{F}_{H1}^{2,p} \left(\frac{e_3}{e_{2,p}} \right)^{1/2}, \quad (79)$$

where the subscript “r” indicates the regularized stability functions. In Eq. (79), the index “2.p” refers to the scheme that utilizes the equilibrium TKE equation but carries transport equations for the scalar variances and scalar covariance. That is, the TKE is determined diagnostically using the steady-state production-dissipation balance, whereas the scalar variances and covariance (and hence the TPE) are determined prognostically with due regard for the third-order turbulent transport⁶. The stability functions $\mathcal{F}_M^{2,p}$ and $\mathcal{F}_{H1}^{2,p}$ of the level 2.p scheme are well-behaved over their entire parameter space. The equilibrium TKE $e_e = e_{2,p}$ is found by solving the equilibrium TKE equation of the level 2.p scheme, which is a cubic equation in e_e . The regularized stability functions given by Eq. (79) are used in the case of growing turbulence, when $e_3/e_{2,p} < 1$. In the case of equilibrium or decaying turbulence, the original, non-modified stability functions of the level 3 (TKESV) scheme are used which are well-behaved at $e_3/e_{2,p} \geq 1$ and pose no problem.

Figure 5 shows the original, non-modified stability functions of the TKESV (level 3) scheme on the $Ri \times e_3/e_{2,p}$ plane at a fixed value of P/e_3 . The stability functions are well-behaved in the case of equilibrium or decaying turbulence, $e_3/e_{2,p} \geq 1$, but become pathological in the case of growing turbulence, $e_3/e_{2,p} < 1$. Figure 6 shows the regularized stability functions of the TKESV (level 3) scheme. As seen from the figure, the stability functions reveal no pathological behaviour.

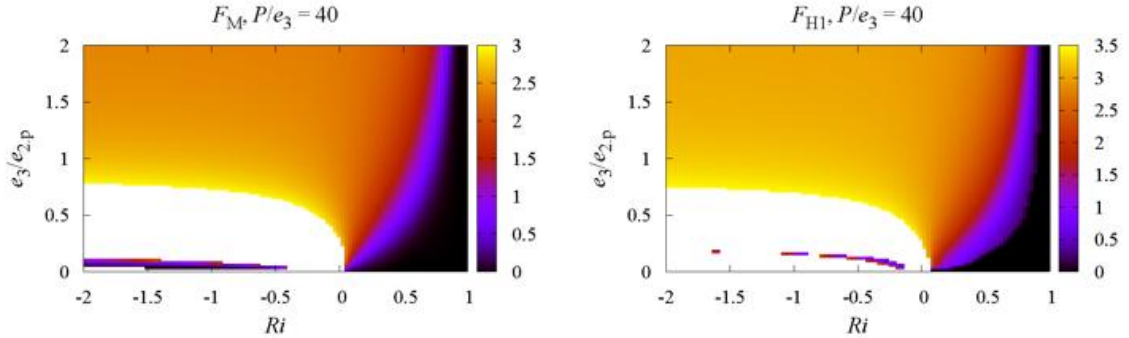


Figure 5: The original, non-regularized momentum-flux $\mathcal{F}_M = \mathcal{F}_M^3$ (left panel) and scalar-flux $\mathcal{F}_{H1} = \mathcal{F}_{H1}^3$ (right panel) stability functions of the TKESV (level 3) scheme as dependent on Ri and $e_3/e_{2,p}$ at a fixed value of $P/e_3 = 40$. The values of stability functions are indicated by the colour scale. The white area is a part of the parameter space where the stability functions are ill-behaved.

It is interesting to draw analogies between Eq. (78) and Eq. (79). As Eq. (78) shows, the regularized level 2.5 stability functions are expressed in terms of the level 2 stability

⁶The letter “p” in the label “2.p” is used to indicate potential energy. In a similar spirit, the level 2.5 scheme may be referred to as the “level 2.k” scheme, where “k” indicates kinetic energy, or, alternatively, the “level 2.e” scheme, where “e” is a conventional notation for the TKE.

functions. For the level 2.5 scheme, the level 2 scheme is the nearest lower-level realizable scheme whose stability functions are well-behaved over the entire parameter space. Likewise, for the level 3 scheme, the level 2.p scheme is the nearest lower-level realizable scheme. The level 2 and the level 2.p schemes differ significantly in the way they treat the scalar variances and covariance. However, both the level 2 and the level 2.p schemes utilize a steady-state equilibrium TKE equation, suggesting that it is the use of the TKE transport equation in combination with the algebraic formulations of the Reynolds stress and scalar fluxes that causes non-realizability of truncated turbulence closure schemes.

Note an important factor $(e_3/e_{2,p})^{1/2}$ in the expressions of the regularized level 3 stability functions, Eq. (79). It is this factor that takes care of a gradual transition of the TKE towards the production-dissipation equilibrium. Dropping the factor $(e_3/e_{2,p})^{1/2}$ in Eq. (79) would result in a too quick response of turbulence to changes in the forcing and in overestimation of momentum and scalar fluxes in the regime of growing TKE. The factor $(e_{2.5}/e_2)^{1/2}$ in Eq. (78) has a similar effect on the behaviour of the level 2.5 scheme.

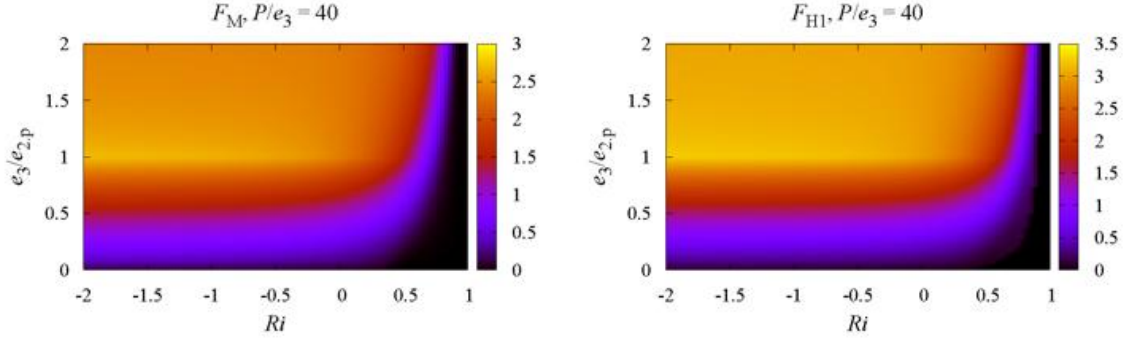


Figure 6: The regularized momentum-flux $\mathcal{F}_M = \mathcal{F}_{Mr}^3$ (left panel) and scalar-flux $\mathcal{F}_{H1} = \mathcal{F}_{H1r}^3$ (right panel) stability functions of the TKESV (level 3) scheme as dependent on Ri and $e/e_e = e_3/e_{2,p}$ at a fixed value of $P/e_3 = 40$. The values of stability functions are indicated by the colour scale. In the case of growing turbulence, $e_3/e_{2,p} < 1$, the stability functions are computed from Eq. (79).

The idea of the regularization method of Helfand and Labraga (1988) is to restore to the second-moment equations some information that has been lost because of truncation. Equation (76) is used to approximately account for (mimic) the effects of the time-rate-of-change and turbulent diffusion in the Reynolds-stress and scalar-flux (and, in the case of level 2.5 scheme, in the scalar-variance and scalar-covariance) equations. An alternative interpretation can be suggested, however. As discussed above, the use Eq. (76) amounts to multiplying the production terms in the truncated equations by a factor $1 - \alpha_e$, where $\alpha_e = (de/dt + \mathcal{D}_e)/\mathcal{G}_e$ depends on time t and vertical coordinate x_3 . Consider, for example, the buoyancy production term in the liquid water potential temperature flux equation (66),

$$- \left(1 - C_b^\theta\right) \tau_\epsilon \beta_3 \langle \theta'_t \theta'_v \rangle, \quad (80)$$

where C_b^θ is a constant that stems from a linear model of the buoyancy contribution to the pressure-scrambling term in the temperature-flux equation. Recall that the use of linear parameterizations of the pressure-scrambling terms is identified as one reason for the failure

of truncated second-order schemes. If Eq. (76) is utilized, the buoyancy production term in the temperature-flux equation becomes

$$-[1 - \alpha_e(t, x_3)] (1 - C_b^\theta) \tau_\epsilon \beta_3 \langle \theta'_l \theta'_v \rangle = - [1 - C_{b*}^\theta(t, x_3)] \tau_\epsilon \beta_3 \langle \theta'_l \theta'_v \rangle, \quad (81)$$

where $C_{b*}^\theta = C_b^\theta + \alpha_e (1 - C_b^\theta)$ is no longer a constant, but a function of t and x_3 . Note that $C_{b*}^\theta = C_b^\theta$ if $\alpha_e = 0$, and the original, non-regularized formulation is recovered. If $\alpha_e = 1$, then $C_{b*}^\theta = 1$, which effectively satisfies the two-component limit constraint of strongly anisotropic turbulence. As discussed in section 5.1, it is not possible to satisfy the TCL constraint within the framework of a linear model of the pressure-scrambling terms if the value of C_b^θ is chosen so that to satisfy the isotropic limit. If Eq. (76) is utilized to modify the truncated temperature-flux equation, both the isotropic and the TCL constraints can be satisfied. Then, the Helfand and Labraga regularization procedure can be viewed as being conceptually similar to the use of non-linear parameterizations of the pressure-scrambling effects.

To conclude this section, we note that the regularized expressions have been obtained for all components of the Reynolds stress and scalar fluxes, not only for $\langle u'_3 u'_1 \rangle$, $\langle u'_3 u'_2 \rangle$, $\langle u'_3 \theta'_l \rangle$, and $\langle u'_3 q'_t \rangle$. Those regularized formulations are not presented here.

10 Interaction with the Underlying Surface

In order to describe the interaction of the boundary-layer turbulence with the underlying surface, the surface fluxes of momentum, heat and moisture should be specified and the boundary conditions for the TKE, scalar variances and scalar covariance should be imposed. The surface fluxes are assumed to be provided by the host atmospheric model (e.g. COSMO or ICON). A consideration of the surface flux calculation procedures is beyond the scope of the present report.

For the TKE, scalar-variance and scalar-covariance, the following boundary conditions at the underlying surface are used in the TKESV-Bas scheme:

$$-C_e^d \tau_\epsilon e \frac{\partial e}{\partial x_3} = 0, \quad (82)$$

$$-C_{\theta\theta}^d \tau_\epsilon e \frac{\partial \langle \theta_l'^2 \rangle}{\partial x_3} = 0, \quad -C_{qq}^d \tau_\epsilon e \frac{\partial \langle q_t'^2 \rangle}{\partial x_3} = 0, \quad -C_{\theta q}^d \tau_\epsilon e \frac{\partial \langle \theta_l' q_t' \rangle}{\partial x_3} = 0. \quad (83)$$

Equations (82) and (83) state that the fluxes of TKE, scalar variances and scalar covariance at the underlying surface are zero. That is, e , $\langle \theta_l'^2 \rangle$, $\langle q_t'^2 \rangle$ and $\langle \theta_l' q_t' \rangle$ are height-constant within the layer immediately adjacent to the underlying surface. This is consistent with the surface-layer similarity (cf. the log-layer relationships given in Appendix A). Notice, however, that the surface-layer relationships (the Monin-Obukhov similarity theory) are applicable to continuous turbulence over a homogeneous surface, and it is, strictly speaking, incorrect to apply the surface-layer similarity relationships over heterogeneous surfaces. Then, the boundary conditions (82) and (83) become inaccurate if a tile approach is used to compute the grid-box mean surface fluxes.

Advanced Features

In order to develop the surface boundary conditions for the scalar variances and covariance that are consistent with the tiled surface schemes, we make use of the following triple

decomposition:

$$f = \langle \bar{f} \rangle + \bar{f}'' + f^s, \quad (84)$$

where f is a generic variable. The angle brackets denote the quantity averaged horizontally over a grid box of a host model. An overbar denotes a mean over a tile, and a double prime denotes a fluctuation of a tile mean quantity about a grid-box mean quantity. The superscript “s” denotes a sub-tile fluctuation. By definition, $\langle \bar{f}'' \rangle = 0$. To simplify the discussion, we take $\bar{f}^s = 0$, although this assumption is not necessary (cf. Mironov and Sullivan, 2016).

Using Eq. (84), we obtain the following expression for the triple-correlation of the vertical velocity, u_3 , and the two scalars, θ_l and q_t :

$$\begin{aligned} \langle u_3' \theta_l' q_t' \rangle &= \left\langle \overline{(u_3'' + u_3^s)} \left(\overline{\theta_l'' + \theta_l^s} \right) \left(\overline{q_t'' + q_t^s} \right) \right\rangle \\ &= \left\langle \overline{u_3'' \theta_l'' q_t''} \right\rangle + \left\langle \overline{u_3'' \theta_l^s q_t^s} \right\rangle + \left\langle \overline{\theta_l'' u_3^s q_t^s} \right\rangle + \left\langle \overline{q_t'' u_3^s \theta_l^s} \right\rangle + \left\langle \overline{u_3^s \theta_l^s q_t^s} \right\rangle. \end{aligned} \quad (85)$$

The first two terms on the r.h.s. of Eq. (85) are zero at the surface because of zero vertical velocity $\overline{u_3}$. The last term on the r.h.s. cannot be estimated unless a high-order closure model is applied to individual tiles. This is usually not the case. The third and the fourth terms on the r.h.s. of Eq. (85) are zero if the grid box of the host model is horizontally homogeneous. If the grid box is heterogeneous, the temperature $\overline{\theta_l}$ and humidity $\overline{q_t}$ differ between the tiles and so do the temperature and humidity fluxes, $\overline{u_3^s \theta_l^s}$ and $\overline{u_3^s q_t^s}$. Then, the third-order velocity-scalar covariance $\langle u_3' \theta_l' q_t' \rangle$, i.e. the flux of temperature-humidity covariance, is generally non-zero at the surface. The expressions for $\langle u_3' \theta_l'^2 \rangle$ and $\langle u_3' q_t'^2 \rangle$ are obtained from Eq. (85) by replacing q_t with θ_l and θ_l with q_t , respectively.

Notice a close analogy between the above analysis and the analysis of Mironov and Sullivan (2016). These authors used large-eddy simulation to explore the second-moment budgets in the stably stratified planetary boundary layer (PBL) over thermally homogeneous and thermally heterogeneous surfaces. Importantly, the LES-based second-moment budgets were estimated with due regard for the sub-grid scale contributions. Taking account of the SGS contributions revealed that the third-order velocity-scalar covariances are non-zero at the heterogeneous surfaces and are crucial for the maintenance of second-moment budgets in the heterogeneous PBL. That finding helped explain the enhanced vertical mixing in the stably-stratified PBL over thermally heterogeneous surfaces.

Based upon the above considerations, we propose the following surface boundary conditions for the scalar variances and scalar covariance that are consistent with the tiled surface schemes:

$$\begin{aligned} -C_{\theta\theta}^d \tau_\epsilon e \frac{\partial \langle \theta_l'^2 \rangle}{\partial x_3} &= 2 \left\langle \overline{\theta_l'' u_3^s \theta_l^s} \right\rangle, & -C_{qq}^d \tau_\epsilon e \frac{\partial \langle q_t'^2 \rangle}{\partial x_3} &= 2 \left\langle \overline{q_t'' u_3^s q_t^s} \right\rangle, \\ -C_{\theta q}^d \tau_\epsilon e \frac{\partial \langle \theta_l' q_t' \rangle}{\partial x_3} &= \left\langle \overline{\theta_l'' u_3^s q_t^s} \right\rangle + \left\langle \overline{q_t'' u_3^s \theta_l^s} \right\rangle. \end{aligned} \quad (86)$$

Note that the surface boundary condition (82) for the TKE remains in force, even though the tile approach may be used. This is readily shown by setting $\theta_l = u_i$ and $q_t = u_i$ in Eq. (85) (summation over repeated indices) and invoking the no-slip boundary condition for the flow velocity, $\overline{u_i} = 0$, at the underlying surface. Note that the term $\langle \overline{u_3^s u_i^s u_i^s} \rangle$ is not necessarily zero at the surface. It cannot be estimated, however, unless a high-order closure model is applied to individual tiles.

The surface boundary conditions given by Eqs. (86) provide an intimate coupling of the scalar variances and covariance with many other quantities characterizing the atmosphere and the soil. In order to illustrate this coupling, consider the moisture and heat balance equations at the underlying surface for individual tiles. The moisture balance equation reads

$$\overline{PP} + \overline{\rho u_3^s q_t^s} = \overline{G_q}, \quad (87)$$

where G_q is the ground moisture flux at the surface, and PP denotes the sum of all forms of precipitation, including (relatively slow) sedimentation of water droplets and ice crystals. Subtracting from Eq. (87) its horizontal mean, multiplying the result with $\overline{q_t''}$ and averaging horizontally, we obtain

$$\left\langle \overline{q_t'' u_3^s q_t^s} \right\rangle = \rho^{-1} \left[\left\langle \overline{q_t'' G_q} \right\rangle - \left\langle \overline{q_t'' PP} \right\rangle \right]. \quad (88)$$

The first term in brackets on the r.h.s. of Eq. (88) is generally non-zero since over heterogeneous surfaces both the total water content and the ground moisture flux vary between the tiles and are likely correlated. There is no good reason to assume that rain, snow, or hail falls differently onto some tiles than onto the others. However, if PP includes sedimentation of water droplets and ice crystals, then the difference between the tiles may be substantial and the covariance $\left\langle \overline{q_t'' PP} \right\rangle$ may appear to be different from zero. For example, if there is fog over some tiles but not over the other tiles, $\overline{PP''} \neq 0$. Rain or snow falling through the fog layers may amplify the influence of fog via seeder-feeder effect.

Consideration of the heat balance of the underlying surface yields the following expression:

$$\begin{aligned} & \left\langle \overline{\theta_l'' w^s \theta_l^s} \right\rangle = \\ & (\rho c_p)^{-1} \left[\left\langle \overline{\theta_l'' G_\theta} \right\rangle - \left\langle \overline{\theta_l'' R_s} \right\rangle - \left\langle \overline{\theta_l'' R_l} \right\rangle - L_v \left(\left\langle \overline{\theta_l'' G_q} \right\rangle - \left\langle \overline{\theta_l'' PP} \right\rangle \right) \right]. \quad (89) \end{aligned}$$

Here, G_θ is the ground heat flux at the surface, R_s is the solar radiation balance at the surface, and R_l is the net long-wave radiation at the surface. All terms on the r.h.s. of Eq. (89) are generally non-zero. The solar radiation balance varies between the tiles because of the difference in the tile albedo, and the long-wave radiation balance varies because of the difference in the tile temperature.

For the flux of temperature-humidity covariance, the following expression holds:

$$\begin{aligned} & \left\langle \overline{\theta_l'' w^s q_t^s} \right\rangle + \left\langle \overline{q_t'' w^s \theta_l^s} \right\rangle = \rho^{-1} \left[\left\langle \overline{\theta_l'' G_q} \right\rangle - \left\langle \overline{\theta_l'' PP} \right\rangle \right] \\ & (\rho c_p)^{-1} \left[\left\langle \overline{q_t'' G_\theta} \right\rangle - \left\langle \overline{q_t'' R_s} \right\rangle - \left\langle \overline{q_t'' R_l} \right\rangle - L_v \left(\left\langle \overline{q_t'' G_q} \right\rangle - \left\langle \overline{q_t'' PP} \right\rangle \right) \right], \quad (90) \end{aligned}$$

where all terms on the r.h.s. of Eq. (90) are generally non-zero over heterogeneous surfaces. If ice is taken into account, a generalized formulation of q_t should be used, θ_l should be replaced with the total water potential temperature, and L_c should be replaced with an effective heat of vapourization-sublimation (see sections 2 and 7).

11 Equation for Scalar Skewness

In this section, a transport equation for the skewness (triple correlation) of the scalar variable s is developed. The s -skewness is required to utilize the double-Gaussian statistical cloud scheme proposed by Naumann et al. (2013) and is only used within the framework of the

extended version of the TKESV scheme. Thus this section discusses *Advanced Features* that are not used within the framework of TKESV-Bas.

Recall that the s variable defined as $s = \mathcal{Q}^{-1}(\langle q_t \rangle - \langle q_{sl} \rangle + q'_t - \mathcal{P}\theta'_l)$ accounts for the combined effect of humidity and temperature fluctuations, and is a measure of local oversaturation/undersaturation (see section 7 for details). A positive s is merely a local value of q_t computed with respect to the linearized saturation specific humidity curve. In order to determine the s skewness, $S_s \equiv \langle s'^3 \rangle / \langle s'^2 \rangle^{3/2}$, the variance of s , $\langle s'^2 \rangle$, and its triple correlation, $\langle s'^3 \rangle$, should be computed. The variance of s is given by

$$\langle s'^2 \rangle = \mathcal{Q}^{-2} (\langle q_t'^2 \rangle - 2\mathcal{P} \langle q_t' \theta_l' \rangle + \mathcal{P}^2 \langle \theta_l'^2 \rangle). \quad (91)$$

It can be computed in a straightforward way using the values of $\langle q_t'^2 \rangle$, $\langle q_t' \theta_l' \rangle$ and $\langle \theta_l'^2 \rangle$ determined within the framework of the TKESV scheme from the scalar (co)variance equations. The triple correlation of s is given by

$$\langle s'^3 \rangle = \mathcal{Q}^{-3} (\langle q_t'^3 \rangle - 3\mathcal{P} \langle q_t'^2 \theta_l' \rangle + 3\mathcal{P}^2 \langle q_t' \theta_l'^2 \rangle - \mathcal{P}^3 \langle \theta_l'^3 \rangle). \quad (92)$$

As Eq. (92) suggests, the determination of $\langle s'^3 \rangle$ requires knowledge of the four third-order scalar correlations. These correlations can be computed from their transport equations, where closure assumptions are required for a number of terms (third-order and fourth-order velocity-scalar correlations and molecular destruction terms). This would make the TKESV scheme unduly complex and computationally expensive. We therefore take a different, more simple approach. We combine the transport equations for $\langle q_t'^3 \rangle$, $\langle q_t'^2 \theta_l' \rangle$, $\langle q_t' \theta_l'^2 \rangle$ and $\langle \theta_l'^3 \rangle$ with due regard for Eq. (92) to formulate a single transport equation for $\langle s'^3 \rangle$. To this end, we neglect the derivatives of \mathcal{P} and \mathcal{Q} with respect to time and space. Although an exact equation for the s -variable triple correlation can easily be derived, this is not required. The exact equation for $\langle s'^3 \rangle$, including time and space derivatives of \mathcal{P} and \mathcal{Q} , is cumbersome. Since \mathcal{P} and \mathcal{Q} depend on the grid-box mean quantities only, the uncertainties associated with neglect of the derivatives of \mathcal{P} and \mathcal{Q} are typically small unless the mean quantities change faster in space and time than higher-order moments (an unlikely situation). Note also that the skewness of s only serves to help determine the fractional cloud cover and its effect on the buoyancy production of the Reynolds stress and scalar fluxes. Then, $\langle s'^3 \rangle$ is in a sense an auxiliary quantity, and it is legitimate to keep the $\langle s'^3 \rangle$ equation reasonably simple at the expense of slightly reduced accuracy.

Combining transport equations for the four third-order moments on the r.h.s. of Eq. (92) and neglecting the derivatives of \mathcal{P} and \mathcal{Q} with respect to t and x_i , we obtain the following equation for the s -variable triple correlation:

$$\frac{1}{3} \left(\frac{\partial}{\partial t} + \langle u_i \rangle \frac{\partial}{\partial x_i} \right) \langle s'^3 \rangle = - \langle u_i' s'^2 \rangle \frac{\partial \langle s \rangle}{\partial x_i} + \langle s'^2 \rangle \frac{\partial \langle u_i' s' \rangle}{\partial x_i} - \frac{1}{3} \frac{\partial \langle u_i' s'^3 \rangle}{\partial x_i} - \epsilon_{s3}, \quad (93)$$

where $\langle s \rangle = \mathcal{Q}^{-1}(\langle q_t \rangle - \langle q_{sl} \rangle)$. The terms on the r.h.s. of Eq. (93) represent production/destruction due to the mean scalar gradient and due to the scalar-flux divergence, fourth-order turbulent transport, and molecular destruction (dissipation), respectively. In order to close Eq. (93), parameterizations of the third-order, $\langle u_i' s'^2 \rangle$, and fourth-order, $\langle u_i' s'^3 \rangle$, velocity-scalar correlations and of the dissipation term, ϵ_{s3} , should be developed.

The dissipation rate of $\langle s'^3 \rangle$ is parameterized through the following algebraic expression:

$$\epsilon_{s3} = \frac{\langle s'^3 \rangle}{3R_{\tau s} \tau_\epsilon}, \quad (94)$$

where $R_{\tau s} = \tau_{s3} / \tau_\epsilon = \langle s'^3 \rangle \epsilon / (3\epsilon \epsilon_{s3})$ is the ratio of the $\langle s'^3 \rangle$ dissipation time scale to the TKE dissipation time scale.

We adopt the following parameterization of the third-order velocity-scalar correlation:

$$\langle u'_i s'^2 \rangle = -C_{us2}^d \tau_\epsilon e \frac{\partial \langle s'^2 \rangle}{\partial x_i} + S_s \langle s'^2 \rangle^{1/2} \langle u'_i s' \rangle, \quad (95)$$

where C_{us2}^d is a dimensionless constant. In the case of nearly isotropic turbulence, the skewness S_s is small and Eq. (95) reduces to the down-gradient diffusion formulation. In the limiting case of strongly skewed PDF of s , the second term on the r.h.s of Eq. (95) becomes dominant. Then, Eq. (95) reduces to the form suggested by the top-hat representation of fluctuating quantities that is fundamental to the mass-flux approach widely used to parameterize cumulus convection in numerical models of the atmosphere. The simplest top-hat mass-flux model is formulated in terms of fractional areas of updraughts, a_u , and downdraughts, $a_d = 1 - a_u$. Alternatively, a PDF can be used which consists of only two Dirac delta functions, i.e. the probabilities of motions to be either updraughts or downdraughts are P_u and P_d , respectively, and $P_u + P_d = 1$. The second term on the r.h.s. of Eq. (95) is basically the mass-flux formulation recast in terms of the quantities used within the second-order closure framework (see Mironov, 2009, for a detailed discussion of the analogies between the mass-flux and the ensemble-mean second-order modelling frameworks). A skewness-dependent parameterization for the flux of potential-temperature variance [given by the second term on the r.h.s. of Eq. (95), where s is replaced with θ] was formulated in Mironov et al. (1999), Abdella and McFarlane (1999) and Abdella and Petersen (2000). An interpolation formula that incorporates both the down-gradient and the skewness-dependent terms was presented in Gryanik and Hartmann (2002). As different from previous studies, we apply these parameterization ideas to the scalar quantity s that accounts for the combined effect of temperature and humidity fluctuations.

The following parameterization of the fourth-order velocity-scalar correlation is adopted:

$$\langle u'_i s'^3 \rangle = 3 \left(1 + \frac{1}{3} S_s^2 \right) \langle s'^2 \rangle \langle u'_i s' \rangle - C_{us3}^d \tau_\epsilon e \frac{\partial \langle s'^3 \rangle}{\partial x_i}, \quad (96)$$

where C_{us3}^d is a dimensionless constant. The first term on the r.h.s. of Eq. (96) represents a generalization of the Millionshchikov hypothesis formulated in Gryanik and Hartmann (2002) and Gryanik et al. (2005) for convective boundary-layer turbulence. In the case of isotropic turbulence, S_s vanishes and the first term on the r.h.s. reduces to the classical Millionshchikov (1941) formulation. It states that the fourth-order moments can be considered as Gaussian, even though the third-order moments are nonzero. In the limiting case of very skewed turbulence, S_s is large and the first term on the r.h.s. of Eq. (96) takes on the form suggested by the top-hat mass-flux approach (cf. the formulation of $\langle u'_i s'^2 \rangle$). The expression $3 \left(1 + \frac{1}{3} S_s^2 \right) = 3 + S_s^2$ amounts to the simplest linear interpolation between the two limiting cases, where dimensionless coefficients 3 and 1 are chosen so that the limiting cases are satisfied exactly. The down-gradient diffusion term, the last term on the r.h.s. of Eq. (96), can be viewed as the smoothing operator that is added to the parameterization of the fourth-order turbulent transport term for numerical reasons. The use of the diffusion term can also be justified on physical grounds. To this end, one needs to consider the transport equation for the fourth-order term $\langle u'_i s'^3 \rangle$ and invoke a number of simplifying assumptions (e.g. use the Rotta-type closure for the pressure-scrambling terms and neglect turbulence anisotropy in the formulations of the mean-gradient terms).

Substituting Eqs. (94), (95) and (96) into Eq. (93) and using the boundary-layer approxi-

mation, we obtain the following equation for the s -variable triple correlation:

$$\begin{aligned} \frac{1}{3} \frac{\partial \langle s'^3 \rangle}{\partial t} = & - \left(S_s \langle s'^2 \rangle^{1/2} \langle u'_3 s' \rangle - C_{us2}^d \tau_\epsilon e \frac{\partial \langle s'^2 \rangle}{\partial x_3} \right) \frac{\partial \langle s \rangle}{\partial x_3} - \langle u'_3 s' \rangle \frac{\partial \langle s'^2 \rangle}{\partial x_3} \\ & + \frac{1}{3} \frac{\partial}{\partial x_3} \left(C_{us3}^d \tau_\epsilon e \frac{\partial \langle s'^3 \rangle}{\partial x_3} - S_s^2 \langle s'^2 \rangle \langle u'_3 s' \rangle \right) - \frac{\langle s'^3 \rangle}{3 R_{\tau s} \tau_\epsilon}. \end{aligned} \quad (97)$$

The following (tentative) estimates of disposable parameters are utilized: $C_{us2}^d = 0.1$, $C_{us3}^d = 0.1$, and $R_{\tau s} = 0.1$.

The surface boundary condition for $\langle s'^3 \rangle$ should be specified that is applicable over both homogeneous and heterogeneous surfaces and is consistent with the tiled surface schemes. To this end, we make use of the triple decomposition (84) and express the fourth-order velocity-scalar covariance as follows:

$$\begin{aligned} \langle u'_3 s'^3 \rangle &= \left\langle (\overline{u_3''} + u_3^s) (\overline{s''} + s^s)^3 \right\rangle \\ &= \langle \overline{u_3''} \overline{s''^3} \rangle + 3 \langle \overline{u_3''} \overline{s''} \overline{s^s} \rangle + \langle \overline{u_3''} \overline{s^s} \overline{s^s} \rangle \\ &+ 3 \langle \overline{s''^2} \rangle \langle \overline{u_3^s} \overline{s^s} \rangle + 3 \langle \overline{s''^2} \overline{u_3^s} \overline{s^s} \rangle + 3 \langle \overline{s''} \overline{u_3^s} \overline{s^s} \rangle + \langle \overline{u_3^s} \overline{s^s} \rangle. \end{aligned} \quad (98)$$

The first three terms on the r.h.s. of Eq. (98) are zero at the surface because of zero vertical velocity $\overline{u_3}$. The last two terms on the r.h.s. cannot be estimated unless a high-order closure model is applied to individual tiles. The remaining two terms are generally non-zero over heterogeneous surfaces.

Using Eq. (98), we propose the following surface boundary condition for $\langle s'^3 \rangle$:

$$3 \left(1 + \frac{1}{3} S_s^2 \right) \langle s'^2 \rangle \langle u'_3 s' \rangle - C_{us3}^d \tau_\epsilon e \frac{\partial \langle s'^3 \rangle}{\partial x_3} = 3 \langle \overline{s''^2} \rangle \langle \overline{u_3^s} \overline{s^s} \rangle + 3 \langle \overline{s''^2} \overline{u_3^s} \overline{s^s} \rangle. \quad (99)$$

Note that Eq. (99) represents the so-called Robin boundary condition, also referred to as the impedance boundary condition, or convective boundary condition. It is a weighted combination of Dirichlet and Neumann boundary conditions that relates the quantity in question ($\langle s'^3 \rangle$ in our case) and its derivative normal to the domain boundary.

12 Conclusions

A turbulence kinetic energy – scalar variance (TKESV) turbulence parameterization scheme is developed. The scheme is formulated in terms of two scalars that are approximately conserved for phase changes in the absence of precipitation. These are the total water specific humidity and the liquid water potential temperature. The TKESV scheme carries prognostic transport equations (including the time-rate-of-change and the third-order turbulent transport terms) for the TKE, for the variances of scalar quantities, and for the scalar covariance. The other second-order moments, namely, the Reynolds stress and the scalar fluxes, are determined through the diagnostic algebraic expressions obtained by neglecting the time-rate-of-change and the triple correlations terms in the respective transport equations.

The focus of the present report is on the baseline version of the TKESV scheme (TKESV-Bas). TKESV-Bas is based on the linear (in the second-order moments involved) parameterizations of the pressure-scrambling terms in the Reynolds-stress and scalar-flux equations, the isotropic down-gradient parameterizations of the third-order transport terms in the TKE

and scalar (co)variance equations, and the algebraic interpolation formula for the turbulence length scale that incorporates a correction term due to stable density stratification. The various time scales, namely, the dissipation time scales in the TKE and the scalar (co)variance equations and the return-to-isotropy time scales in the Reynolds-stress and scalar-flux equations, are set proportional to each other and are expressed in terms of turbulence length scale and the TKE. The simplified boundary conditions for the scalar variances and covariance at the underlying surface are used that do not account for the surface heterogeneity within a grid box of a host atmospheric model. The effect of latent heat release/consumption on the buoyancy production/destruction of the Reynolds stress (including half of its trace, the TKE) and of the scalar fluxes is taken into account through the use of a statistical cloud scheme. The cloud scheme makes use of a combination of Gaussian and exponential PDFs of linearized saturation deficit/excess (s variable). The exponential PDF is used at strong grid-box mean undersaturation and is designed to account, in a rather approximate way, for the shallow cumulus regime. In that regime, mixing is known to be dominated by convective plumes although the fractional cloud cover is typically low. The so-called stability functions that appear in the algebraic formulations for the Reynolds stress and scalar fluxes are considered in much detail. The stability functions resulting from the truncated Reynolds-stress and scalar-flux equations (where the third-order and the time-rate-of-change terms are neglected) with the linear parameterizations of the pressure-scrambling terms are ill-behaved over a certain range of governing parameters (e.g. mean velocity shear and mean buoyancy gradient). Using plausible physical arguments, regularized stability functions are developed that are well-behaved over their entire parameter space and cause no pathological behaviour of the Reynolds stress and scalar fluxes.

It is the baseline version of the TKESV scheme in the boundary-layer approximation (i.e. the one-dimensional TKESV-Bas) that is intended for use in NWP models ICON and COSMO in the near future. In the medium-term prospective, an extended version of the scheme (TKESV-Ext) can be used. TKESV-Ext incorporates a number of advanced features discussed in the respective sections of the present report. These include improved formulations of the pressure-scrambling terms and of the third-order transport terms, non-local formulation of the turbulence length scale, lower boundary conditions for the scalar (co)variances that account for the surface heterogeneity and are consistent with the tile approach to compute surface fluxes, allowance for cloud ice through the use of the ice-liquid water potential temperature, and a statistical cloud scheme capable of describing cumulus regimes. The utilization of an advanced statistical cloud scheme, e.g. the scheme proposed by Naumann et al. (2013), requires knowledge of the scalar skewness. A prognostic transport equation for the skewness (triple correlation) of the s variable that accounts for the combined effect of humidity and temperature fluctuations is derived in section 11.

The TKESV-Bas scheme is implemented into the NWP models ICON and COSMO. Testing of TKESV-Bas is underway. Details of the implementation and results from numerical experiments will be reported in subsequent publications. Results of testing of an earlier version of the TKESV scheme through off-line single-column numerical experiments and through parallel experiments with the full-fledged COSMO model (including the entire data assimilation cycle) are reported in Machulskaya and Mironov (2013).

Acknowledgments.

The authors are grateful to Vittorio Canuto, Evgeni Fedorovich, Jean-Francois Geleyn, Vincent Larson, Ann Kristin Naumann, Matthias Raschendorfer, Bodo Ritter, Axel Seifert, and Peter Sullivan for useful discussions.

13 Appendices

Appendix A. Modelling Pressure-Scrambling Terms in the Reynolds-Stress and Scalar-Flux Equations

In this section, we demonstrate how models (parameterizations) of the pressure-scrambling terms in the Reynolds-stress and the scalar-flux equations are developed. By way of illustration, the formulation for the potential temperature θ is considered. Other scalar quantities, e.g. θ_l and q_t , are treated in the same way. We restrict our consideration to the parameterizations of Π_{ij} and $\Pi_{\theta i}$ which are linear in terms of the second-order moments of fluctuating fields. Some non-linear parameterizations of the pressure-scrambling terms are briefly discussed in section 5.1.

Decomposition

Taking the divergence of the transport equation for the fluctuating velocity, a Poisson equation for the fluctuating pressure is obtained. It reads

$$\frac{\partial^2 p'}{\partial x_k^2} = -\frac{\partial^2}{\partial x_k \partial x_l} (u'_k u'_l - \langle u'_k u'_l \rangle) - \beta_k \frac{\partial \theta'}{\partial x_k} - 2\epsilon_{kml} \Omega_m \frac{\partial u'_l}{\partial x_k} - 2 \frac{\partial \langle u_k \rangle}{\partial x_l} \frac{\partial u'_l}{\partial x_k}. \quad (\text{A.1})$$

The fluctuating pressure is decomposed into the contributions due to the non-linear turbulence interactions (denoted by the subscript t), buoyancy (subscript b), the Coriolis effects (subscript c), and mean-velocity shear (subscript s),

$$p' = p'_t + p'_b + p'_c + p'_s, \quad (\text{A.2})$$

which are found by solving the following set of Poisson equations:

$$\begin{aligned} \frac{\partial^2 p'_t}{\partial x_k^2} &= -\frac{\partial^2}{\partial x_k \partial x_l} (u'_k u'_l - \langle u'_k u'_l \rangle), & \frac{\partial^2 p'_b}{\partial x_k^2} &= -\beta_k \frac{\partial \theta'}{\partial x_k}, \\ \frac{\partial^2 p'_c}{\partial x_k^2} &= -2\epsilon_{kml} \Omega_m \frac{\partial u'_l}{\partial x_k}, & \frac{\partial^2 p'_s}{\partial x_k^2} &= -2 \frac{\partial \langle u_k \rangle}{\partial x_l} \frac{\partial u'_l}{\partial x_k}. \end{aligned} \quad (\text{A.3})$$

The (formal) solutions to Eqs. (A.3) read (Chou, 1945; Ristorcelli et al., 1995; Shih, 1996)

$$\begin{aligned} p_t &= \frac{1}{4\pi} \int_{Vol} \left(\frac{\partial^2 u''_k u''_l}{\partial x''_k \partial x''_l} - \frac{\partial^2 \langle u_k u_l \rangle''}{\partial x''_k \partial x''_l} \right) \frac{dVol}{|\mathbf{x} - \mathbf{x}''|}, & p_b &= \frac{1}{4\pi} \int_{Vol} \beta''_k \frac{\partial \theta''}{\partial x''_k} \frac{dVol}{|\mathbf{x} - \mathbf{x}''|}, \\ p_c &= \frac{1}{4\pi} \int_{Vol} 2\epsilon_{kml} \Omega_m \frac{\partial u''_l}{\partial x''_k} \frac{dVol}{|\mathbf{x} - \mathbf{x}''|}, & p_s &= \frac{1}{4\pi} \int_{Vol} 2 \frac{\partial U''_k}{\partial x''_l} \frac{\partial u''_l}{\partial x''_k} \frac{dVol}{|\mathbf{x} - \mathbf{x}''|}, \end{aligned} \quad (\text{A.4})$$

where double-primed quantities are evaluated as functions of the integration variable. Small letters denote turbulent fluctuations, and capital letters denote mean quantities (this notation is used temporarily to avoid confusion between primed and double-primed quantities).

Using (A.2), the pressure-scrambling terms Π_{ij} and $\Pi_{\theta i}$ are decomposed into the contributions due to the non-linear turbulence interactions (superscript t), buoyancy (superscript b), the Coriolis effects (superscript c), and mean-velocity shear (superscript s),

$$\Pi_{ij} = \Pi^t_{ij} + \Pi^b_{ij} + \Pi^c_{ij} + \Pi^s_{ij}, \quad \Pi_{\theta i} = \Pi^t_{\theta i} + \Pi^b_{\theta i} + \Pi^c_{\theta i} + \Pi^s_{\theta i}. \quad (\text{A.5})$$

With due regard for Eqs. (A.4) these contributions are given by

$$\begin{aligned}
\Pi_{ij}^t &= - \left\langle p_t \left(\frac{\partial u_i}{\partial x_j} + \frac{\partial u_j}{\partial x_i} \right) \right\rangle = \frac{1}{4\pi} \int_{Vol} \left(\frac{\partial^3 \langle u_k'' u_l'' u_i \rangle}{\partial x_k'' \partial x_l'' \partial x_j''} + \frac{\partial^3 \langle u_k'' u_l'' u_j \rangle}{\partial x_k'' \partial x_l'' \partial x_i''} \right) \frac{dVol}{|\mathbf{x} - \mathbf{x}''|}, \\
\Pi_{ij}^b &= - \left\langle p_b \left(\frac{\partial u_i}{\partial x_j} + \frac{\partial u_j}{\partial x_i} \right) \right\rangle = \frac{1}{4\pi} \int_{Vol} \beta_k'' \left(\frac{\partial^2 \langle \theta'' u_i \rangle}{\partial x_k'' \partial x_j''} + \frac{\partial^2 \langle \theta'' u_j \rangle}{\partial x_k'' \partial x_i''} \right) \frac{dVol}{|\mathbf{x} - \mathbf{x}''|}, \\
\Pi_{ij}^c &= - \left\langle p_c \left(\frac{\partial u_i}{\partial x_j} + \frac{\partial u_j}{\partial x_i} \right) \right\rangle = \frac{1}{4\pi} \int_{Vol} 2\epsilon_{kml} \Omega_m \left(\frac{\partial^2 \langle u_l'' u_i \rangle}{\partial x_k'' \partial x_j''} + \frac{\partial^2 \langle u_l'' u_j \rangle}{\partial x_k'' \partial x_i''} \right) \frac{dVol}{|\mathbf{x} - \mathbf{x}''|}, \\
\Pi_{ij}^s &= - \left\langle p_s \left(\frac{\partial u_i}{\partial x_j} + \frac{\partial u_j}{\partial x_i} \right) \right\rangle = \frac{1}{4\pi} \int_{Vol} 2 \frac{\partial U_k''}{\partial x_l''} \left(\frac{\partial^2 \langle u_l'' u_i \rangle}{\partial x_k'' \partial x_j''} + \frac{\partial^2 \langle u_l'' u_j \rangle}{\partial x_k'' \partial x_i''} \right) \frac{dVol}{|\mathbf{x} - \mathbf{x}''|}, \quad (\text{A.6})
\end{aligned}$$

and

$$\begin{aligned}
\Pi_{\theta i}^t &= \left\langle \theta \frac{\partial p_t}{\partial x_i} \right\rangle = \frac{1}{4\pi} \int_{Vol} \frac{\partial^3 \langle u_k'' u_l'' \theta \rangle}{\partial x_k'' \partial x_l'' \partial x_i''} \frac{dVol}{|\mathbf{x} - \mathbf{x}''|}, \\
\Pi_{\theta i}^b &= \left\langle \theta \frac{\partial p_b}{\partial x_i} \right\rangle = \frac{1}{4\pi} \int_{Vol} \beta_k'' \frac{\partial^2 \langle \theta'' \theta \rangle}{\partial x_k'' \partial x_i''} \frac{dVol}{|\mathbf{x} - \mathbf{x}''|}, \\
\Pi_{\theta i}^c &= \left\langle \theta \frac{\partial p_c}{\partial x_i} \right\rangle = \frac{1}{4\pi} \int_{Vol} 2\epsilon_{kml} \Omega_m \frac{\partial^2 \langle u_l'' \theta \rangle}{\partial x_k'' \partial x_i''} \frac{dVol}{|\mathbf{x} - \mathbf{x}''|}, \\
\Pi_{\theta i}^s &= \left\langle \theta \frac{\partial p_s}{\partial x_i} \right\rangle = \frac{1}{4\pi} \int_{Vol} 2 \frac{\partial U_k''}{\partial x_l''} \frac{\partial^2 \langle u_l'' \theta \rangle}{\partial x_k'' \partial x_i''} \frac{dVol}{|\mathbf{x} - \mathbf{x}''|}, \quad (\text{A.7})
\end{aligned}$$

where quantities without double primes are evaluated at the point where Π_{ij} and $\Pi_{\theta i}$ are determined. The Π_{ij}^t and $\Pi_{\theta i}^t$ contributions are often referred to as slow parts and Π_{ij}^b , Π_{ij}^c , Π_{ij}^s , $\Pi_{\theta i}^b$, $\Pi_{\theta i}^c$ and $\Pi_{\theta i}^s$ as rapid parts, respectively, of the pressure-scrambling terms.

The integrals in Eqs. (A.6) and (A.7) are taken over the entire flow domain. In practice, however, the two-point correlations are assumed to diminish rapidly with distance from the point where the pressure terms are evaluated. Then, the volume of integration is reduced to a small region in the immediate vicinity of that point, and Π_{ij} and $\Pi_{\theta i}$ are modelled in terms of local quantities.

Slow Parts of Π_{ij} and $\Pi_{\theta i}$

We utilize the return-to-isotropy parameterizations (Rotta, 1951; Monin, 1965) for the slow (return-to-isotropy) contributions to the pressure-scrambling terms. They read

$$\Pi_{ij}^t = C_t^u \frac{\langle u_i u_j \rangle - \frac{2}{3} \delta_{ij} e}{\tau_{ru}} = C_t^u \frac{a_{ij}}{\tau_{ru}}, \quad \Pi_{\theta i}^t = C_t^\theta \frac{\langle u_i \theta \rangle}{\tau_{r\theta}}, \quad (\text{A.8})$$

where τ_{ru} and $\tau_{r\theta}$ are the relaxation return-to-isotropy time scales, and C_t^u and C_t^θ are dimensionless constants.

It is customary in geophysical and engineering applications to take the relaxation time scales τ_{ru} and $\tau_{r\theta}$ to be proportional to the TKE dissipation time scale $\tau_\epsilon = e/\epsilon$, that is $\tau_{ru} = \tau_{r\theta} = \tau_\epsilon$, where dimensionless proportionality constants are set to one as they always occur in combination with the other constants. Estimates of C_t^u and C_t^θ vary over a wide range. Values of C_t^u from 1 to 3 and of C_t^θ from 2 to 10 have been proposed (see e.g. Launder et al., 1975; Zeman and Tennekes, 1975; Zeman and Lumley, 1976; Dakos and Gibson, 1987; Speziale et al., 1991; Kenjereš and Hanjalić, 1995; Hanjalić et al., 1996; Craft et al., 1996; Dol et al., 1997; Hanjalić, 1999; Girimaji, 2000; Mironov, 2001; Hanjalić, 2002; Umlauf and Burchard, 2005). We adopt the estimates of $C_t^u = 1.8$ and $C_t^\theta = 5.0$, keeping in mind that some tuning may appear to be necessary. In particular, the estimate of $C_t^\theta = 3.0$ is found by a number of authors to be more appropriate for (mostly) buoyancy-driven flows.

Buoyancy Contributions to Π_{ij} and $\Pi_{\theta i}$

The formal expressions for the buoyancy, the Coriolis and the mean-velocity shear contributions (the so-called rapid contributions) to the pressure-scrambling terms are given by the second, the third and the fourth members of Eqs. (A.6) and (A.7), respectively. Assuming that the mean fields are approximately homogeneous over a distance of the order of the integral turbulence length scale, β_k can be taken outside the integrals (the same is true for $2\partial U_k/\partial x_l$ in the expressions for the mean-velocity shear contributions to the pressure-scrambling terms considered below). Then, the buoyancy contributions to the pressure-scrambling terms can be represented in the form (see e.g. Shih, 1996)

$$\Pi_{ij}^b = -\beta_k \left(X_{kij}^b + X_{kji}^b \right), \quad \Pi_{\theta i}^b = -\beta_k Y_{ki}^b. \quad (\text{A.9})$$

where, in view of the second members of Eqs. (A.6) and (A.7),

$$X_{kij}^b = -\frac{1}{4\pi} \int_{Vol} \frac{\partial^2 \langle \theta'' u_i \rangle}{\partial x_k'' \partial x_j''} \frac{dVol}{|\mathbf{x} - \mathbf{x}''|}, \quad Y_{ki}^b = -\frac{1}{4\pi} \int_{Vol} \frac{\partial^2 \langle \theta'' \theta \rangle}{\partial x_k'' \partial x_i''} \frac{dVol}{|\mathbf{x} - \mathbf{x}''|}. \quad (\text{A.10})$$

The tensors X_{kij} and Y_{ki} satisfy the following constraints:

$$\text{symmetry} \quad X_{kij}^b = X_{jik}^b, \quad Y_{ki}^b = Y_{ik}^b, \quad (\text{A.11})$$

$$\text{continuity} \quad X_{kii}^b = 0, \quad (\text{A.12})$$

$$\text{normalization} \quad X_{kik}^b = \langle u_i \theta \rangle, \quad Y_{kk}^b = \langle \theta^2 \rangle. \quad (\text{A.13})$$

Within the limits of linear approximations (in the second-order moments of fluctuating fields, i.e. in $\langle u_i u_j \rangle$, $\langle u_i \theta \rangle$ and $\langle \theta^2 \rangle$), the most general forms of X_{kij}^b and Y_{ki}^b that satisfy the symmetry constraints (A.11) are the following tensor polynomials:

$$X_{kij}^b = \alpha_1 \delta_{kj} \langle u_i \theta \rangle + \alpha_2 (\delta_{ki} \langle u_j \theta \rangle + \delta_{ji} \langle u_k \theta \rangle), \quad Y_{ki}^b = \gamma_1 \delta_{ki} \langle \theta^2 \rangle. \quad (\text{A.14})$$

Satisfying the continuity (A.12) and the normalization (A.13) constraints, we obtain $\alpha_1 = 2/5$, $\alpha_2 = -1/10$ and $\gamma_1 = 1/3$. With these estimates, Eqs. (A.9) and (A.14) yield the following formulations:

$$\Pi_{ij}^b = -\frac{3}{10} \left(\beta_i \langle u_j \theta \rangle + \beta_j \langle u_i \theta \rangle - \frac{2}{3} \delta_{ij} \beta_k \langle u_k \theta \rangle \right), \quad \Pi_{\theta i}^b = -\frac{1}{3} \beta_i \langle \theta^2 \rangle. \quad (\text{A.15})$$

Note that Eq. (A.15) contains no free parameters; the numerical values of all dimensionless coefficients in the expressions for Π_{ij}^b and $\Pi_{\theta i}^b$ are fixed by mathematical constraints.

Coriolis Contributions to Π_{ij} and $\Pi_{\theta i}$

Parameterizations of the Coriolis contributions to the pressure-scrambling terms are developed analogously to parameterizations of the buoyancy contributions. The Coriolis contributions are represented as

$$\Pi_{ij}^c = -2\epsilon_{kml}\Omega_m (X_{klij}^c + X_{klji}^c), \quad \Pi_{\theta i}^c = -2\epsilon_{kml}\Omega_m Y_{kli}^c, \quad (\text{A.16})$$

where

$$X_{klij}^c = -\frac{1}{4\pi} \int_{Vol} \frac{\partial^2 \langle u_l'' u_i \rangle}{\partial x_k'' \partial x_j''} \frac{dVol}{|\mathbf{x} - \mathbf{x}''|}, \quad Y_{kli}^c = -\frac{1}{4\pi} \int_{Vol} \frac{\partial^2 \langle u_l'' \theta \rangle}{\partial x_k'' \partial x_i''} \frac{dVol}{|\mathbf{x} - \mathbf{x}''|}. \quad (\text{A.17})$$

The tensor Y_{kli}^c is exactly the same tensor as X_{kij}^b that appears in the parameterization of Π_{ij}^b , see Eqs. (A.9)–(A.14). The tensor X_{klij}^c satisfies the following constraints:

$$\text{symmetry} \quad X_{klij}^c = X_{kilj}^c, \quad X_{klij}^c = X_{jlik}^c, \quad (\text{A.18})$$

$$\text{continuity} \quad X_{klli}^c = 0, \quad (\text{A.19})$$

$$\text{normalization} \quad X_{klik}^c = \langle u_l u_i \rangle. \quad (\text{A.20})$$

Within the limits of a linear approximation, the most general form of X_{klij}^c that satisfies the symmetry constraints (A.18) is

$$\begin{aligned} X_{klij}^c &= 2e [\alpha_1 \delta_{li} \delta_{kj} + \alpha_2 (\delta_{lk} \delta_{ji} + \delta_{lj} \delta_{ki})] \\ &+ \alpha_3 \delta_{li} a_{kj} + \alpha_4 \delta_{kj} a_{li} + \alpha_5 (\delta_{ij} a_{kl} + \delta_{lj} a_{ki} + \delta_{ki} a_{lj} + \delta_{lk} a_{ji}). \end{aligned} \quad (\text{A.21})$$

Satisfying the continuity (A.19) and the normalization (A.20) constraints, we obtain $\alpha_1 = 2/15$, $\alpha_2 = -1/30$, $\alpha_3 = -1/3 - 11\alpha_5/3$ and $\alpha_4 = 1/3 - 4\alpha_5/3$. Using Eqs. (A.16), (A.14) and (A.21) along with these estimates, we obtain

$$\Pi_{ij}^c = -\frac{2}{3} (2 + 7\alpha_5) (\epsilon_{imk} \Omega_m a_{kj} + \epsilon_{jmk} \Omega_m a_{ki}), \quad \Pi_{\theta i}^c = -\epsilon_{imk} \Omega_m \langle u_k \theta \rangle, \quad (\text{A.22})$$

with only one free coefficient α_5 . An estimate of $\alpha_5 = -1/10$ was adopted in a number of studies (e.g Shih, 1996; Hanjalić, 1999).

Mean-Velocity Shear Contributions to Π_{ij} and $\Pi_{\theta i}$

The contributions to the pressure-scrambling terms due to the mean-velocity shear are parameterized in the same way as the contributions due to the Coriolis effects. The mean-velocity shear contributions are represented as

$$\Pi_{ij}^s = -2 \frac{\partial U_k}{\partial x_l} (X_{klij}^s + X_{klji}^s), \quad \Pi_{\theta i}^s = -2 \frac{\partial U_k}{\partial x_l} Y_{kli}^s, \quad (\text{A.23})$$

where

$$X_{klij}^s = -\frac{1}{4\pi} \int_{Vol} \frac{\partial^2 \langle u_l'' u_i \rangle}{\partial x_k'' \partial x_j''} \frac{dVol}{|\mathbf{x} - \mathbf{x}''|}, \quad Y_{kli}^s = -\frac{1}{4\pi} \int_{Vol} \frac{\partial^2 \langle u_l'' \theta \rangle}{\partial x_k'' \partial x_i''} \frac{dVol}{|\mathbf{x} - \mathbf{x}''|}. \quad (\text{A.24})$$

As is easy to see, the tensors X_{klij}^s and Y_{kli}^s are exactly the same tensors as X_{klij}^c and Y_{kli}^c , respectively, that appear in the parameterization of the Coriolis contributions to the

pressure-scrambling terms. Using the results of the previous sub-section, we obtain

$$\begin{aligned}\Pi_{ij}^s &= -\frac{4}{5}S_{ij}e + 6\alpha_5 \left(S_{ik}a_{kj} + S_{jk}a_{ki} - \frac{2}{3}\delta_{ij}S_{kl}a_{kl} \right) \\ &\quad - \frac{2}{3}(2 + 7\alpha_5)(W_{ik}a_{kj} + W_{jk}a_{ki}), \\ \Pi_{\theta i}^s &= -\left(\frac{3}{5}S_{ik} + W_{ik} \right) \langle u'_k \theta' \rangle,\end{aligned}\tag{A.25}$$

where S_{ij} and W_{ij} are the symmetric and the antisymmetric parts, respectively, of the mean-velocity gradient tensor.

Resulting Expressions for Π_{ij} and $\Pi_{\theta i}$

Combining Eqs. (A.8) with $\tau_{ru} = \tau_{r\theta} = \tau_\epsilon$, (A.15), (A.22) and (A.25) and returning to the notation with primes, we obtain the following parameterizations of the pressure-scrambling terms in the Reynolds-stress and the temperature-flux equations that are linear in the second-order moments of fluctuating fields:

$$\begin{aligned}\Pi_{ij} &= C_t^u \frac{a_{ij}}{\tau_\epsilon} \\ &\quad - C_{s1}^u S_{ij}e - C_{s2}^u \left(S_{ik}a_{kj} + S_{jk}a_{ki} - \frac{2}{3}\delta_{ij}S_{kl}a_{kl} \right) - C_{s3}^u (W_{ik}a_{kj} + W_{jk}a_{ki}) \\ &\quad - C_b^u \left(\beta_i \langle u'_j \theta' \rangle + \beta_j \langle u'_i \theta' \rangle - \frac{2}{3}\delta_{ij}\beta_k \langle u'_k \theta' \rangle \right) \\ &\quad - 2C_c^u (\epsilon_{imk}\Omega_m a_{kj} + \epsilon_{jmk}\Omega_m a_{ki}),\end{aligned}\tag{A.26}$$

$$\Pi_{\theta i} = C_t^\theta \frac{\langle u'_i \theta' \rangle}{\tau_\epsilon} - \left(C_{s1}^\theta S_{ij} + C_{s2}^\theta W_{ij} \right) \langle u'_j \theta' \rangle - C_b^\theta \beta_i \langle \theta'^2 \rangle - 2C_c^\theta \epsilon_{imj}\Omega_m \langle u'_j \theta' \rangle,\tag{A.27}$$

where $C_t^u = 1.8$, $C_{s1}^u = 4/5$, $C_{s2}^u = -6\alpha_5$, $C_{s3}^u = \frac{2}{3}(2 + 7\alpha_5)$, $C_b^u = 3/10$, $C_c^u = \frac{1}{3}(2 + 7\alpha_5)$, $C_t^\theta = 5.0$, $C_{s1}^\theta = 3/5$, $C_{s2}^\theta = 1$, $C_b^\theta = 1/3$ and $C_c^\theta = 1/2$ are dimensionless coefficients. The only yet undetermined coefficient α_5 can be estimated by satisfying one or the other additional constraint. One way to determine α_5 is to require that the second-moment equations of the TKESV scheme subject to the surface-layer approximation yield the classical logarithmic velocity profile. Details are given in next sub-section.

Logarithmic Velocity Profile Constraints

Consider a fluid layer just above a flat rigid surface where (i) turbulence is stationary and horizontally homogeneous, and (ii) the effects of buoyancy, reference frame rotation, advection and third-order transport are negligible. It is further assumed that (iii) the surface layer is a small portion of the PBL, so that the directional wind shear is negligible, and turbulent fluxes can be considered approximately height-constant, equal to their surface values (in other words, changes of fluxes over the surface layer are small compared to their changes over the entire PBL). Under the assumptions (i)–(iii), the TKE equation (12) reduces to a balance between the shear production and the dissipation,

$$-\langle u'_i u'_k \rangle \frac{\partial \langle u_i \rangle}{\partial x_k} - \epsilon = 0,\tag{A.28}$$

and the Reynolds-stress equation (18) with due regard for the parameterization (21) of the pressure-scrambling term reduces to a balance between the shear production and pressure redistribution,

$$\begin{aligned} & -C_t^u \frac{a_{ij}}{\tau_\epsilon} - \left(\frac{4}{3} - C_{s1}^u \right) e S_{ij} - (1 - C_{s2}^u) \left(a_{ik} S_{jk} + a_{jk} S_{ik} - \frac{2}{3} \delta_{ij} a_{kl} S_{kl} \right) \\ & - (1 - C_{s3}^u) (a_{ik} W_{jk} + a_{jk} W_{ik}) = 0, \end{aligned} \quad (\text{A.29})$$

where the deviatoric part ϵ_{ij}^d of the Reynolds-stress dissipation tensor is incorporated into the parameterization of the slow part Π_{ij}^t of the pressure redistribution term.

In the near-surface layer subject to the above assumptions (i)–(iii), the mean-velocity profile is logarithmic, and the following well-known relations hold true:

$$l = \kappa x_3, \quad -\langle u'_1 u'_3 \rangle = u_*^2, \quad e = C_e u_*^2, \quad \frac{\partial \langle u_1 \rangle}{\partial x_3} = \frac{u_*}{\kappa x_3}. \quad (\text{A.30})$$

Here, κ is the von Kármán constant whose conventional value is 0.4, C_e is a dimensionless constants, and u_* is the surface friction velocity. The x_1 horizontal axis is taken to be aligned with the surface stress so that $\langle u'_2 u'_3 \rangle = 0$ and $\langle u_2 \rangle = 0$ (in the horizontally-homogeneous layer over a rigid surface, $\langle u_3 \rangle = 0$ by virtue of continuity).

It is straightforward to verify by substituting (A.30) into (A.28), where ϵ is expressed in terms of e and l through (31) and (35), that the logarithmic-layer TKE budget, Eq. (A.28), is satisfied if

$$C_\epsilon = C_e^{-3/2}. \quad (\text{A.31})$$

Using the estimate of $C_e = 3.33$ (e.g. Umlauf and Burchard, 2003; Umlauf et al., 2003), we obtain $C_\epsilon = 0.165$.

With the x_1 -axis aligned with $\langle u'_1 u'_3 \rangle$, the only non-zero components of S_{ij} and W_{ij} are $S_{13} = S_{31} = W_{13} = -W_{31}$. Then, Eq. (A.29) yields the following expressions for the Reynolds-stress components in the near-surface log-layer:

$$a_{12} = a_{23} = 0, \quad (\text{A.32})$$

$$\begin{aligned} & \left\{ 1 - \frac{4}{3} \left(\frac{1 - C_{s2}^u}{C_t^u} \right)^2 (\tau_\epsilon S_{13})^2 + 4 \left(\frac{1 - C_{s3}^u}{C_t^u} \right)^2 (\tau_\epsilon W_{13})^2 \right\} a_{13} \\ & + \frac{1}{C_t^u} \left(\frac{4}{3} - C_{s1}^u \right) \tau_\epsilon S_{13} e = 0, \end{aligned} \quad (\text{A.33})$$

$$\begin{aligned} & a_{11} + \frac{\tau_\epsilon}{C_t^u} \left[\frac{2}{3} (1 - C_{s2}^u) S_{13} + 2 (1 - C_{s3}^u) W_{13} \right] a_{13} = 0, \\ & a_{22} - \frac{\tau_\epsilon}{C_t^u} \left[\frac{4}{3} (1 - C_{s2}^u) S_{13} \right] a_{13} = 0, \\ & a_{33} + \frac{\tau_\epsilon}{C_t^u} \left[\frac{2}{3} (1 - C_{s2}^u) S_{13} - 2 (1 - C_{s3}^u) W_{13} \right] a_{13} = 0, \end{aligned} \quad (\text{A.34})$$

Substituting Eqs. (17), (35), (A.30) and (A.31) along with the expressions $S_{13} = W_{13} = \frac{1}{2} \frac{\partial \langle u_1 \rangle}{\partial x_3}$, $C_{s2}^u = -6\alpha_5$ and $C_{s3}^u = \frac{2}{3}(2 + 7\alpha_5)$ into Eq. (A.33), we obtain the following quadratic equation for the disposable coefficient α_5 :

$$44\alpha_5^2 - 4\alpha_5 - \left[1 + \frac{9C_t^u}{4} \left(\frac{4}{3} - C_{s1}^u \right) - \frac{9}{2} \left(\frac{C_t^u}{C_e} \right)^2 \right] = 0. \quad (\text{A.35})$$

The physically meaningful negative root of Eq. (A.35) is given by

$$\alpha_5 = \frac{1}{22} \left[1 - (1 + 11C_\alpha^*)^{1/2} \right], \quad C_\alpha^* = 1 + \frac{9C_t^u}{4} \left(\frac{4}{3} - C_{s1}^u \right) - \frac{9}{2} \left(\frac{C_t^u}{C_e} \right)^2. \quad (\text{A.36})$$

Using $C_{s1}^u = 4/5$, $C_t^u = 1.8$ and $C_e = 3.33$, we obtain $\alpha_5 = -0.164$.

With due regard for Eqs. (17), (35), (A.30), (A.31) and (A.33) and the expressions for $S_{13} = W_{13}$, C_{s2}^u and C_{s3}^u given above, Eqs. (A.34) yield the following estimates of the velocity variances in the near-surface log-layer:

$$\begin{aligned} \langle u_1'^2 \rangle &= \frac{2C_e}{3} \left(1 - \frac{4\alpha_5}{C_t^u} \right) u_*^2, \\ \langle u_2'^2 \rangle &= \frac{2C_e}{3} \left(1 - \frac{1 + 6\alpha_5}{C_t^u} \right) u_*^2, \\ \langle u_3'^2 \rangle &= \frac{2C_e}{3} \left(1 + \frac{1 + 10\alpha_5}{C_t^u} \right) u_*^2. \end{aligned} \quad (\text{A.37})$$

It should be pointed out that with the above estimates of C_t^u , C_e and α_5 the velocity variances are always non-negative, i.e. the realizability requirements are satisfied.

Appendix B. Disposable Constants and Parameters of TKESV-Bas

Estimates of disposable constants and parameters of the baseline version of the TKESV scheme are summarized in Table 1. The values of $C_{s2}^u = 3/5$ and $C_{s3}^u = 13/15$ correspond to $\alpha_5 = -1/10$ [Eq. (26) with $F_l = 0$], i.e. to the one-component or two-component limit of anisotropic turbulence. These optional estimates are given in parentheses.

Table 1: Disposable Constants and Parameters of TKESV-Bas

Constant/ Parameter	Estimate	Equation for	Equation Nos.	Comments
C_e^d	0.1	e	(60)	
$C_{\theta\theta}^d$	0.1	$\langle \theta_l'^2 \rangle$	(61)	
C_{qq}^d	0.1	$\langle q_t'^2 \rangle$	(62)	
$C_{\theta q}^d$	0.1	$\langle \theta_l' q_t' \rangle$	(63)	
R_τ	0.5	$\langle \theta_l'^2 \rangle, \langle q_t'^2 \rangle,$ $\langle \theta_l' q_t' \rangle$	(61)–(63)	
C_ϵ	0.165	τ_ϵ	(64)	$= C_e^{-3/2}$
κ	0.4	l	(64)	
C_{lb}	1.0	l	(64)	
l_∞	200 m	l	(64)	
C_t^u	1.8	$\langle u_i' u_j' \rangle$	(65)	
C_{s1}^u	4/5	$\langle u_i' u_j' \rangle$	(65)	
C_{s2}^u	0.986 (3/5)	$\langle u_i' u_j' \rangle$	(65)	$= -6\alpha_5$
C_{s3}^u	0.567 (13/15)	$\langle u_i' u_j' \rangle$	(65)	$= \frac{2}{3}(2 + 7\alpha_5)$
C_b^u	3/10	$\langle u_i' u_j' \rangle$	(65)	
C_t^θ	5.0	$\langle u_i' \theta_l' \rangle$	(66)	
C_{s1}^θ	3/5	$\langle u_i' \theta_l' \rangle$	(66)	
C_{s2}^θ	1	$\langle u_i' \theta_l' \rangle$	(66)	
C_b^θ	1/3	$\langle u_i' \theta_l' \rangle$	(66)	
C_t^q	5.0	$\langle u_i' q_t' \rangle$	(67)	
C_{s1}^q	3/5	$\langle u_i' q_t' \rangle$	(67)	
C_{s2}^q	1	$\langle u_i' q_t' \rangle$	(67)	
C_b^q	1/3	$\langle u_i' q_t' \rangle$	(67)	
C_e	3.33		(A.30)	Required to estimate C_ϵ through (A.31) and α_5 through (A.36)
α_5	-0.164 (-1/10)		(A.36), or (26)	Required to estimate C_{s2}^u and C_{s3}^u

Appendix C. Turbulence Potential Energy

The quantity P defined by Eqs. (73) and (74) naturally appears in the equations for the Reynolds stress and scalar fluxes. It is characteristic of the potential energy of turbulent flow and can therefore be referred to as the turbulence potential energy (TPE). By way of illustration, consider the temperature-stratified fluid where potential temperature θ is the only thermodynamic variable that affects buoyancy. Then, $q_l = 0$, $q_t = 0$, $\theta_l = \theta$, $\mathcal{I}_\theta = 1$, $N^2 = -\beta_3 \partial \langle \theta \rangle / \partial x_3$, and Eq. (73) is simplified to give

$$P = \tau_\epsilon^2 \beta_3^2 \langle \theta'^2 \rangle. \quad (\text{C.1})$$

The definition of TPE is not unique, however. For example, the following definition of TPE has been used in the analyses of atmospheric turbulence (see e.g. Zilitinkevich et al., 2007; Mauritsen et al., 2007):

$$P_N = \frac{1}{2} N^{-2} \beta_3^2 \langle \theta'^2 \rangle. \quad (\text{C.2})$$

A transport equation for P_N can be readily derived using the transport equation for buoyancy (potential temperature) variance. Assuming that N^2 varies slowly in space and time and using the boundary-layer approximation, we obtain

$$\frac{\partial P_N}{\partial t} = \beta_3 \langle u'_3 \theta' \rangle - \frac{1}{2} \frac{\partial}{\partial x_3} \left(\frac{\beta_3^2}{N^2} \langle u'_3 \theta'^2 \rangle \right) - \frac{\beta_3^2}{N^2} \epsilon_{\theta\theta}, \quad (\text{C.3})$$

In the boundary-layer approximation, the transport equation for the TKE, $e \equiv \frac{1}{2} \langle u_i'^2 \rangle$, reads

$$\begin{aligned} \frac{\partial e}{\partial t} = & -\beta_3 \langle u'_3 \theta' \rangle - \left(\langle u'_1 u'_3 \rangle \frac{\partial \langle u_1 \rangle}{\partial x_3} + \langle u'_2 u'_3 \rangle \frac{\partial \langle u_2 \rangle}{\partial x_3} \right) \\ & - \frac{\partial}{\partial x_3} \left(\frac{1}{2} \langle u'_3 u_i'^2 \rangle + \langle u'_3 p' \rangle \right) - \epsilon. \end{aligned} \quad (\text{C.4})$$

The term $-\beta_3 \langle u'_3 \theta' \rangle$ on the r.h.s. of Eq. (C.4) (the buoyancy flux) appears with the opposite sign on the r.h.s. of Eq. (C.3). It describes the conversion of the TPE into the TKE that occurs in unstable density (buoyancy) stratification, and vice versa where the stratification is stable. The use of TPE defined through Eq. (C.2) is advantageous as it makes the TPE transport equation particularly convenient and facilitates the analysis of turbulence energetics. For example, Eqs. (C.3) and (C.4) can be added, leading to the total (TPE+TKE) turbulence energy equation that has been used by some researchers in the analyses of stably-stratified turbulent flows (e.g. Zilitinkevich et al., 2007; Mauritsen et al., 2007; Zilitinkevich et al., 2009, 2013).

Note, however, that the TPE defined through Eq. (C.2) is a well-defined quantity (non-negative and finite) only if the flow is stably stratified ($N^2 > 0$). The quantity P_N bears a close analogy to the available potential energy defined as a part of the total potential energy of the stratified flow that can be converted into kinetic energy (see e.g. Vallis, 2006, for a comprehensive discussion). Where the buoyancy stratification is neutral ($N^2 = 0$) or unstable ($N^2 < 0$), P_N is infinite or negative and is not really convenient to use. For the Earth's atmosphere, where the buoyancy stratification is due to both temperature and humidity and the thermodynamics is strongly complicated by phase changes, a TPE transport equation as simple and elegant as Eq. (C.3) is difficult to derive. It is therefore advantageous to work with the variance and covariance equations for the scalar quantities that can be derived from the first principles in a fairly straightforward way. The quantity P defined by Eqs. (73)

and (74), or by Eq. (C.1) in the case of temperature-stratified flow, is merely a diagnostic quantity that naturally appears in the equations for the Reynolds stress and scalar fluxes. It has the physical meaning of turbulence potential energy but a separate transport equation for P is actually not needed.

Appendix D. Stability Functions in Shear-Free Flow

Consider a simple case of shear-free flow. With $S_{ij} = W_{ij} = 0$ (no mean velocity shear), the Reynolds-stress and scalar-flux equations (65)–(67) are considerably simplified (recall that the reference frame rotation is also neglected, $\Omega_i = 0$). The off-diagonal components of the Reynolds stress tensor are zero, $\langle u'_1 u'_2 \rangle = \langle u'_1 u'_3 \rangle = \langle u'_2 u'_3 \rangle = 0$, and so are the horizontal components of the scalar fluxes, $\langle u'_1 \theta'_l \rangle = \langle u'_2 \theta'_l \rangle = 0$ and $\langle u'_1 q'_l \rangle = \langle u'_2 q'_l \rangle = 0$. The diagonal components of the Reynolds stress tensor (i.e. the velocity variances) are given by

$$\langle u'^2_1 \rangle = \langle u'^2_2 \rangle = \frac{2}{3}e - \frac{2(1 - C^u_b)}{3C^u_t} \tau_\epsilon (-\beta_3 \langle u'_3 \theta'_v \rangle), \quad (\text{C.1})$$

$$\langle u'^2_3 \rangle = \frac{2}{3}e + \frac{4(1 - C^u_b)}{3C^u_t} \tau_\epsilon (-\beta_3 \langle u'_3 \theta'_v \rangle), \quad (\text{C.2})$$

and the vertical scalar fluxes are given by

$$\langle u'_3 \theta'_l \rangle = -\mathcal{F}_{\text{H1}} \tau_\epsilon e \frac{\partial \langle \theta_l \rangle}{\partial x_3} - \mathcal{F}_{\text{H2}} \tau_\epsilon \beta_3 \langle \theta'_l \theta'_v \rangle, \quad (\text{C.3})$$

$$\langle u'_3 q'_l \rangle = -\mathcal{F}_{\text{H1}} \tau_\epsilon e \frac{\partial \langle q_l \rangle}{\partial x_3} - \mathcal{F}_{\text{H2}} \tau_\epsilon \beta_3 \langle q'_l \theta'_v \rangle, \quad (\text{C.4})$$

$$\mathcal{F}_{\text{H1}} = \left[1 + \frac{4(1 - C^u_b)}{3C^u_t C^\theta_t} \tau_\epsilon^2 N^2 \right]^{-1} \left[\frac{2}{3C^\theta_t} + \frac{4(1 - C^u_b)(1 - C^\theta_b)P}{3C^u_t (C^\theta_t)^2 e} \right], \quad (\text{C.5})$$

$$\mathcal{F}_{\text{H2}} = \frac{1 - C^\theta_b}{C^\theta_t}, \quad (\text{C.6})$$

where N^2 and P are given by Eqs. (72)–(74), and $C^q_t = C^\theta_t$ and $C^q_b = C^\theta_b$ are used to obtain Eq. (C.4). In the shear-free limit, \mathcal{F}_{H2} is merely a constant and \mathcal{F}_{H1} is a function of $\tau_\epsilon^2 N^2$ and P/e . There is no problem with the stability function \mathcal{F}_{H1} in the case of stable buoyancy stratification, where N^2 is positive (with the x_3 -axis directed vertically upward, $\beta_3 < 0$). If the stratification is unstable, $N^2 < 0$ and the expression in the denominator (first set of square brackets) on the the r.h.s. of Eq. (C.5) may approach zero or become negative, leading to physically meaningless values of \mathcal{F}_{H1} .

A similar problem with the stability functions is encountered within the framework of a one-equation closure scheme that carries prognostic transport equation for the TKE whereas all other second-moment equations, including the scalar-variance and scalar-covariance equations, are reduced to diagnostic algebraic expressions. By way of illustration, we further simplify the discussion and consider a temperature-stratified flow, where moisture effects are neglected and $\theta_l = \theta$. Within the framework of the one-equation TKE scheme, the following down-gradient formulation for the vertical potential-temperature flux holds:

$$\langle u'_3 \theta'_l \rangle = -\mathcal{F}_{\text{H}} \tau_\epsilon e \frac{\partial \langle \theta \rangle}{\partial x_3}, \quad (\text{C.7})$$

$$\mathcal{F}_{\text{H}} = \frac{2}{3C^\theta_t} \left\{ 1 + \left[\frac{4(1 - C^u_b)}{3C^u_t C^\theta_t} + 2R_\tau \frac{1 - C^\theta_b}{C^\theta_t} \right] \tau_\epsilon^2 N^2 \right\}^{-1}. \quad (\text{C.8})$$

As Eq. (C.8) suggests, \mathcal{F}_{H} may become infinite or negative in convective conditions, where $N^2 < 0$.

References

- Abdella, K. and McFarlane, N. (1999). Reply. *J. Atmos. Sci.*, 56:3482–3483.
- Abdella, K. and Petersen, A. C. (2000). Third-order moment closure through the mass-flux approach. *Boundary-Layer Meteorol.*, 95:303–318.
- Baldauf, M., Seifert, A., Förstner, J., Majewski, D., Raschendorfer, M., and Reinhardt, T. (2011). Operational convective-scale numerical weather prediction with the COSMO model: description and sensitivities. *Mon. Weather Rev.*, 139:3887–3905.
- Bannon, P. R. (2007). Virtualization. *J. Atmos. Sci.*, 64:1405–1409.
- Bechtold, P., Cuijpers, J. W. M., Mascart, P., and Trouilhet, P. (1995). Modeling of trade wind cumuli with a low-order turbulence model: Toward a unified description of Cu and Sc clouds in meteorological models. *J. Atmos. Sci.*, 52:455–463.
- Bechtold, P., Fravallo, C., and Pinty, J. P. (1992). Modeling of trade wind cumuli with a low-order turbulence model: Toward a unified description of Cu and Sc clouds in meteorological models. *J. Atmos. Sci.*, 49:1723–1744.
- Betts, A. K. (1973). Non-precipitating cumulus convection and its parameterization. *Quart. J. Roy. Meteorol. Soc.*, 99:178–196.
- Betts, A. K. (1986). A new convective adjustment scheme. Part I: Observational and theoretical basis. *Quart. J. Roy. Meteorol. Soc.*, 112:677–691.
- Blackadar, A. K. (1962). The vertical distribution of wind and turbulent exchange in neutral atmosphere. *J. Geophys. Res.*, 67:3095–3102.
- Bougeault, P. (1981). Modeling the trade-wind cumulus boundary layer. Part I: Testing the ensemble cloud relations against numerical data. *J. Atmos. Sci.*, 38:2414–2428.
- Bougeault, P. and André, J.-C. (1986). On the stability of the third-order turbulence closure for the modeling of the stratocumulus-topped boundary layer. *J. Atmos. Sci.*, 43:1574–1581.
- Bougeault, P. and Lacarrère, P. (1989). Parameterization of orography-induced turbulence in a mesobeta-scale model. *Mon. Weather Rev.*, 117:1872–1890.
- Brost, R. A. and Wyngaard, J. C. (1978). A model study of the stably stratified planetary boundary layer. *J. Atmos. Sci.*, 35:1427–1440.
- Chou, P.-Y. (1945). On velocity correlation and the solution of the equation of turbulent fluctuation. *Quart. Appl. Math.*, 3:38–54.
- Craft, T. J., Ince, N. Z., and Launder, B. E. (1996). Recent developments in second-moment closure for buoyancy-affected flows. *Dynam. Atmos. Oceans*, 23:99–114.
- Dakos, T. and Gibson, M. M. (1987). On modelling the pressure terms of the scalar flux equations. In et al., F. D., editor, *Turbulent Shear Flows 5*, pages 7–18, Berlin. Springer.
- Daly, B. J. and Harlow, F. H. (1970). Transport equations in turbulence. *Phys. Fluids*, 13:2634–2649.
- Deardorff, J. W. (1976). Usefulness of liquid-water potential temperature in a shallow-cloud model. *J. Appl. Meteorol.*, 15:98–102.

- Dol, H. S., Hanjalić, K., and Kenjereš, S. (1997). A comparative assessment of the second-moment differential and algebraic models in turbulent natural convection. *Int. J. Heat and Fluid Flow*, 18:4–14.
- du Vachat, R. J. (1989). Comment on “Design of a nonsingular level 2.5 second-order closure model for the prediction of atmospheric turbulence”. *J. Atmos. Sci.*, 46:1631–1632.
- Girimaji, S. S. (2000). Pressure-strain correlation modelling of complex turbulent flows. *J. Fluid Mech.*, 422:91–123.
- Golaz, J.-C., Larson, V. E., and Cotton, W. R. (2002). A PDF-based model for boundary layer clouds. Part I: Method and model description. *J. Atmos. Sci.*, 59:3540–3551.
- Gryanik, V. M. and Hartmann, J. (2002). A turbulence closure for the convective boundary layer based on a two-scale mass-flux approach. *J. Atmos. Sci.*, 59:2729–2744.
- Gryanik, V. M., Hartmann, J., Raasch, S., and Schröter, M. (2005). A refinement of the millionshchikov quasi-normality hypothesis for convective boundary layer turbulence. *J. Atmos. Sci.*, 62:2632–2638.
- Hanjalić, K. (1999). Second-moment turbulence closures for CFD: Needs and prospects. *IJCFD*, 12:67–97.
- Hanjalić, K. (2002). One-point closure models for buoyancy-driven turbulent flows. *Ann. Rev. Fluid Mech.*, 34:321–347.
- Hanjalić, K., Kenjereš, S., and Durst, F. (1996). Natural convection in partitioned two-dimensional enclosures at high Rayleigh numbers. *Int. J. Heat Mass Tran.*, 39:1407–1427.
- Hanjalić, K. and Launder, B. (2011). *Modelling Turbulence in Engineering and the Environment. Second-Moment Routes to Closure*. Cambridge University Press.
- Hassid, S. and Galperin, B. (1994). Modeling rotating flows with neutral and unstable stratification. *J. Geophys. Res.*, 99:12,533–12,548.
- Heinze, R., Mironov, D., and Raasch, S. (2015). Second-moment budgets in cloud-topped boundary layers: A large-eddy simulation study. *J. Adv. Model. Earth Syst.*, 7.
- Helfand, H. M. and Labraga, J. C. (1988). Design of a nonsingular level 2.5 second-order closure model for the prediction of atmospheric turbulence. *J. Atmos. Sci.*, 45:113–132.
- Helfand, H. M. and Labraga, J. C. (1989). Reply. *J. Atmos. Sci.*, 46:1633–1635.
- Jones, W. P. and Musogno, P. (1988). Closure of Reynolds stress and scalar flux equation. *Phys. Fluids*, 31:3589–3604.
- Kenjereš, S. and Hanjalić, K. (1995). Prediction of turbulent thermal convection in concentric and eccentric horizontal annuli. *Int. J. Heat Fluid Fl.*, 18:429–439.
- Kenjereš, S. and Hanjalić, K. (2000). Convective rolls and heat transfer in finite-length Rayleigh-Bénard convection: A two-dimensional numerical study. *Phys. Rev. E.*, 62:7987–7998.
- Kenjereš, S. and Hanjalić, K. (2002). Combined effects of terrain orography and thermal stratification on pollutant dispersion in a town valley: a T-RANS simulation. *J. Turbulence*, 3:1–25.

- Lappen, C.-L. and Randall, D. A. (2001). Toward a unified parameterization of the boundary layer and moist convection. Part II: Lateral mass exchanges and subplume-scale fluxes. *J. Atmos. Sci.*, 58:2037–2051.
- Larson, V. E., Wood, R., Field, P. R., Golaz, J.-C., Haar, T. H. V., and Cotton, W. R. (2001). Small-scale and mesoscale variability of scalars in cloudy boundary layers: One-dimensional probability density functions. *J. Atmos. Sci.*, 58:1978–1994.
- Launder, B. E., Reece, G. J., and Rodi, W. (1975). Progress in the development of a Reynolds-stress turbulence closure. *J. Fluid Mech.*, 68:537–566.
- Lazeroms, W. M. J., Brethouwer, G., Wallin, S., and Johansson, A. V. (2013). An explicit algebraic reynolds-stress and scalar-ux model for stably stratified flows. *J. Fluid Mech.*, 723:91–125.
- Lazeroms, W. M. J., Brethouwer, G., Wallin, S., and Johansson, A. V. (2015). Efficient treatment of the nonlinear features in algebraic reynolds-stress and heat-flux models for stratified and convective flows. *Int. J. Heat and Fluid Flow*, 53:15–28.
- Lazeroms, W. M. J., Svensson, G., Bazile, E., Brethouwer, G., Wallin, S., and Johansson, A. V. (2016). Study of transitions in the atmospheric boundary layer using explicit algebraic turbulence models. *Boundary-Layer Meteorol.*, 161:19–47.
- Lewellen, D. S. and Lewellen, W. S. (2004). Buoyancy flux modeling for cloudy boundary layers. *J. Atmos. Sci.*, 61:1147–1160.
- Lilly, D. K. (1968). Models of cloud-topped mixed layers under a strong inversion. *Quart. J. Roy. Meteorol. Soc.*, 94:292–309.
- Lumley, J. L. (1975). Pressure-strain correlation. *Phys. Fluids*, 18:750.
- Machulskaya, E. (2015). Clouds and convection as subgrid-scale distributions. In Plant, R. S. and Yano, J.-I., editors, *Parameterization of Atmospheric Convection. Volume 2: Current Issues and New Theories*, chapter 25, pages 377–422. World Scientific, Imperial College Press.
- Machulskaya, E. and Mironov, D. (2013). Implementation of TKE–Scalar Variance mixing scheme into COSMO. COSMO Newsletter 13. Available from <http://www.cosmo-model.org>.
- Mauritsen, T., Svensson, G., Zilitinkevich, S. S., Esau, I., Enger, L., and Grisogono, B. (2007). A total turbulent energy closure model for neutrally and stably stratified atmospheric boundary layers. *J. Atmos. Sci.*, 64:4113–4126.
- Mellor, G. L. (1977). The Gaussian cloud model relations. *J. Atmos. Sci.*, 34:356–358.
- Mellor, G. L. and Yamada, T. (1974). A hierarchy of turbulence closure models for planetary boundary layers. *J. Atmos. Sci.*, 31:1791–1806.
- Mellor, G. L. and Yamada, T. (1982). Development of a turbulence closure model for geophysical fluid problems. *Rev. Geophys.*, 20:851–875.
- Millionshchikov, M. D. (1941). On the theory of homogeneous isotropic turbulence. *Doklady Acad. Nauk SSSR*, 32:611–614.
- Mironov, D. V. (2001). Pressure–potential-temperature covariance in convection with rotation. *Quart. J. Roy. Meteorol. Soc.*, 127:89–110.

- Mironov, D. V. (2009). Turbulence in the lower troposphere: second-order closure and mass-flux modelling frameworks. In Hillebrandt, W. and Kupka, F., editors, *Interdisciplinary Aspects of Turbulence*, volume 756 of *Lect. Notes Phys.*, pages 161–221. Springer-Verlag.
- Mironov, D. V., Gryanik, V. M., Lykossov, V. N., and Zilitinkevich, S. S. (1999). Comments on “A New Second-Order Turbulence Closure Scheme for the Planetary Boundary Layer” by K. Abdella and N. McFarlane. *J. Atmos. Sci.*, 56:3478–3481.
- Mironov, D. V. and Sullivan, P. P. (2016). Second-moment budgets and mixing intensity in the stably stratified atmospheric boundary layer over thermally heterogeneous surfaces. *J. Atmos. Sci.*, 73:449–464.
- Monin, A. S. (1965). On the symmetry properties of turbulence in the near-surface layer of air. *Izv. Atmos. Oceanic Phys.*, 1:25–30.
- Monin, A. S. and Yaglom, A. M. (1971). *Statistical Fluid Mechanics*, volume 1. MIT Press, Cambridge, Massachusetts.
- Nakanishi, M. and Niino, H. (2004). An improved Mellor-Yamada level-3 model with condensation physics: its design and verification. *Boundary-Layer Meteorol.*, 112:1–31.
- Naumann, A. K., Seifert, A., and Mellado, J. P. (2013). A refined statistical cloud closure using double-Gaussian probability density functions. *Geosci. Model Dev.*, 6:1641–1657.
- Otić, I., Grötzbach, G., and Wörner, M. (2005). Analysis and modelling of the temperature variance equation in turbulent natural convection for low-Prandtl-number fluids. *J. Fluid Mech.*, 525:237–261.
- Pope, S. B. (2000). *Turbulent Flows*. Cambridge University Press.
- Raschendorfer, M. (1999). Special topic: The new turbulence parameterization of LM. Quarterly Report of the Operational NWP-Models of the Deutscher Wetterdienst, 19.
- Raschendorfer, M. (2001). The new turbulence parameterization of LM. COSMO Newsletter 1. Available from <http://www.cosmo-model.org>.
- Ristorcelli, J. R., Lumley, J. L., and Abid, R. (1995). A rapid-pressure covariance representation consistent with the Taylor-Proudman theorem materially frame indifferent in the two-dimensional limit. *J. Fluid Mech.*, 292:111–152.
- Rotta, J. C. (1951). Statistische Theorie nichthomogener Turbulenz. 1. *Zs. Phys.*, 129:547–572.
- Shih, T.-H. (1996). Constitutive relations and realizability of single-point turbulence closures. In M. Hallböck, D. S. Henningson, A. V. Johansson, and P. H. Alfredsson, editor, *Turbulence and Transition Modelling*, pages 155–192. Kluwer Acad. Publ., Dordrecht, etc.
- Shih, T.-H. and Lumley, J. L. (1985). Modeling of pressure correlation terms in Reynolds stress and scalar flux equations. Technical Report FDA-85-03, Sibley School of Mechanical and Aerospace Engineering, Cornell University.
- Sommeria, G. and Deardorff, J. W. (1977). Subgrid-scale condensation in models of non-precipitating clouds. *J. Atmos. Sci.*, 34:344–355.
- Speziale, C. G. (1985). Modeling the pressure gradient-velocity correlation of turbulence. *Phys. Fluids*, 28:69–71.

- Speziale, C. G., Sarkar, S., and Gatski, T. B. (1991). Modeling the pressure-strain correlation of turbulence: an invariant dynamical system approach. *J. Fluid Mech.*, 227:245–272.
- Stull, R. (1973). Inversion rise model based on penetrative convection. *J. Atmos. Sci.*, 30:1092–1099.
- Tompkins, A. M. (2003). Impact of temperature and humidity variability on cloud cover assessed using aircraft data. *Quart. J. Roy. Meteorol. Soc.*, 129:2151–2170.
- Tompkins, A. M. (2005). The parameterization of cloud cover. Technical memorandum, European Centre for Medium-Range Weather Forecasts, Reading, U.K.
- Umlauf, L. and Burchard, H. (2003). A generic length-scale equation for geophysical turbulence models. *Journal of Marine Research*, 61:235–265.
- Umlauf, L. and Burchard, H. (2005). Second-order turbulence closure models for geophysical boundary layers. A review of recent work. *Cont. Shelf Res.*, 25:795–827.
- Umlauf, L., Burchard, H., and Hutter, K. (2003). Extending the $k - \omega$ turbulence model towards oceanic applications. *Ocean Modelling*, 5:195–218.
- Vallis, G. K. (2006). *Atmospheric and Oceanic Fluid Dynamics. Fundamentals and Large-scale Circulation*. Cambridge University Press, Cambridge, etc.
- Wyngaard, J. C. (1975). Modeling the planetary boundary layer – extension to the stable case. *Boundary-Layer Meteorol.*, 9:441–460.
- Yamada, T. (1977). A numerical experiment on pollutant dispersion in a horizontally-homogeneous atmospheric boundary layer. *Atmos. Environ.*, 11:1015–1024.
- Zeman, O. (1981). Progress in the modeling of planetary boundary layers. *Ann. Rev. Fluid Mech.*, 13:253–272.
- Zeman, O. and Lumley, J. L. (1976). Modeling buoyancy driven mixed layers. *J. Atmos. Sci.*, 33:1974–1988.
- Zeman, O. and Tennekes, H. (1975). A self-contained model for the pressure terms in the turbulent stress equations of the neutral atmospheric boundary layer. *J. Atmos. Sci.*, 32:1808–1813.
- Zeman, O. and Tennekes, H. (1977). Parameterization of the turbulent energy budget at the top of the daytime atmospheric boundary layer. *J. Atmos. Sci.*, 34:111–123.
- Zilitinkevich, S. S., Elperin, T., Kleeorin, N., iV. L’vov, and Rogachevskii, I. (2009). Energy- and flux-budget turbulence closure model for stably stratified flows. Part II: the role of internal gravity waves. *Boundary-Layer Meteorol.*, 133:139–164.
- Zilitinkevich, S. S., Elperin, T., Kleeorin, N., and Rogachevskii, I. (2007). Energy- and flux-budget (EFB) turbulence closure model for stably stratified flows. Part I: steady-state, homogeneous regimes. *Boundary-Layer Meteorol.*, 125:167–191.
- Zilitinkevich, S. S., Elperin, T., Kleeorin, N., Rogachevskii, I., and Esau, I. (2013). A hierarchy of energy- and flux-budget (EFB) turbulence closure models for stably-stratified geophysical flows. *Boundary-Layer Meteorol.*, 146:341–373.
- Zilitinkevich, S. S. and Mironov, D. V. (1992). Theoretical model of thermocline in a fresh-water basin. *J. Phys. Oceanogr.*, 22:988–996.

List of COSMO Newsletters and Technical Reports

(available for download from the COSMO Website: www.cosmo-model.org)

COSMO Newsletters

- No. 1: February 2001.
- No. 2: February 2002.
- No. 3: February 2003.
- No. 4: February 2004.
- No. 5: April 2005.
- No. 6: July 2006.
- No. 7: April 2008; Proceedings from the 8th COSMO General Meeting in Bucharest, 2006.
- No. 8: September 2008; Proceedings from the 9th COSMO General Meeting in Athens, 2007.
- No. 9: December 2008.
- No. 10: March 2010.
- No. 11: April 2011.
- No. 12: April 2012.
- No. 13: April 2013.
- No. 14: April 2014.
- No. 15: July 2015.
- No. 16: July 2016.

COSMO Technical Reports

- No. 1: Dmitrii Mironov and Matthias Raschendorfer (2001):
Evaluation of Empirical Parameters of the New LM Surface-Layer Parameterization Scheme. Results from Numerical Experiments Including the Soil Moisture Analysis.
- No. 2: Reinhold Schrodin and Erdmann Heise (2001):
The Multi-Layer Version of the DWD Soil Model TERRA-LM.
- No. 3: Günther Doms (2001):
A Scheme for Monotonic Numerical Diffusion in the LM.
- No. 4: Hans-Joachim Herzog, Ursula Schubert, Gerd Vogel, Adelheid Fiedler and Roswitha Kirchner (2002):
LLM - the High-Resolving Nonhydrostatic Simulation Model in the DWD-Project LIT-FASS.
Part I: Modelling Technique and Simulation Method.

- No. 5: Jean-Marie Bettems (2002):
EUCOS Impact Study Using the Limited-Area Non-Hydrostatic NWP Model in Operational Use at MeteoSwiss.
- No. 6: Heinz-Werner Bitzer and Jürgen Steppeler (2004):
Documentation of the Z-Coordinate Dynamical Core of LM.
- No. 7: Hans-Joachim Herzog, Almut Gassmann (2005):
Lorenz- and Charney-Phillips vertical grid experimentation using a compressible non-hydrostatic toy-model relevant to the fast-mode part of the 'Lokal-Modell'.
- No. 8: Chiara Marsigli, Andrea Montani, Tiziana Paccagnella, Davide Sacchetti, André Walser, Marco Arpagaus, Thomas Schumann (2005):
Evaluation of the Performance of the COSMO-LEPS System.
- No. 9: Erdmann Heise, Bodo Ritter, Reinhold Schrodin (2006):
Operational Implementation of the Multilayer Soil Model.
- No. 10: M.D. Tsyrlunikov (2007):
Is the particle filtering approach appropriate for meso-scale data assimilation ?
- No. 11: Dmitrii V. Mironov (2008):
Parameterization of Lakes in Numerical Weather Prediction. Description of a Lake Model.
- No. 12: Adriano Raspanti (2009):
COSMO Priority Project "VERification System Unified Survey" (VERSUS): Final Report.
- No. 13: Chiara Marsigli (2009):
COSMO Priority Project "Short Range Ensemble Prediction System" (SREPS): Final Report.
- No. 14: Michael Baldauf (2009):
COSMO Priority Project "Further Developments of the Runge-Kutta Time Integration Scheme" (RK): Final Report.
- No. 15: Silke Dierer (2009):
COSMO Priority Project "Tackle deficiencies in quantitative precipitation forecast" (QPF): Final Report.
- No. 16: Pierre Eckert (2009):
COSMO Priority Project "INTERP": Final Report.
- No. 17: D. Leuenberger, M. Stoll and A. Roches (2010):
Description of some convective indices implemented in the COSMO model.
- No. 18: Daniel Leuenberger (2010):
Statistical analysis of high-resolution COSMO Ensemble forecasts in view of Data Assimilation.
- No. 19: A. Montani, D. Cesari, C. Marsigli, T. Paccagnella (2010):
Seven years of activity in the field of mesoscale ensemble forecasting by the COSMO-LEPS system: main achievements and open challenges.
- No. 20: A. Roches, O. Fuhrer (2012):
Tracer module in the COSMO model.

- No. 21: Michael Baldauf (2013):
A new fast-waves solver for the Runge-Kutta dynamical core.
- No. 22: C. Marsigli, T. Diomede, A. Montani, T. Paccagnella, P. Louka, F. Gofa, A. Corigliano (2013):
The CONSENS Priority Project.
- No. 23: M. Baldauf, O. Fuhrer, M. J. Kurowski, G. de Morsier, M. Müllner, Z. P. Piotrowski, B. Rosa, P. L. Vitagliano, D. Wójcik, M. Ziemiański (2013):
The COSMO Priority Project 'Conservative Dynamical Core' Final Report.
- No. 24: A. K. Miltenberger, A. Roches, S. Pfahl, H. Wernli (2014):
Online Trajectory Module in COSMO: a short user guide.
- No. 25: P. Khain, I. Carmona, A. Voudouri, E. Avgoustoglou, J.-M. Bettems, F. Grazzini (2015):
The Proof of the Parameters Calibration Method: CALMO Progress Report.
- No. 26: D. Mironov, E. Machulskaya, B. Szintai, M. Raschendorfer, V. Perov, M. Chumakov, E. Avgoustoglou (2015):
The COSMO Priority Project 'UTCS' Final Report.
- No. 27: J.-M. Bettems (2015):
The COSMO Priority Project 'COLOBOC': Final Report.
- No. 28: Ulrich Blahak (2016):
RADAR_MIE_LM and RADAR_MIELIB - Calculation of Radar Reflectivity from Model Output.
- No. 29: M. Tsyrlnikov and D. Gayfulin (2016):
A Stochastic Pattern Generator for ensemble applications.

COSMO Technical Reports

Issues of the COSMO Technical Reports series are published by the *COnsortium for Small-scale MOdelling* at non-regular intervals. COSMO is a European group for numerical weather prediction with participating meteorological services from Germany (DWD, AWGeophys), Greece (HNMS), Italy (USAM, ARPA-SIMC, ARPA Piemonte), Switzerland (MeteoSwiss), Poland (IMGW), Romania (NMA) and Russia (RHM). The general goal is to develop, improve and maintain a non-hydrostatic limited area modelling system to be used for both operational and research applications by the members of COSMO. This system is initially based on the COSMO-Model (previously known as LM) of DWD with its corresponding data assimilation system.

The Technical Reports are intended

- for scientific contributions and a documentation of research activities,
- to present and discuss results obtained from the model system,
- to present and discuss verification results and interpretation methods,
- for a documentation of technical changes to the model system,
- to give an overview of new components of the model system.

The purpose of these reports is to communicate results, changes and progress related to the LM model system relatively fast within the COSMO consortium, and also to inform other NWP groups on our current research activities. In this way the discussion on a specific topic can be stimulated at an early stage. In order to publish a report very soon after the completion of the manuscript, we have decided to omit a thorough reviewing procedure and only a rough check is done by the editors and a third reviewer. We apologize for typographical and other errors or inconsistencies which may still be present.

At present, the Technical Reports are available for download from the COSMO web site (www.cosmo-model.org). If required, the member meteorological centres can produce hardcopies by their own for distribution within their service. All members of the consortium will be informed about new issues by email.

For any comments and questions, please contact the editor:

Massimo Milelli
Massimo.Milelli@arpa.piemonte.it